Sonochemistry and Sonocatalysis: Current Progress, Existing Limitations, and Future Opportunities in Sustainable Chemistry.

Quang Thang Trinh,[1,*] Nicholas Golio,[2] Yuran Cheng,[1,3] Haotian Cha,[1] Kin Un Tai,[1] Lingxi Ouyang,[1,4] Jun Zhao,[5] Tuan Sang Tran,[1] Tuan Khoa Nguyen,[1] Jun Zhang,[1,6] Hongjie An,[1,4] Zuojun Wei,[3] Francois Jerome,[2] Prince Nana Amaniampong,[2,*] Nam-Trung Nguyen[1,*].

[1]*Queensland Micro and Nanotechnology Centre, Griffith University, 170 Kessel Road, Nathan, QLD 4111, Australia.*

[2]*CNRS, Institut de Chimie des Milieux et Matériaux de Poitiers (IC2MP), Université de Poitiers, Bat B1 (ENSI-Poitiers), 1 rue Marcel Doré, 86073 Poitiers, France.*

[3]*Key Laboratory of Biomass Chemical Engineering of the Ministry of Education, College of Chemical and Biological Engineering, Zhejiang University, Hangzhou, Zhejiang, 310058, P.R. China.*

[4]*School of Environment Science, Griffith University, 170 Kessel Road, Nathan, QLD 4111, Australia.*

[5]*Department of Biology, Hong Kong Baptist University, Hong Kong, China.*

[6]*School of Engineering and Built Environment, Griffith University, 170 Kessel Road, Nathan, QLD 4111, Australia.*

Corresponding authors:

q.trinh@griffith.edu.au (Q.T.T.)

prince.nana.amaniampong@univ-poitiers.fr (P.N.A.)

nam-trung.nguyen@griffith.edu.au (N.-T.N.)

Abstract.

Sonocatalysis is a specialised field within sonochemistry that leverages the interaction between ultrasound and solid catalysts to enhance the rate and selectivity of chemical reactions. As a non-traditional catalytic activation method, sonocatalysis can profoundly modify reaction mechanisms and unlock novel activation pathways that are not typically accessible through standard catalysis. This unique approach offers new opportunities for driving reactions under milder conditions while potentially improving selectivity and efficiency. This review highlights the recent progress in sonocatalytic applications aligned with several United Nations Sustainable Development Goals, including environmental remediation, sonotherapy, and biomass conversion. In these applications, we explore the underlying sonocatalytic mechanisms and the interaction between solid catalysts and ultrasound, which drive the enhanced reactivity. A key feature of this manuscript is its comprehensive analysis of the primary technical challenges in sonocatalysis, specifically its low energy efficiency and the complexity of reaction control. To address these hurdles, we examine various effective strategies, such as the incorporation of nanostructured catalytic cavitation agents and the design of advanced microfluidic sonoreactors. These innovations improve energy transfer, control bubble dynamics, and enhance catalytic activity under ultrasound. Furthermore, we implement molecular modelling to gain fundamental insights into the mechanisms fundamental to the effectiveness of sonocatalysts. This approach provides a deeper understanding of how nanostructured catalysts interact with ultrasonic fields, guiding the design of next-generation catalytic materials. The integration of nanostructured catalytic cavitation agents**,** microfluidic reactor technologies, and computational molecular modelling forms a trilateral synergistic platform that unlocks new potential in sonocatalysis. This multidisciplinary framework paves the way for significant advancements in sustainable chemistry, offering innovative solutions to global challenges in energy, health, and environmental sustainability.

1. Introduction

Sonochemistry is an evolving field that explores the unique effects of ultrasound on chemical systems, with profound implications for industrial, environmental, and biomedical applications.[1-5] In recent years, the ability of ultrasound to enhance various chemical processes has led to its adoption in fields such as ultrasound-assisted extraction, crystallisation, chemical synthesis, material fabrication, and non-invasive therapies.[6-10] The operational frequency range for sonochemistry typically lies between 20 kHz to 1 MHz, enabling a wide array of chemical transformations and material processing techniques that are otherwise challenging under conventional methods. The versatility and effectiveness of ultrasound have made it an indispensable tool in industries like food processing, pharmaceuticals, material science, and environmental remediation.[11-13] One of the most striking features of sonochemistry is its ability to accelerate reaction rates, alter reaction pathways, and modify physical properties under relatively mild conditions. Unlike conventional chemical reactions, which often rely on high temperatures and/or pressures, sonochemical processes occur via the non-thermal effects of ultrasound, thereby providing more energy-efficient and selective routes for chemical transformations. For example, ultrasound-assisted synthesis has been employed to produce nanoparticles, polymers, and porous materials, while sono-crystallisation has been used to control crystal size and purity in pharmaceutical applications.[14-18]

The primary mechanism driving many sonochemical processes is acoustic cavitation—the formation, growth, and violent collapse of bubbles in a liquid medium under ultrasonic irradiation. When these bubbles collapse, they generate localised extreme conditions, including high temperatures (up to 5000 K), high pressures (hundreds of atmospheres), and intense shear forces.[19-22] This results in microstreaming, microjetting, pyrolysis, sonoluminescence, and the generation of highly reactive radicals. The localised energy generated by cavitation creates a unique microenvironment that can induce chemical reactions, alter reaction kinetics, and facilitate material synthesis under ambient conditions.[23-26] For example, acoustic cavitation has been employed to synthesise materials such as metallic nanoparticles and oxide films, which are difficult to achieve

using traditional methods.[14, 15, 27] Furthermore, sonochemistry has been instrumental in improving the bioavailability of drugs, where cavitation aids in the breakdown of biological barriers, enhancing drug delivery systems through sonoporation or ultrasound-triggered drug release.[28-30] Despite the promising potential of cavitation, its random and uncontrolled nature, both spatially and temporally, poses significant challenges in optimising sonochemical processes. Cavitation events can occur unpredictably, leading to side reactions, unintended material degradation, and inefficient energy usage. These limitations become particularly problematic in industrial applications, where process consistency and efficiency are critical.

To address these challenges, researchers have explored various strategies to better control cavitation. Traditionally, exogenous gas nuclei, such as micro- and nanobubbles, are introduced to initiate cavitation. However, microbubbles have inherent limitations, such as their short circulation half-life and rapid destruction under ultrasound. More recently, alternative nucleation agents like phase-change droplets and solid cavitation agents have been proposed. Phase-change droplets provide a more stable platform for cavitation initiation, but they still suffer from size limitations and are not suitable for long-term applications.[31, 32] Solid cavitation agents, particularly those developed for biomedical applications, offer more promise than other techniques.[33-35] These materials, often composed of metal oxides or nanostructured surfaces, provide stable nucleation sites for cavitation and are able to be engineered for use in broader industrial applications. For example, TiO_2 nanoparticles and carbon-based nanomaterials have been used as solid cavitation agents to improve the control and efficiency of ultrasound-assisted reactions.[36, 37] These agents enhance cavitation by reducing the threshold acoustic energy required, allowing for more precise control over where and when cavitation occurs. A key limitation of current sonochemical methods is their reliance on uncontrolled cavitation for the generation of radical species, often requiring continuous high-powered ultrasound over long durations. This is not only energy-intensive but also increases the likelihood of undesired side reactions and reduces the overall efficiency and selectivity of the chemical process.

Sonocatalysis, an emerging sub-field of sonochemistry, seeks to address these inefficiencies by integrating a heterogeneous catalyst into the ultrasonic field. The solid catalyst interacts with the ultrasound-induced radicals and absorbs the cavitation energy, thus facilitating more controlled reactions.[38-42] For instance, catalysts such as TiO_2 or ZnO have been introduced in environmental remediation efforts to work synergistically with ultrasound to degrade pollutants in water.[39, 42] The combination of ultrasound with solid catalysts enhances the degradation rates of organic contaminants, such as dyes and pharmaceuticals, while reducing the required energy input.

However, a significant challenge remains: the physical distance separating cavitation events and the catalytic surface, which limits the efficiency of energy transfer. Cavitation primarily occurs in the bulk liquid, while catalytic reactions take place on the solid surface, meaning that the full potential of the combined ultrasound-catalyst system is not realised. To overcome these challenges, several approaches are being explored. The use of nanostructured catalytic cavitation agents provides one avenue for increasing the surface area available for cavitation while reducing the energy barrier for bubble formation. These nanostructures can serve as both nucleation sites for cavitation and as active catalytic surfaces, thereby bridging the gap between ultrasound energy and catalytic activity. Another promising development is the design of microfluidic sonoreactors, which offer enhanced control over cavitation events by confining the reaction space and optimising the flow of reactants. In microfluidic systems, the interaction between ultrasound and the fluid can be precisely controlled, allowing for more uniform cavitation and reducing energy losses. In addition, the integration of computational molecular modelling is becoming increasingly important for understanding the fundamental mechanisms of sonocatalysis to better guide the design of novel nanostructured materials. By simulating the interaction between ultrasound, cavitation, and solid catalysts, researchers seek to optimise the system parameters in order to maximise the efficiency and selectivity.

In this review, we summarise the history of sonochemistry and describe the recent developments of sonochemistry and sonocatalysis for sustainable chemistry. We analyse in detail the existing technical hurdles for further developing these technologies and give a perspective on harnessing the

nanostructured catalytic cavitation agents and the power of microfluidics in sonocatalysis. In this review, computational molecular modelling, nanostructured catalytic cavitation agents, and microfluidic solutions are proposed to be integrated into a sonocatalytic platform for the first time. The result is a three-pronged approach that leverages different aspects of sonochemistry to accelerate advancements sustainable chemistry.

2. The evolution of sonochemistry

2.1. Application of sound waves in chemistry (Sonochemistry)

Sonochemistry refers to the use of sound with high-frequency vibration in the ultrasonic range as the energy source for chemical processes. The frequencies of sound are expressed in units of Hertz (Hz), where 1 Hz corresponds to one cycle of sound per second. The audible range of sound (human hearing range) is from 20 Hz–20 kHz, while sound with higher frequencies (20 kHz – 200 MHz) cannot be heard by human ears and is called "ultrasound" (Figure 1a).[43] At very high frequencies, there is significant energy loss of ultrasonic irradiation due to molecular motion, resulting in negligible chemical effects. Consequently, the frequency range higher than 1 MHz is mainly used for medical imaging applications. On the other hand, the frequency range from 20 kHz to 1 MHz is of particular interest to the chemistry community since it retains enough chemical effects to carry out chemical reactions.[43] Under ultrasonic irradiation, cycles of bubble nucleation, growth, and collapse (referred to as cavitation) occur continuously and generate highly active radicals which are very useful in facilitating chemical reactions with high activity and selectivity.[44] The collapse of cavitation bubbles creates extreme local conditions of ultra-high temperature and pressure, initiating free radicals which can catalyse chemical reactions. Therefore, the field of sonochemistry aims to study the effect of acoustic cavitation in liquids for enhancing chemical activity, and how cavitation affects chemical reactions and processes.

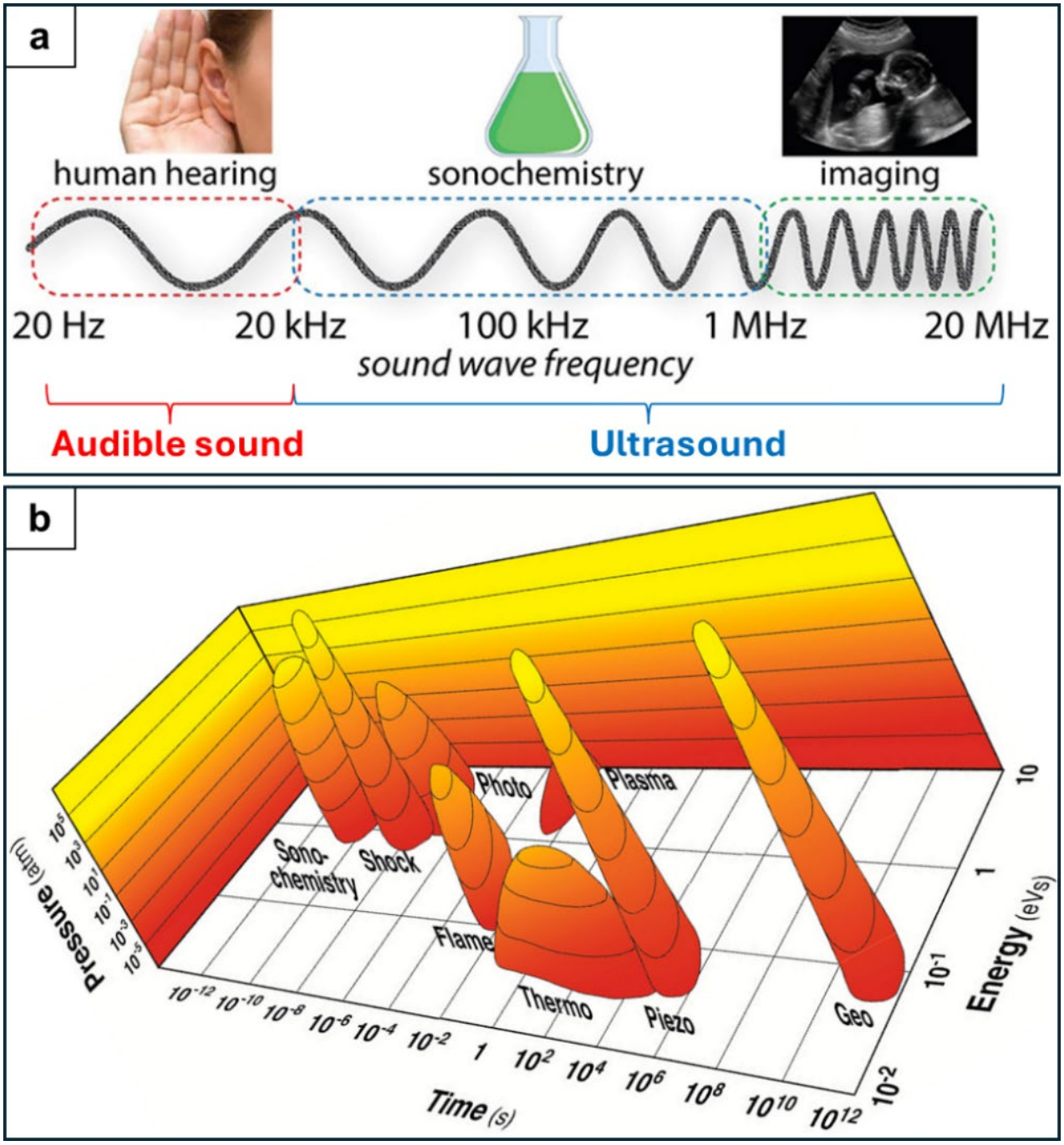

Figure 1. (a) Frequency range of sound and their applications, reproduced with permission from McKenzie et al.[43] Copyright 2019, John Wiley and Sons. (b) Comparison of the parameters that control chemical reactivity (time, pressure, and energy) for various forms of chemistry, reproduced with permission from Suslick et al.[45] Copyright 2018, American Chemical Society.

In conventional thermochemical approaches, operating parameters such as temperature, pressure, and reaction time are tuned to control the equilibrium of the chemical process. The temperature determines the amount of kinetic energy inherent in the system, and the pressure controls the interatomic collision density. Temperature, pressure, and reaction time form the three-dimensional (3D) space over which reaction conditions are tuned in order to optimise a given chemical application (Figure 1b). However, in many cases, simply tuning these parameters does not enable

adequate control of the reaction rate and selectivity or the optimal parameters require too much energy expenditure to be a viable solution. Thus, alternative chemical pathways have emerged in an attempt to solve this bottleneck. The cornerstone of these alternative chemical pathways is that chemical reactions are driven by external triggers, such as electrical potentials (electrochemistry), photons (photochemistry), plasma (plasma-chemistry), and ultrasound (sonochemistry). Among these external triggers, ultrasound holds great promise due to its unique combination of short reaction times, high generated pressures, and high reaction energies compared to other traditional energy sources (Figure 1b).

Figure 1b shows that sonochemistry is characterised by the high energy amount (from 1 to 10 eV) which is introduced in a very short time (~10^{-10} s) and under an extremely high pressure (up to 10^3 atm). These features provide an energy equivalent comparable to shock-tube chemistry and photochemistry, except for the fact that the energy provided by ultrasound is thermal in nature. Other approaches, such as flame-chemistry in flash pyrolysis, thermochemistry, or geochemistry (the chemistry behind major geological systems), produce lower levels of energy and feature with a longer reaction duration of more than 6 orders of magnitude. Due to its unique characteristics, sonochemical reactions can occur in extreme temperature-pressure conditions in a very short duration (on the order of microseconds), resulting in unprecedented high activity and selectivity. The speed of reaction under ultrasound enables experimentation with chemical reagents whose operating conditions are normally prohibitive and thus difficult to use by conventional routes.

2.2. A 'sound' story (History of sonochemistry)

Figure 2 briefly summarises the history of sonochemistry. Following the introduction of the concept of ultrasound in 1794, acoustic cavitation was the first observed phenomenon in water reported by Thornycroft and Barnaby in 1895.[46] They observed that the propeller of the torpedo boat destroyer HMS Daring was eroded and pitted by the so-called "cavitation events", which involved the generation and implosion of large bubbles occurring during the movement of the blades. In 1917, Rayleigh explained this phenomenon using mathematical models of the formation, growth, and collapse of vapor bubbles in an incompressible fluid.[47] However, despite the early discovery of

cavitation, its first useful application in chemistry was only observed in 1927 by Loomis, Wood, and Richards. Their application marked the first usage of the chemical effects of high-frequency ultrasound for accelerating reactions, facilitating particle aggregation, and even as a disinfectant.[48, 49] Their research became the landmark in sonochemistry and strongly influenced the subsequent development of the field. In 1934, Frenzel and Shultes observed the first instance of "sono-luminescence" – the emission of light in liquid samples due to cavitation caused by ultrasonic irradiation.[50] Several important developments in sonochemistry occurred subsequent to these discoveries, including the effects of ultrasound on electrochemistry in 1935[51] and the application of ultrasound in organic chemistry in 1938.[52] At this time, the applications of ultrasound in chemical and biological processes became more widespread leading to the seminal Richards' review paper entitled "Supersonic phenomena" in 1939.[53]

In 1950, Weissler et al. studied the aqueous oxidation of potassium iodide under ultrasonic irradiation and found that the short-lived reactive species generated from cavitation were able to induce the secondary oxidation of iodide (I^-) to triiodide (I_3^-), which could be easily detected by spectrophotometry.[54] This research laid the foundation for the development of chemical dosimetry method to evaluate the efficiency of the sonochemical Weissler reaction, which is still largely used in the present day. In 1951, Nolting et al. reported a modelling study on the dynamics of acoustic bubbles,[55] contributing to understanding the thermodynamic properties of cavitation and predicting the extremely high temperature of 10,000 K inside cavitation bubbles. Due to this extremely high temperature, sonochemistry is also called "hot-spot chemistry". Those discoveries later led to the term "sonochemistry" coined by Weissler, a pioneering scientist in the field of ultrasound applications in chemistry, in his seminal paper.[56] The detection of highly active radicals (H and OH) formed during ultrasonic cavitation and the microjet effect produced upon bubble collapse were also reported in 1956[57] and 1961,[58] respectively. However, despite this ground-breaking research, the field of sonochemistry was not widely recognised until the 1980s. According to a Scopus search, the term "sonochemistry" only appeared 8 times in research papers from 1953 to 1986.

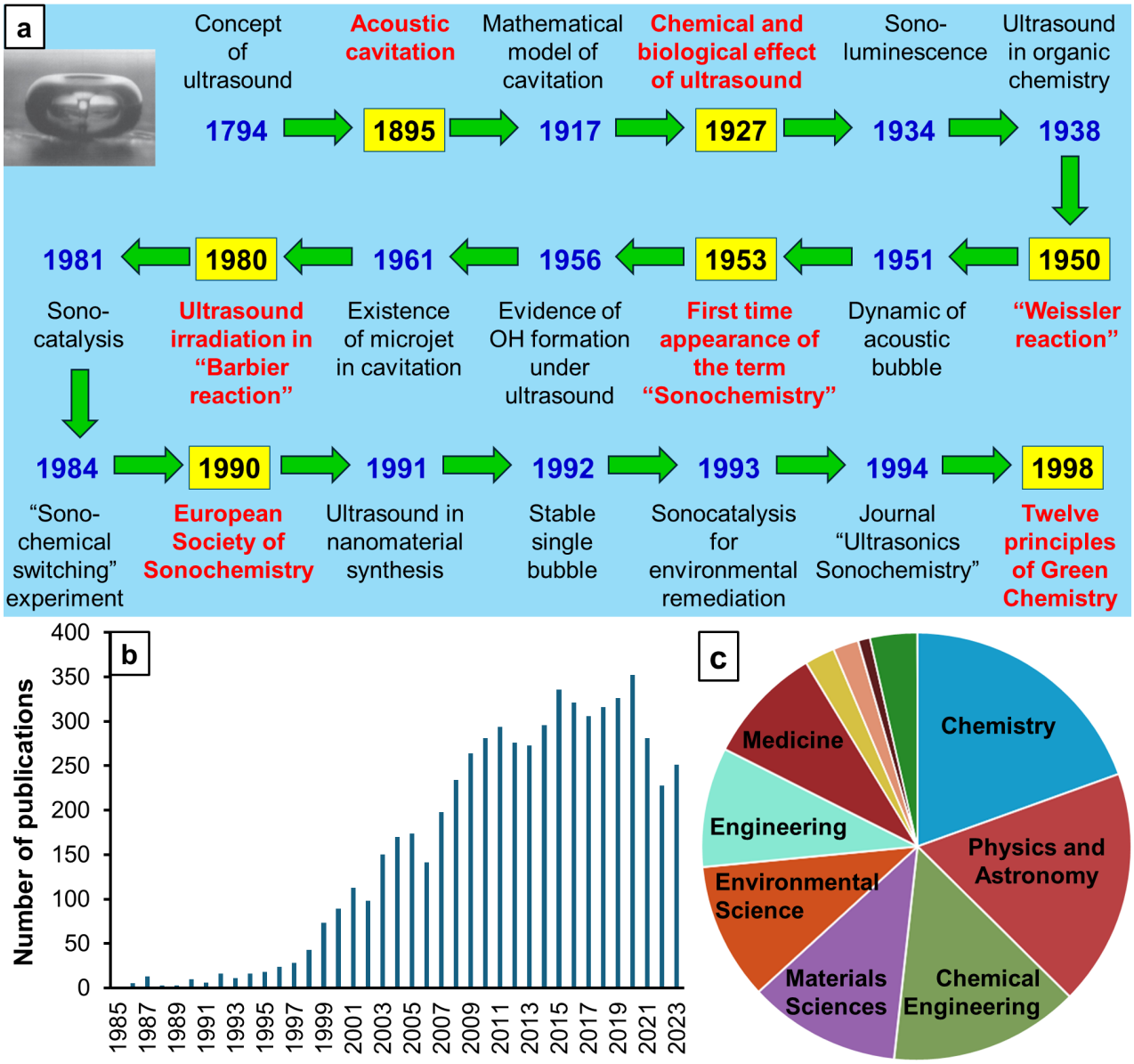

Figure 2. (a) The revolution of sonochemistry. Inserted image shows a microjet bubble produced during sono-chemical cavitation. Some important landmarks in the history of sonochemistry are highlighted in red. (b) Number of publications with the keyword "sonochemistry" in different years, from Scopus search in September 2024. (c) Subject areas of research with the keywords "sonochemistry", from Scopus search in September 2024.

In 1980, the term "sonochemistry" re-emerged in the review on acoustic cavitation by Neppiras,[23] marking the rebirth of sonochemistry as a distinct discipline. In the 1980s, great successes in the development of piezoelectric materials and transducers consequently made the commercialisation of ultrasonic equipment more affordable.[59] Different types of ultrasound apparatus, such as the ultrasound bath, the ultrasound horn and ultrasound probes with controllable power and frequencies became available. The availability of this technology boosted the number of studies on the application of ultrasound in chemical and biological processes, as was evidenced by the appearance of the term "sonochemistry" more than 100 times in published papers between 1980 and 1995

(Figure 2b). Some landmark discoveries in this period are (i) the highly effective "Barbier reaction", which is the organometallic reaction between a carbonyl group and an alkyl halide under ultrasonic irradiation, reported by Luche et al. in 1980;[60] (ii) the use of the term "sonocatalysis" by Suslick et al. in 1981[61] relating to olefin isomerization catalysed by iron carbonyl catalysts, which was drastically enhanced under high frequency ultrasonic conditions; and (iii) the Ando's "sonochemical switching" in organic synthesis in 1984,[62] where ultrasound changed the reaction pathway from electrophilic to nucleophilic for the reaction between benzyl bromide and toluene. These achievements and the works from prominent scientists of this period (for example, Timothy Mason at Coventry University, Jean-Louis Luche at Joseph Fourier University and Kenneth Suslick at the University of Illinois at Urbana-Champaign) laid the foundation for the development of modern sonochemistry, resulting in the establishment of the European Society of Sonochemistry in 1990[63] and the Elsevier journal dedicated to sonochemistry, Ultrasonics Sonochemistry, in 1994.[64] One important achievement in this period is the success of Gaitan et al. in stabilising a single bubble under ultrasonic irradiation and studying sonoluminesence during its expansion and contraction in 1992.[65] This discovery established the fundamental framework to characterise acoustic bubbles, which is still being used at present. The application of ultrasound was quickly expanded beyond organic synthesis and found great successes in other areas, such as nanomaterials synthesis, environmental remediation, medical therapy, and biological engineering (Figure 2c). In 1998, Paul Anastas and John Warner published a paper entitled "Twelve principles of Green Chemistry", outlying the set of principles that "*reduces or eliminates the use or generation of hazardous substances in the design, manufacture and applications of chemical products*".[66] Based on these principles, sonochemistry is widely accepted as a "green" process. For example, recent developments in the field of sonocatalysis for biomass conversion and polymer degradation proved that it could make a prominent contribution towards sustainable and eco-friendly chemistry and a circular economy.[67-75]

2.3. Acoustic Cavitation: The engine of sonochemistry

Ultrasonic waves locally change the density of the fluid and are measured as pressure perturbations. With sufficient acoustic intensity, these waves disrupt the tensile forces of the liquid, forming a vapor cavity, or bubble, in the liquid.[76] During the propagation of ultrasound in liquid media, bubbles are expanded and compressed in response to the alternate rarefaction and compression cycles of the ultrasound. This process results in the accumulation of energy inside the bubbles as their radius changes (Figs. 3a,b).[77-79] At a certain size, bubbles implode and release their stored energy. The formation of bubbles and their subsequent size oscillation are called "cavitation", Figure 3a. Cavitation events are accompanied by sudden increases in local pressure (up to several MPa) and local temperature (up to thousands of degrees Celsius).[45, 80] The extent of the effect of imploding cavitation bubbles in a liquid depends on the applied frequency. For instance, Low Frequency Ultrasound (LFUS) (20-80 kHz) generates few large cavitation bubbles (~170 μm at 20 kHz).[78] Bubble implosion during LFUS irradiation mainly induces physical effects, such as shock waves and high speed jets.[81] Therefore, LFUS is often used in applications such as the erosion/deagglomeration of particles and the breaking long chain polymers.

In contrast, High Frequency Ultrasound (HFUS, > 100 kHz) generates a large number of small sized cavitation bubbles (5-6 μm).[82] The implosion of these bubbles is substantially accelerated by the inertia of the surrounding fluid, propelling radicals into the bulk solution (Fig. 3c). The propelled radicals can initiate further chemical reactions. Under an appropriate acoustic intensity, cavitation bubble implosion results in emission of a short flash of light (50-500 ps), a phenomenon known as sonoluminescence.[83, 84] Light emission with wavelengths between 200-800 nm suggests a high local temperature of approximately 5,000 K at the cavitation site.[85] Suslick et al. investigated the sonoluminescence of a single bubble and reported that the energy released during cavitation bubble implosion is strong enough to induce chemical reactions.[80, 84] Reactions induced by this energy release include the homolytic dissociation of water to H• and •OH radicals (water sonolysis) and the formation of NO_2^- by N_2 dissociation and its subsequent oxidation by O_2 or H_2O.[78] The size (3-200 μm), lifetime (0.4 μs at 500 Hz, 10 μs at 20 kHz), and stability of cavitation bubbles depend on

various factors, including the acoustic frequency, the acoustic intensity, physicochemical properties of the liquid, the presence of a dissolved gas, and the bulk solution temperature and pressure.[82, 86]

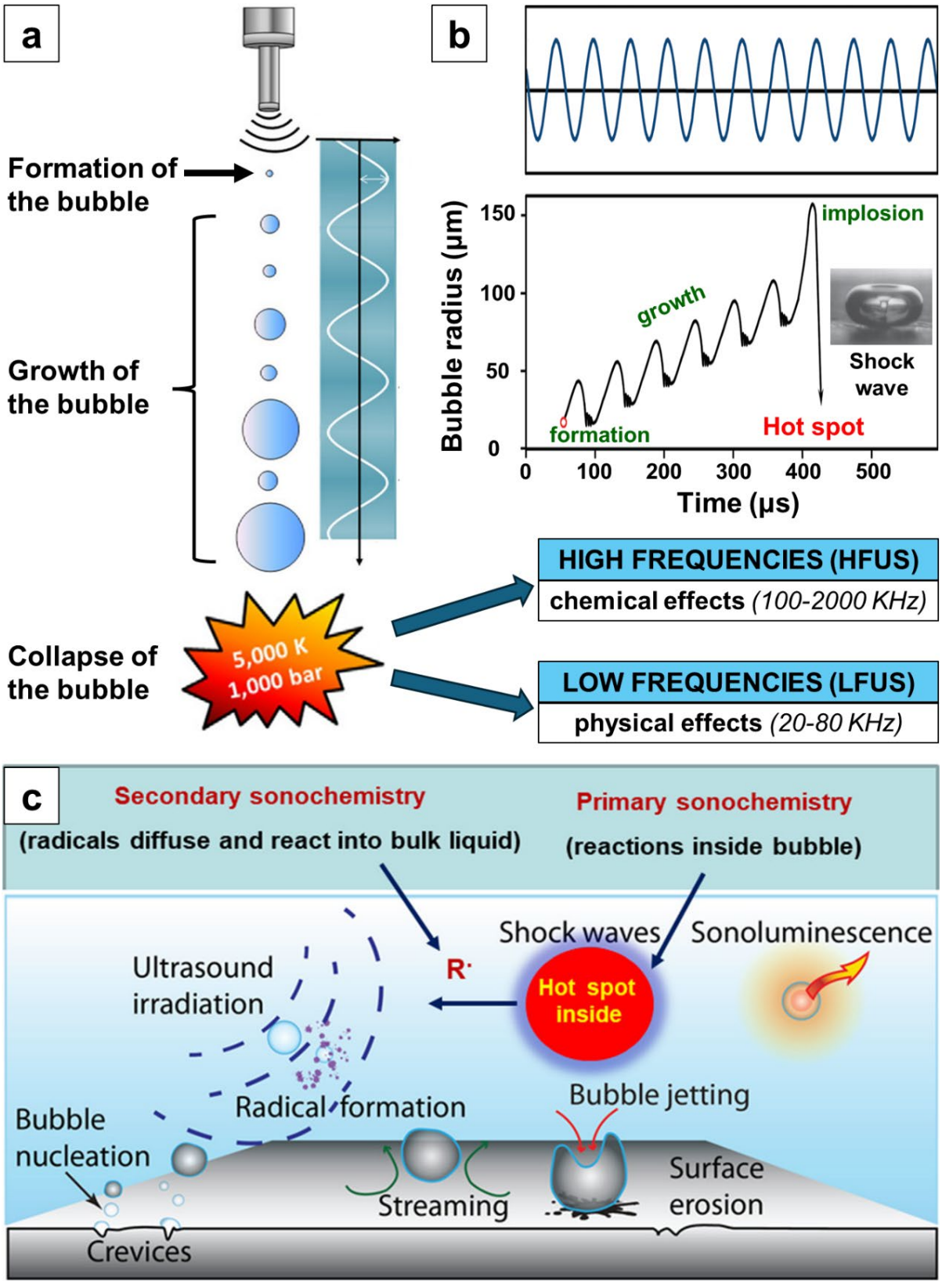

Figure 3. (a) Cavitation events under ultrasonic irradiation, reproduced with permission from Chatel et al.[87] Copyright 2016, Elsevier. (b) The change of bubble size during the cavitation, reproduced with permission from Xu et al.[77] Copyright 2013, Royal Society of Chemistry. (c) Chemical and physical effects induced by acoustic cavitation, reproduced from an open access publication.[88]

The radical composition inside a cavitation bubble depends on the gaseous atmosphere, the identity of the surrounding liquid, and the presence of dissolved solutes.[78, 79] For instance, high vapor pressure liquids or solutes can diffuse inside of the cavitation bubble where they are instantaneously pyrolyzed. These pyrolysis reactions form additional radicals and co-products from radical recombination. Once these cavitation bubbles implode, the radicals are propelled into the solution where they can recombine (e.g. forming H_2O_2 and H_2, during water sonolysis) or oxidise the solutes, opening an unconventional method to synthesise a wide range of chemicals.[88] The chemical effect induced by sonochemistry can be significantly leveraged when it is controlled using heterogeneous catalysts. In some cases, the integration of sonochemical reactions with heterogeneous catalysts resulted in a reactivity increase by nearly a millionfold.[84] The next section summarises the general application areas of sonochemistry without the assistance of a catalyst. Section 3 is dedicated to more detailed applications of sonocatalysis, where the sonochemical reactions are facilitated by the presence of solid catalysts.

2.4. Application areas of Sonochemistry

According to the "Twelve principles of Green Chemistry" outlined by Anastas and Warner,[66] sonochemical applications are generally considered to be environmental friendly and sustainable. Some of the main advantages of sonochemistry are its potential for tuning selectivity, enhancing process efficiency, avoiding the use of toxic chemicals or reagents, reducing waste, and consuming renewable energy resources such as electricity from solar energy. All of these features make sonochemistry a safe and energy efficient discipline. Chatel et al. analysed the relationships between sonochemistry and green engineering[89] based on the "Twelve principles of Green Engineering" of Anastas and Zimmerman,[90] focusing on different chemical processes and their energy efficiencies. Recently, Sivakumar et al. introduced the concept of "7E"[91] to rationalise the seven different aspects of efficiency when analysing the use of sonochemistry in industries. These seven categories include process efficiency, product and scale-up efficiency, environmental efficiency, productivity efficiency, energy efficiency, cost efficiency, and sustainability efficiency (Figure 4a).

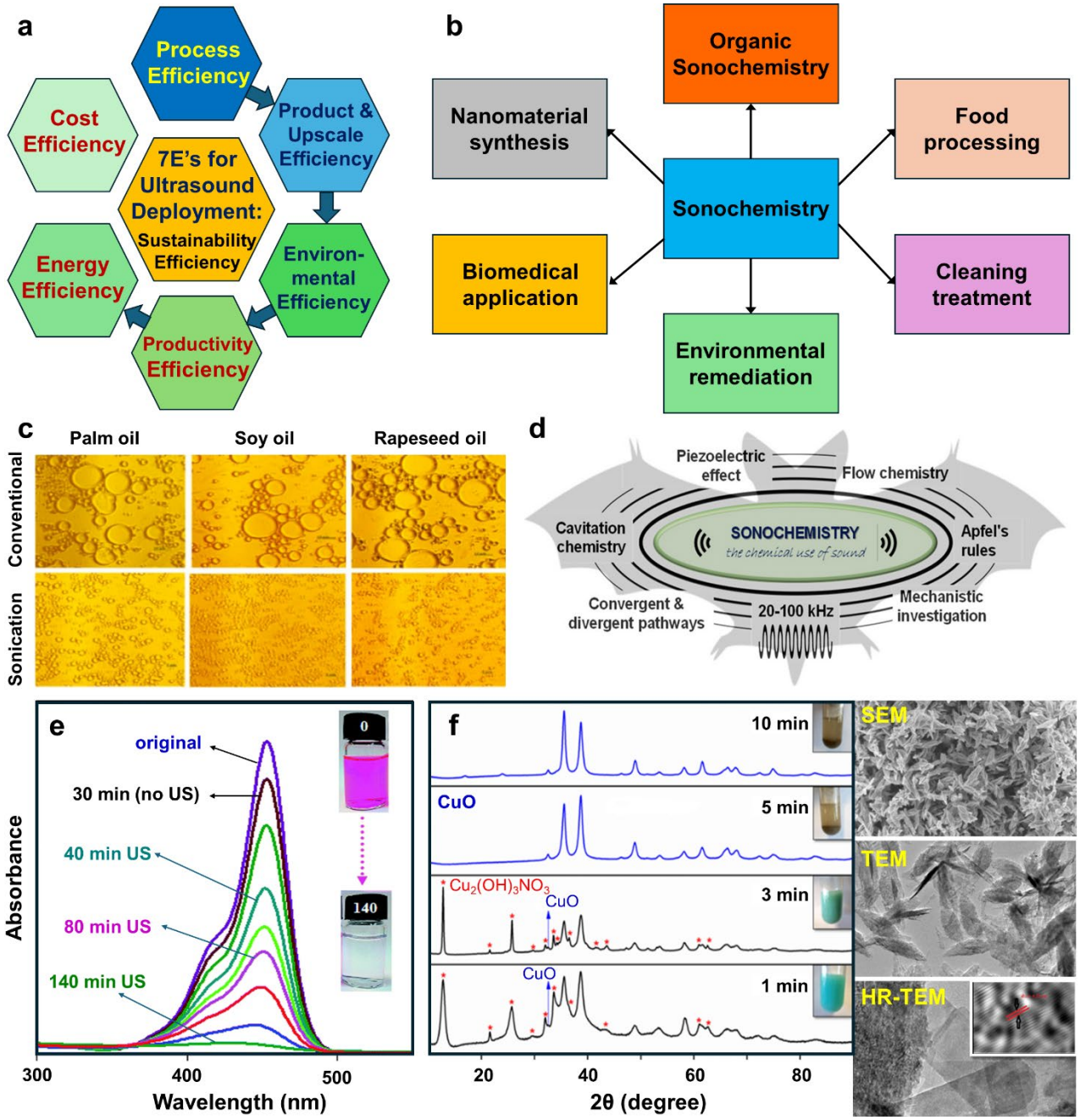

Figure 4. (a) The concept of "7E" for evaluating ultrasonic efficiency in processing systems. (b) General application areas of sonochemistry. (c) Optical microscopy images of oil-in-water emulsions obtained via sonication and conventional methods (high-shear homogenization), reproduced with permission from Taha et al.[92] Copyright 2018, Elsevier. (d) The potentiality of sonochemistry in synthetic organic chemistry, reproduced from an open access publication.[88] (e) UV-vis absorption spectra of the sonodegradation process of Rhodamin B (RhB as a function of irradiation time, reproduced from an open access publication.[93] (f) XRD patterns showing the structural changes in CuO sonocatalysts at different ultrasonic irradiation times, reproduced with permission from Amaniampong et al.[67] Copyright 2018, Royal Society of Chemistry.

Sonochemistry is used in many diverse areas of applications, including cleaning treatments, food and diary sonoprocessing, organic sonochemistry, environmental remediation, biomedical applications, and nanomaterials synthesis (Figure 4b). These applications leverage both the physical and chemical effects of sonochemistry. Physical effects induced primary from LFUS are widely

used in cleaning and food processing. Although these processes are sometimes categorised as "*false sonochemistry applications*",[94] they are driven by cavitation events which are at the core of sonochemistry and utilise some of their chemical effects[95]. In cleaning applications, liquid jet and shockwave effects cause structural changes, such as material fragmentation, ductile material deformation, and the removal of surface contamination.[30] Sonochemical cleaning is more efficient than conventional methods, such as water washing, mechanical abrasion, UV treatments, and aqueous chemical disinfection. This enhanced efficiency comes from two main advantages supplied by ultrasound: (i) improved mass transport and (ii) localised mechanical shear force at the treated surface of the material, which both help to loosen the adhesion between the contaminated particles on the surface.[96, 97] Important operational parameters need to be optimised to obtain the best performance, including ultrasonic power, frequency, and temperature of the ultrasonic irradiation. Recently, mathematical models have been proposed to predict how the cleaning efficiency will be translated on an industrial scale.[98-100] Despite the promising results achieved at the laboratory scale, the application of ultrasound-assisted cleaning at an industrial scale still remains a significant challenge, requiring more technological development before it becomes economically feasible.

The strong physical effects generated from cavitation induced by LFUS have also been used in many food processes and in the dairy industry,[101]. The main driving force for ultrasound-induced extraction in food applications is the generation of micro-jets during asymmetrical cavitation near the solvent and cell tissue interface, disrupting the cell walls and enhancing the transport of solutes into solvent.[102] This phenomenon facilitates the extraction of specific compounds from natural products with higher yields and shorter times at ambient temperatures, avoiding the use of a large amount of solvent and heating in conventional methods. Some successful applications of sono-extraction have been reported for the collection of polyphenols from an orange peel[103] and from purple corn pericarp,[104] β-carotene from fresh carrots,[105] pectin from grapefruit[106] and from a pomegranate peel,[107] C-phycocyanin from *Spirulina platensis,*[108] caffeine from green coffee beans,[109] and other high value-added products, such as antioxidant compounds, anthocyanins, chlorophyll, and flavonoids.[110-113] In emulsification and de-emulsification processes, high shear

forces, intense shock waves and micro-jets generated by cavitation at the boundary between two immiscible liquid phases promote the disruption of droplets into the dispersion medium, facilitating the formation of stable 10-100 nm nanoemulsion droplets. Figure 4c shows an example of oil-in-water nanoemulsions produced using ultrasound-assisted processes. Ultrasound significantly improves the quality and homogeneity of the nanoemulsions over the conventional method.[92] Nanoemulsions have broad applications in food, cosmetic, and pharmaceutical industries due to their high bioavailability, low turbidity, and low polydispersity and have been efficiently produced from the ultrasonic emulsification and de-emulsification.[114-120] However, technical challenges in scaling up the processes are currently hindering their application at an industrial scale.

The application of ultrasound in cleaning, extraction, and emulsion described above predominantly uses the physical effects of cavitation and does not take advantage of its full chemical potential. The chemical effects of sonochemistry are much more significant in other applications, including in organic synthesis (called organic sonochemistry), water remediation, nanomaterials synthesis, and in medical applications (Figure 4b). Loomis, Wood, and Richards originally reported the role of sonochemistry in organic synthesis in 1927 (Fig. 2a), thus marking the birth of sonochemistry. However, sonochemistry only started to receive significant attention from organic chemists only after the 1950s, when better ultrasound generators were available. There are many recent examples of ultrasound's success in producing chemicals with higher yield and selectivity than conventional synthesis schemes in the literature.[121-123]

In polymer synthesis, which is a specific area of organic synthesis, sonochemistry contributed to facilitating polymerization with a higher yield and superior quality.[43] The frequency range generally applied to organic sonochemistry is from 20-100 kHz (Fig. 4d). For example, Jayarajan et al. observed that the selective substitution reaction at the meta position of the arenes ring could not occur without sonication, however, in an ultrasonic bath with a frequency of 37 kHz (Figure 5a) they were able to achieve a yield of 98%.[124] The use of higher frequency ultrasound is not as common in organic sonochemistry, but it usually results in unprecedentedly high activity.[44, 68, 74] Both the chemical and physical effects of sonochemistry play an important role in facilitating

organic chemistry reactions. Physical effects enhance mass transfer, while chemical effects accelerate the activity and selectivity of the reactions.

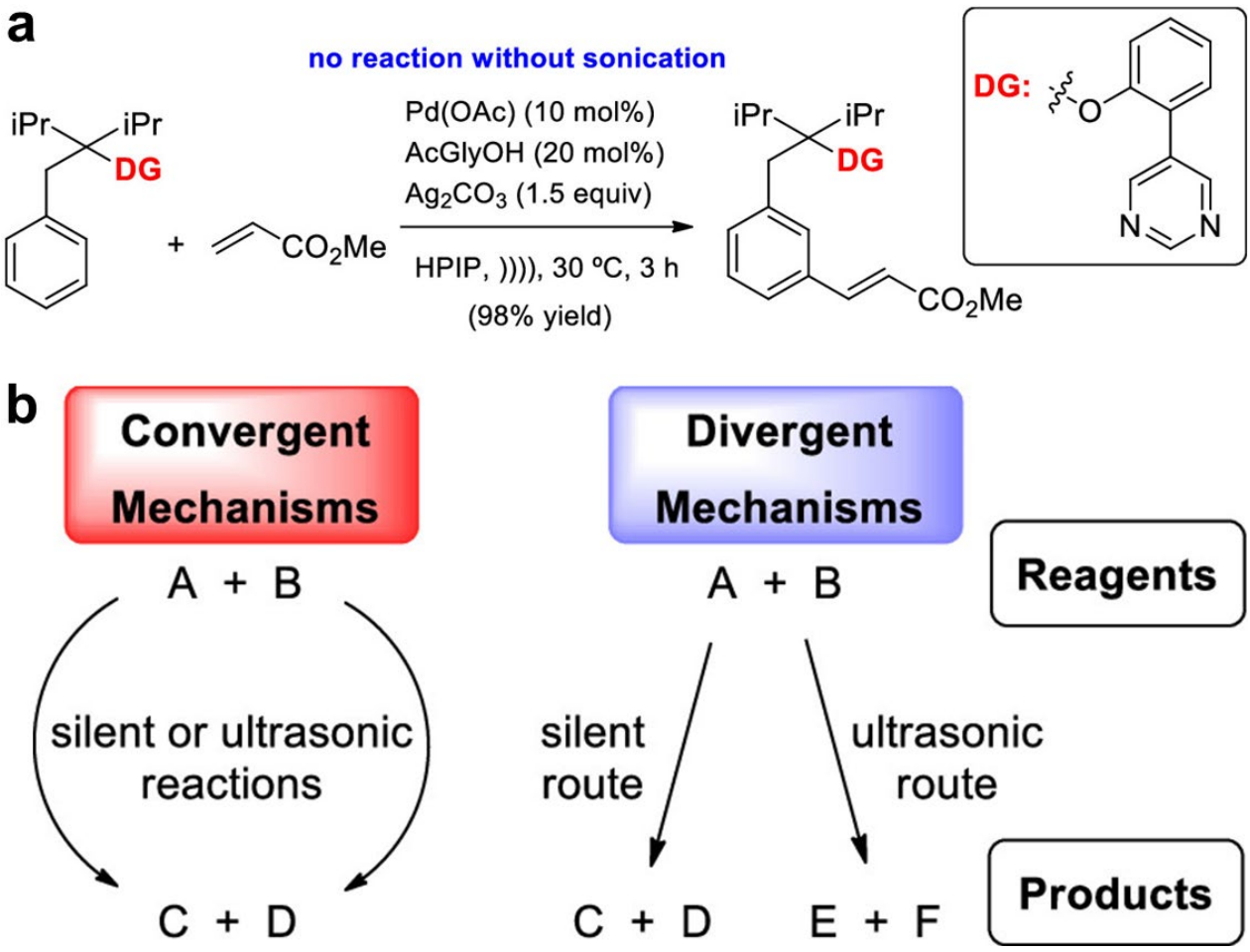

Figure 5. (a) Direct and selective meta-C−H substitution of arenes mediated by ultrasound, reproduced with permission from Jayarajan et al.[124] Copyright 2020, John Wiley and Sons. (b) Classification of organic sonochemical reactions from a mechanistic perspective, reproduced from an open access publication.[88]

In the early days of sonochemistry, Luche et al.[125] classified organic sonochemistry into three classes based which effect was dominant: class 1 was driven by the free radicals generated by cavitation in homogeneous reactions, class 2 was driven by mechanical effects in heterogeneous media, and class 3 combined the features both classes 1 and 2, while also involving the transfer of a single electron in a key step. Among the three classes, class 1 and class 3 were considered to be "*true sonochemistry*", while class 2 was classified as "*false sonochemistry*". On the other hand, modern sonochemistry categorises organic sonochemical reactions into two categories, convergent and divergent, according to a mechanistic point of view (Figure 5b).[88] Organic sonochemistry follows the Apfel rules, which state that the acoustic parameters and calibration of ultrasonic devices

need to be designed appropriately to ensure the accuracy and reproducibility of experimental results (Fig. 4d).[88, 126] The integration of recent technological innovations with organic sonochemical techniques, such as piezo-redox chemistry,[127-131] flow-chemistry[132-139] and automation chemistry[140-145] demonstrates the high potential impact of organic sonochemistry in synthetic and nonsynthetic applications under eco-friendly conditions.

The chemical effects of sonochemistry are even more pronounced in environmental remediation applications, owing to the highly reactive oxygen species (ROS) generated by cavitation (e.g., •OH, $•O_2$, and •OOH). Thus, environmental remediation via sonochemistry is classified as an advanced oxidation process (AOP).[146, 147] Because of its use of relatively few chemicals and operation under ambient conditions, environmental sonochemical remediation is considered to be a "green process" and is extensively applied to remove both inorganic or organic pollutants in wastewater treatment[147-149] and in soil,[150-152] sludge[153-155] and sediment remediation.[150] Volatile organic pollutions can be pyrolyzed inside cavitation bubbles due to the extremely reactive environment present inside the bubble. In addition, oxidative degradation of these organic compounds can occur at the bubble/liquid boundary, where radicals are formed simultaneously with the formation of the cavitation bubble, or in the bulk solution where active radicals are released after bubble collapse.

Sonochemical remediation has also been successfully used to eliminate a wide range of hazardous pollutants, including polycyclic aromatic hydrocarbons, pharmaceuticals, pesticides, fungicides, dyes, and pigments, with high efficiency.[146-148, 156-158] For instance, Andani et al. reported 96% efficiency for Rhodamin B degradation using sonotreatment in an ultrasonic bath with a frequency of 37 kHz (Fig. 4e).[93] This efficiency was 12-fold higher than that of a conventional process without the added benefits of sonochemistry. Important parameters for efficient sonochemical treatment are the frequency, the power of the ultrasonic waves, and the irradiation time. Ultrasound with higher frequencies (200 to 600 kHz) are typically applied for wastewater treatment due to the need for a high density of ROS, whereas lower frequencies (20-40 kHz) are often used in sludge and soil remediation.[150, 159] One challenge of sonochemical treatment is the fast quenching of active oxygen species in the bulk solution (only 10% of active radicals are present in

the bulk solution). Therefore, sonochemistry has the potential to be combined with another AOP processes, such as Fenton oxidation,[160] ozonation[150, 156] and coagulation, to enhance the wastewater treatment.[161] We note that sono-elimination of hazardous compounds might not always result in their complete degradation to H_2O and CO_2, and therefore it is important to carefully track the identity of by-products formed in order to ensure that there is no secondary environmental toxicity.[79, 162] To date, most sonochemical treatments for environmental remediation are developed at laboratory scale for a simulated wastewater composition, and is not yet feasible for commercial scale.[163] Efforts are being made in this field to enhance the technology and economic feasibility of sonotreatment processes at a larger scale. These efforts include designing more effective reactors, developing continuous processes, and optimising their energy consumption.[79]

Sonochemistry also shows promising biomedical applications in eliminating diseases as well in drug delivery for cancer treatment. In this context, sonochemistry can be applied to improve the efficiency of current cancer treatment methods, which are often expensive, time consuming, and lack selectively in targeting cancer cells.[164] Exogenous medical microbubbles generated during sonochemical cavitation facilitate the delivery of cancer treating drugs to affected cells by stabilising the plasma concentration within the therapeutic range.[165-167] Due to its high accuracy, high specificity, and non-invasive nature, sonochemistry has been used as a therapy for curing brain tumours,[162] xenograft tumours,[168] breast cancer cells,[169] melanoma cancer cells,[170] and head and neck cancer cells.[171] With its ability to stabilise nanoemulsions, sonochemistry is also used in a wide range of drug delivery applications, including topical, ocular, oral, and intravenous methods.[119, 167, 172, 173] In these applications, high frequencies are usually applied (500kHz-1MHz). Much higher efficiency has been reported for ultrasound-assisted drug deliveries.[174] Recently, a combination of sonochemistry and nanostructured catalysts, called sonodynamic therapy, has received great interest for its effectiveness in treating cancer.[175-177] The presence of nanostructured catalysts accelerates and enhances the formation of highly active oxidative agents, which can selectively destroy cancer cells without inducing side effects,[170, 178] demonstrating the potential of using sonochemistry in cancer treatments.

One particularly useful application of sonochemistry is nanomaterials synthesis (including metal oxides, nanoparticles, core-shell structures, metal alloys, and 2D materials),[179-184] which benefits from the corporation of both the physical and chemical effects of sonochemical cavitation events. Nanomaterials play an important role in biomedicine, catalysis, environmental sciences and energy storage.[185-189] The exposed facet,[190, 191] particle size,[192, 193] and morphology[194] of nanomaterials are crucial to their properties. Controlling these structural features with conventional methods is challenging at nanoscale and usually requires rigorous conditions (high temperature), hazardous reagents, solvents, and surfactants, as well as long preparation times. Advantages of sonochemical synthesis are the short synthesis time, use of ambient conditions (room temperature) and environmentally friendly reactants, and a lack of template or surfactant, making it a "green chemical synthesis*"* of nanomaterials. One example of sonochemical synthesis is presented in Fig. 4f for the preparation of CuO nanoleaves.[67] The nanostructured CuO material was obtained after 5 minutes of sonication synthesis time at 25 ºC, resulting in a highly crystalline and uniform 2D morphological structure. By contrast, conventional methods that utilise surfactants and high calcination temperatures (>400 °C) in a time-consuming and energy expensive synthesis result in a much lower quality material. The catalyst prepared via sonochemistry also exhibited much higher stability in the conversion of glycerol than the catalyst prepared through conventional methods.[67]

Physical effects from cavitation events, such as microstreaming, high-speed microjets, and high-intensity shockwaves, contribute to enhanced heat and mass transfer during the synthesis of nanomaterials, resulting in fine control over the material's morphology. In addition, due to an increase in collision probability caused by transient cavitation and the fast-cooling rate of sonochemical processes (~10^{10} K/s), the growth of large particles is inhibited, resulting in the formation of small and highly uniform particle sizes with large specific surface area and high porosity. Chemical effects of sonochemistry also help to control the structure of the synthesised nanomaterials. Primary sonochemistry activates the initial reagents as they are incorporated inside a cavitation bubble leading to the production of precursors for nanoparticle nucleation. Secondary sonochemistry releases a large quantity of active radicals into the bulk solution upon cavitation

bubble implosion. These radicals attach to the nuclei of the nanoparticles, altering the surface energy and serving as structural template to control the exposed facet and morphology during the growth of nanomaterials. Key parameters that need to be carefully controlled in order to achieve the desired properties of the synthesised materials are the ultrasonic frequency, power, sonication time, and ultrasonic activation mode. Usually, low frequency ultrasound (20-100 kHz) with a high intensity is employed in nanomaterials synthesis. Many materials, including metals, metal oxides, sulphides, alloys, composites, and amorphous materials, have been synthesised using this technique. This illustrates the power and great potential of sonochemistry as a process intensification technique in materials science. Although sonochemical nanomaterial synthesis is still not ready for large scale applications, it is expected to play an increasingly significant role in accelerating the production of next generation engineered materials.

3. Sonocatalysis.

3.1. What is Sonocatalysis?

Sonochemical reactions can be classified into three types according to the nature of cavitation: homogeneous sonochemistry, heterogeneous sonochemistry, and sonocatalysis, which represents the intersection of the two (Figure 6). In homogeneous sonochemistry, cavitation events occur in the liquid phase, generating active radicals that facilitate chemical reactions. Therefore, the key features of homogeneous sonochemistry are the chemical effects occurring in the liquid phase. In heterogeneous sonochemistry, the cavitation events occur in immiscible liquid-liquid or solid-liquid systems. The cavitation collapse generates shockwaves and microjets that enhance mass transport and accelerate chemical reactions. Sonocatalysis is a special application area where both the chemical and physical effects of ultrasound are leveraged to accelerate reactions in heterogeneous systems. In sonocatalysis, either phase of a liquid-liquid system, or the solid phase in a solid-liquid system acts as a catalyst to accelerate the chemical reaction occurring in the bulk liquid. The presence of this catalytic phase significantly enhances the rate of the reaction under ultrasonic irradiation, which has the potential to reach a million-fold enhancement in the reaction rate when compared to conventional process using the same catalyst in the absence of ultrasound.

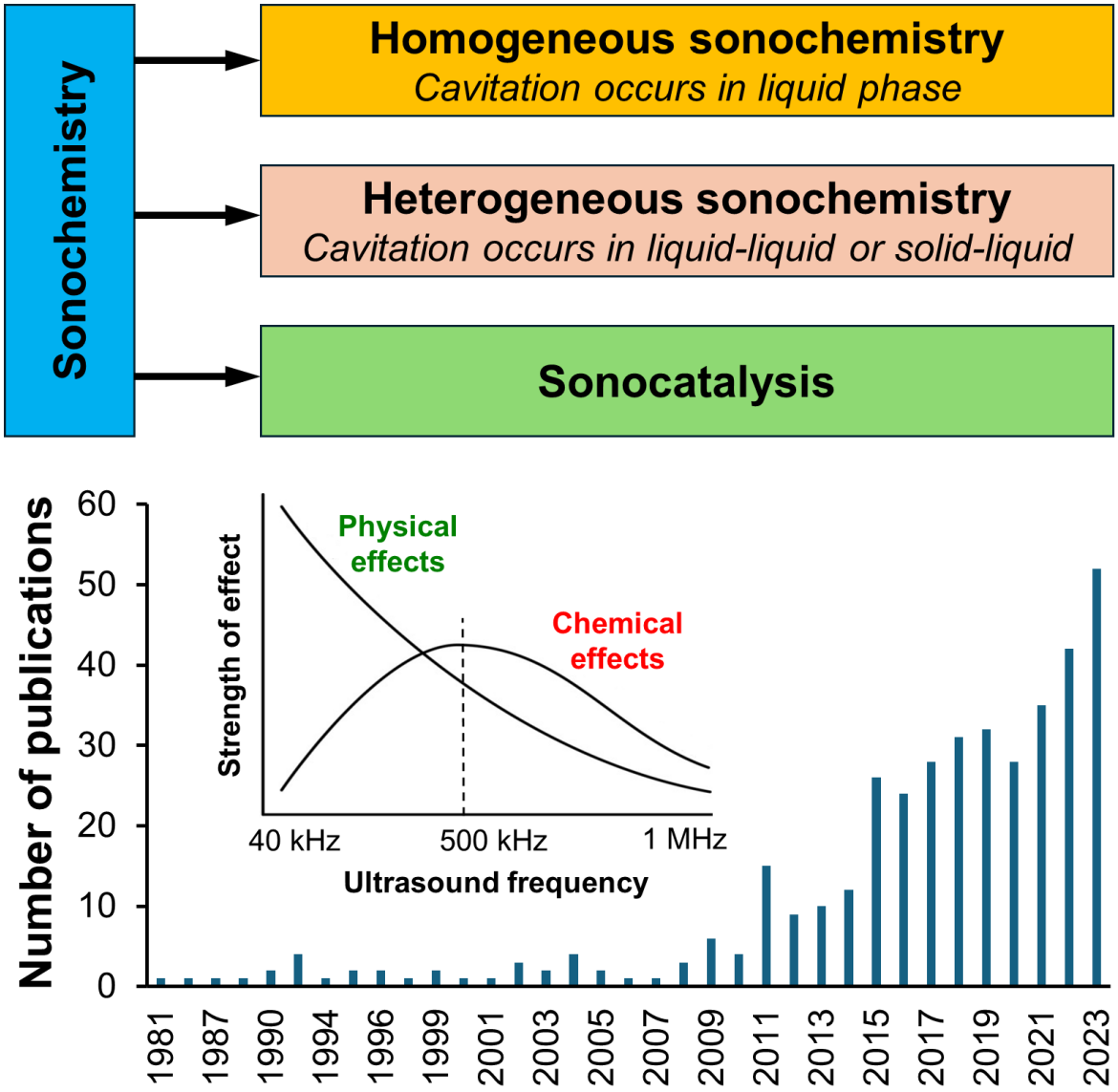

Figure 6. Classification of sonochemical reactions (top) and number of publications with the keyword "sonocatalysis" in different years, from Scopus search, September 2024 (bottom). Insert image shows the variation of the two primary effects that enhance sonochemical reactions (shear force and reactive radical formation) with the applied ultrasound frequency, reproduced with permission from McKenzie et al.[43] Copyright 2019, John Wiley and Sons.

Whether the physical or chemical effects of ultrasound are dominant depends on the operating conditions of the process. The most important parameter in determining the dominant mechanism is the applied frequency of the ultrasound. At the lower frequency range (<100 kHz), physical effects dominate, while radical formation is often negligible (insert figure in Fig. 6). These processes are called low frequency ultrasound (LFUS). In LFUS systems, the physical effects of cavitation, such as mixing, catalyst dispersion, and coke removal, are exploited for improving reaction rates. For example, LFUS has been used to accelerate the iron-catalysed oxidation of glucose by hydrogen peroxide. The formation of radicals increases when higher frequency ultrasound is used, but radical production decreases beyond a threshold value (Fig.6). At elevated frequencies, cavitation bubbles

collapse long before reaching their resonant size, thus decreasing the efficiency of active radical production. In addition, at higher frequencies, the energy supplied by ultrasonic irradiation is predominantly transformed into kinetic energy for molecular motion/vibration, resulting in the suppression of chemical effects. Consequently, the range from 200-500 kHz, called high frequency ultrasound (HFUS) is considered to be the best range for maximising the chemical effects of sonocatalysis. In the presence of nanoparticles, the formation of cavitation bubbles occurs preferentially on the nanoparticle surface via heterogeneous nucleation. In this way, radicals produced inside cavitation bubbles can be transferred to a nano-designed catalytic surface by the high-speed jets generated from the implosion of cavitation bubbles, offering promising tools for better control of the reaction selectivity.

Suslick et al. were the first to introduce the term of sonocatalysis in 1981.[61] In their study of olefin isomerisation under ultrasonic irradiation, they observed that the rate of isomerization of 1-alkenes on organometallic iron carbonyl compounds was 10^5 times higher than that of traditional thermal reactions. Starting from 2015, sonocatalysis witnessed a renaissance in response to the urgent need for the development of new emerging green technologies that could address the United Nations Sustainable Development Goals. Since then, sonocatalysis has steadily received a great deal of attention from the global research community, as evidenced by the continuous upward trend in scientific publications (Fig. 6). In the following sections, we describe in more detail the recent success of sonocatalysis in wastewater treatment, medical therapy and biomass conversion. We focus on analysing the mechanism by which sonocatalysis outperforms conventional approaches in these applications to emphasise its potential in establishing a more sustainable society.

3.2. Sonocatalysis in wastewater treatment

The increasing accumulation of organic contamination in wastewater effluents, including organic dyes, antibiotics, pesticides, and pharmaceutically active compounds, poses a severe threat to the living ecosystem, biodiversity, and human health.[195-198] One of the UN Sustainable Development Goals (SDG) states that ensuring accessibility to “clean and accessible water” will be crucial for the sustainable development of humans by 2030.[185] Therefore, it is an urgent task for the research

community to develop efficient methods to tackle this challenge. Recently, sonocatalytic approaches to wastewater treatment has attracted great interest as a highly effective and green alternative. According to a Scopus search, sonocatalysis for wastewater treatment contributes to more than 70% of total applications of sonocatalysis from 2018 to 2023. Excellent recent reviews in this application can be found by Wang et al.,[199] Soni et al.,[200] Liu et al.,[201] Abdi et al.,[202] and Dhull et al.[203]

There are two mechanisms by which sonocatalysts eliminate organic contaminants in wastewater: (1) direct contaminant degradation by the catalyst under ultrasound and (2) catalyst-enhanced sonolysis, which in turn decomposes contaminants (Figure 7a). Jun et al. demonstrated these two mechanisms in the removal of methylene blue (MB) and acid blue 80 (AB) on the $Ti_3C_2T_x$ MXene catalyst under ultrasonic irradiation.[204] In the first mechanism, enhanced the mass transfer caused by cavitation bubble implosion facilitated the adsorption of methylene blue (MB) on the catalyst surface and significantly increased its degradation activity. While acid blue 80 (AB) could not be degraded directly using $Ti_3C_2T_x$ MXene catalysts under silent conditions (i.e., without ultrasound), the presence of $Ti_3C_2T_x$ MXene catalysts enhanced the rate of water sonolysis, resulting in a higher density of ROS (H_2O_2 and •OH radicals), which in turn caused degradation. In order to make sonocatalysts more efficient in wastewater treatment, they are engineered to have different morphologies that maximise their activity. Ucar fabricated Cu-dopamine nanoflowers that exhibited high specific area and good activity for the degradation of methylene blue.[205] Dastborhan et al. prepared the nanocomposite MoS2/carbon nano tubes in flower-like shapes as an efficient catalyst for the sonocatalytic degradation of hydroxychloroquine (Fig. 7b).[206] Similarly, Saravanakumar et al. produced sonocatalyst microrods of $CoTiO_3/Ti_3C_2T_x$ MXene that had high activity in bisphenol A (BPA) degradation (Fig. 7c).[207] Materials ranging from metal oxides,[203, 208] substrate-supported metal nanoparticles, metal sulphides,[209] metal phosphides, porous organic polymers, metal-organic frameworks (MOF)[202, 210] and MXenes[211] have been broadly developed for sonocatalytic water remediation. Recently the combination of different semiconductor phases with suitable valence band and conduction band potentials to construct a Z-scheme heterostructure is a research “hotspot” in sonocatalysis due to the fact that the presence of conductive channels, broaden the optical

response range and intensify the redox driving force.[212-215] Qiao et al. has managed to prepare the Z-scheme $KTaO_3/FeVO_4/Bi_2O_3$ nanocomposite (Fig. 7d), which showed excellent sonocatalytic activity for the degradation of antibiotic ceftriaxone.[216]

In order to properly evaluate the performance of sonocatalysis, Qiu et al. collected experimental data from the sonocatalytic degradation of several microorganisms in water and plotted the rate constant of sonodegradation with and without the presence of the catalyst, Fig. 7e.[198] The database includes sono-elimination of *Escherichia coli (*E-coli) at 39 kHz and 200W (Study 1),[217] Legionella pneumophila at 36 kHz and 300W (Study 2),[218] E-coli at 36 kHz and 300W (Study 3),[219] and salicylic acid oxidation (Study 4) at 36 kHz and 200W on Al_2O_3 and TiO_2 catalysts. Figure 6e shows that the sonocatalytic activity of Al_2O_3 is at least 10-fold higher than the activity of ultrasound alone, illustrating the need for sonocatalysis. Since Al_2O_3 does not have any catalytic activity for contaminant degradation without ultrasonic irradiation, the enhancement of sonocatalytic contaminant degradation was attributed to the catalyst enhancing cavitation. Figure 6e also shows that the efficiency of TiO_2 is 1.4–3.8 times better than that of Al_2O_3, and this was attributed to the synergistic effect between TiO_2 and ultrasound in generating higher density of ROS (enhanced cavitation by TiO_2) and in inducing the photo-thermal-catalytic effect (enhanced catalytic activity of TiO_2 by sonochemistry).[198] A more quantitative method to show the power of sonocatalysis involves benchmarking sonocatalytic efficiency against the effects of sonolysis, adsorption, and the summation of those two individual effects (adsorption+sonolysis), as in Fig. 7f.[220, 221] In the sonocatalytic degradation of sulfadiazine on a MXene-MOF catalyst, Ranjith et al.[220] measured the rate constant of contaminant removal via catalytic adsorption (in the absence of ultrasound) and via sonolysis only (in ultrasound without catalysts), and via both contaminant removal methods combined. In Figure 7f, the degradation rate coefficient obtained for sonocatalysis far exceeds the result obtained for all other experiments, highlighting the synergy between catalysts that are active under ultrasound and sonolysis. A synergy index (SI), which is computed using the formula in Fig. 7f, is a convenient metric for expressing the synergy of sonocatalysis, which can be used to benchmark the performance of different catalysts for the sono-degradation of the same contaminant.

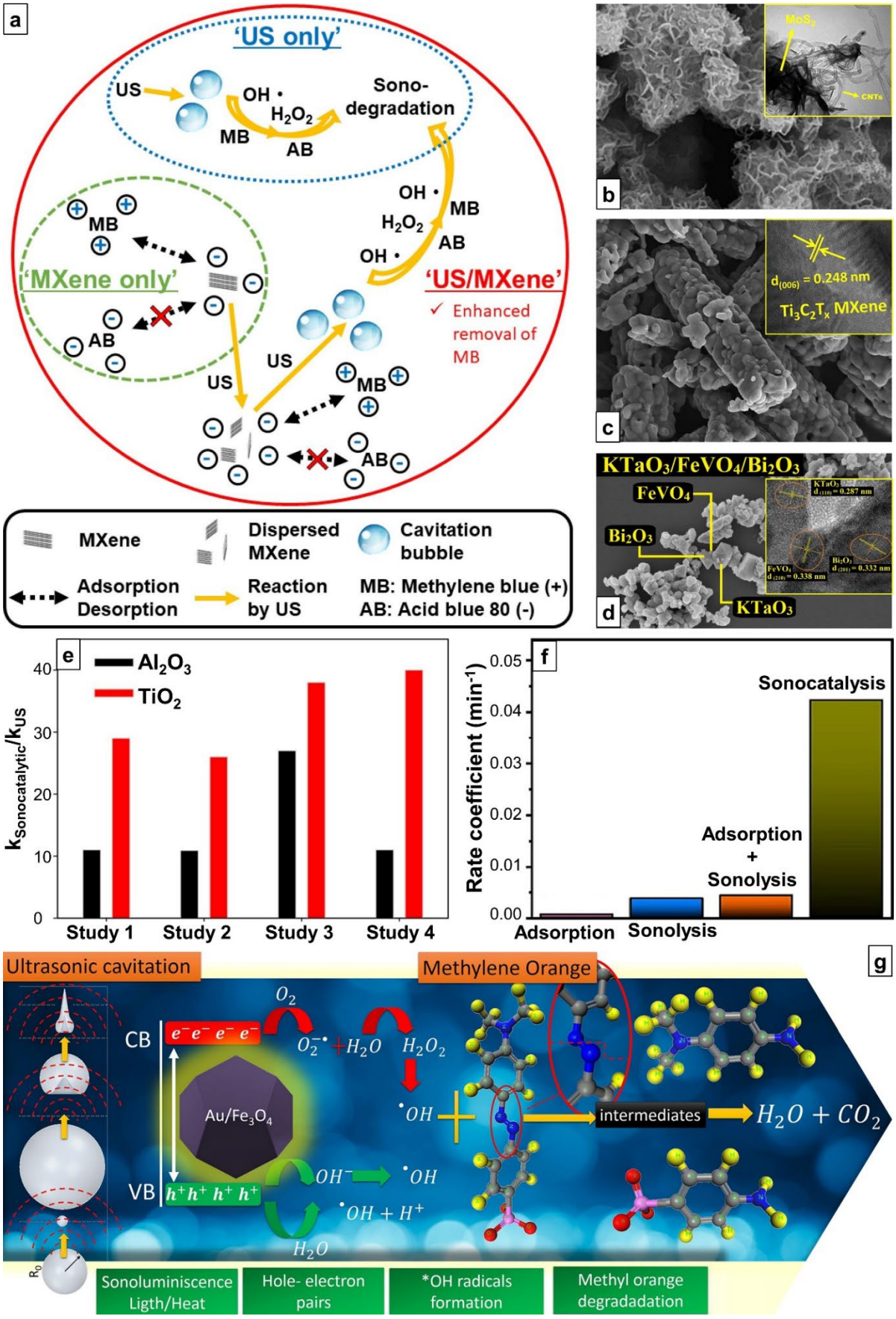

Figure 7. (a) Mechanism for the sonocatalytic removal of organic dyes, reproduced with permission from Jun et al.[204] Copyright 2020, Elsevier. (b) SEM and TEM images of MoS_2/carbon nano tubes (CNT) nanoflower for the sonocatalytic degradation of hydroxychloroquine, reproduced with permission from Dastborhan et al.[206] Copyright 2022, Elsevier. (c) SEM and HR-TEM images of $CoTiO_3$-MXene microrods as sonocatalysts in bisphenol A degradation, reproduced with permission from Saravanakumar et al.[207] Copyright 2021, Elsevier. (d) SEM and HR-TEM images of Z-scheme

$KTaO_3/FeVO_4/Bi_2O_3$ nanocomposite in the sonocatalytic degradation of ceftriaxone sodium antibiotic, reproduced with permission from Qiao et al.[216] Copyright 2019, Elsevier. (e) Enhancement of the sonocatalytic activities compare to the activities in silent conditions for the elimination of E-coli (Study 1), Legionella pneumophila (Study 2), E-coli (Study 3) and salicylic acid oxidation (Study 4) on Al_2O_3 and TiO_2, reproduced with permission from Qiu et al.[198] (f) Synergistic effect in the sonocatalytic degradation of sulfadiazine on MXene-MOF nanocomposite, reproduced with permission from Ranjith et al.[220] Copyright 2018, Elsevier. (g) Sono-degradation mechanism of methyl orange by Au/Fe_3O_4 nanoparticles, reproduced with permission from Ruiz-Baltazar.[222] Copyright 2021, Elsevier.

Finally, efforts have been made to obtain a more detailed understanding of the sonocatalytic mechanism for water treatment via molecular modelling. Ruíz-Baltazar et al.[222] conducted a comprehensive characterization of Au/Fe_3O_4 catalysts and proposed a mechanism for the sonodegradation of methyl orange using computational simulations (Fig. 7g). Their results showed that cavitation bubble implosion generates sufficient light and heat (via sonoluminescence) to create electron-hole pairs in the conduction band (CB) and the valence band (VB) at the interface between Au and Fe_3O_4. These electron-hole pairs were active in facilitating water sonolysis, producing a high density of •OH radicals, which are essential for methyl orange degradation, Fig. 7g. Experimental results showed that an excellent sonocatalytic efficiency of 91.2% was obtained after a short reaction time of 15 min. This detailed mechanistic understanding of sonocatalyst operation is helpful in aiding the design of other sonocatalytic wastewater treatment methods in the future.

3.3. Sonocatalysis in medical therapy

After applications involving sonocatalysis for wastewater treatment, the second largest application of sonocatalysis (~25% according to a Scopus search from 2018 to 2023) is for medical therapy. Sonocatalysts are being applied in cancer therapy, antibacterial therapy, and therapeutic nanomedicine. Previously, sonochemistry was used to enhance the penetration range and drug efficiency in photodynamic therapy, which is a well-developed stimuli-responsive and non-invasive method for tumour treatment.[4, 5] In photodynamic therapy, a photo-responsive drug is activated with photoenergy, releasing active radicals that kill cancer cells with minimal side effects. However, the penetration depth of light in photodynamic therapy is up to 1cm and is therefore only able to access skin and prostate cells. Consequently, photodynamic therapy is not effective to treat cancer cells for major internal organs (e.g., liver, pancreas, kidney) which would require a penetration depth larger

than 7 cm. On the other hand, the penetration depth of radiation therapy is much larger than photodynamic therapy, allowing it to be applied in treating deeper tumour sites. However, the downside is that the strength of the radiation is too strong, causing severe damage on neighbouring normal tissues. The penetration depth of sonotherapy (therapy using ultrasound) is ~10 cm, which is ideal for accessing the major organ tissues without using harmful radiation. Recently, the application of sonocatalysis in medical therapy, called sonodynamic therapy (SDT), has been receiving a lot of attention from researchers, especially in cancer treatment, both as an individual strategy or in cooperation with photodynamic therapy. Cancer is considered a global health challenge, and it is among one of the most common threats to human health. The risk of cancer is intensified due to the fast-changing climate and intensive industrialization that drastically change our living environments. Therefore, the development of sustainable technologies, like sonodynamic therapy, that are highly effective for cancer treatment are vital to the improvement of human health.

Due to the complex reactions occurring inside of cancer cells, the detailed mechanism for the effectiveness of sonocatalytic therapy is not yet fully understood. Despite this, extensive efforts are being made to gain more insight into the processes occurring during catalytic sonotherapy. It is widely proposed that therapy mechanisms including sonocatalysis function via mechanical, chemical, and thermal effects. Mechanical effects, such as microstreaming, microjets, and shockwaves, are produced by acoustic cavitation and act on cell structures, causing necrosis or cell death. Thermal effects result from the release of heat stored inside a bubble during implosion, activating thermal necrosis of the tumour tissues located in proximity to the cavitation bubbles. However, the most impactful factor of sonocatalytic therapy is its chemical effect, stemming from the production of highly active radical species. Reactive oxygen species (ROS) generated during bubble collapse can destroy tumour cells through cell apoptosis. However, the presence of these ROS triggers two subsequent feedback reactions from the tumour microenvironment (TME): hypoxia which suppresses the production of ROS and an over-expressed glutathione (GSH) which consumes the existing ROS, resulting in decreased therapeutic efficacy. These two feedback reactions and the high level of H_2O_2 accumulated from water sonolysis can have the undesired effect

of actually promoting the growth and metastasis of cancer cells. After periods of sufficiently long exposure, this might eventually cause the tumour cells to become drug and immune resistant. Therefore, another important role of the catalyst is to regulate the TME to reduce these risk factors and enhance the efficiency of sonotherapy. Designing sonocatalysts that generate a high density of ROS and are able to tune the TME is vital to the improvement of sonocatalytic therapies.

Liu et al. succeeded in preparing ultrathin-FeOOH-coated MnO_2 nanospheres (denoted as MO@FHO) that were used as bifunctional sonocatalysts that both promoted ROS generation and inhibited the TME.[223] Figure 8a presents the anticancer mechanism of this material. Figure 8b shows the in-vivo experimental efficiency of tumour treatment on mice. MnO_2 acts as the catalytic center, and its catalytic activity is accelerated by the FeOOH phase, jointly producing a high density of ROS, including •OH, $\bullet O_2^-$, and singlet $^1O_2$ species, under ultrasonic irradiation. In addition, the interaction between the MnO_2 core and the FeOOH shell created intrinsic multivalent metal ions at the interfacial zone of MO@FHO that catalysed H_2O_2 decomposition to relieve tumour hypoxia and reduce the GSH (Fig. 8a). In-vitro experiments showed that the ROS yield of MO@FHO under ultrasound was much higher than compared to the control case without the catalyst. The MO@FHO was also able to disrupt the metabolic equilibrium of the cells and regulate the TME. In-vivo tests on mice with MBA-MD-231 breast cancer cell indicated a significant inhibition of tumour growth (Fig. 8b). Alleviation of tumour hypoxia was confirmed by immunostaining assays analysing the indicators HIF-1α and VEGF. This study created a strategy for designing highly effective nano-catalysts for sonotherapy that are active in ROS generation and are capable of regulating the TME.

The light (via sonoluminescence), heat (via solvent pyrolysis) and piezoelectric potential (via piezoelectric effect) generated during cavitation events also enhance the activity of sonocatalysts. In particular, bubble collapse has the ability to modify the electronic properties of the catalytic material by changing its bandgap and/or improving the separation of electron–hole pairs, increasing the production of ROS. As a result of these effects, the sonocatalytic nanoagents (SCNs) used in therapeutic applications are also called “sonosensitisers”. Advanced SCNs with high therapy efficiency are constructed from a wide range of materials, including organic materials (e.g.,

phenothiazine compounds, fluoroquinolone antibiotics, porphyrins, and xanthenes), inorganic materials (e.g., noble metal nanoparticles, transition metal oxides, sulphides, carbon-based nanomaterials, quantum dots, piezoelectric materials, and Z-scheme and S-scheme heterostructures), and organic/inorganic hybrid nanoparticles (e.g., metal organic frameworks (MOFs), zeolitic imidazolate framework (ZIFs), and covalent organic frameworks (COFs)). The efficiency of sonocatalytic nanoagents (SCN) in generating ROS and their effect in TME regulation can be greatly enhanced by combining SDT with other techniques. These techniques incorporating SDT include high-intensity focused ultrasound-based SDT, SDT-assisted sonoporation, SDT-assisted photothermal therapy (SDT-PTT), SDT-assisted chemotherapy (SDT-CDT), SDT-assisted gas therapy, and SDT-assisted photodynamic therapy (SDT-PDT) (Figure 8c).[224] The recent development of novel sonocatalytic nanoagents and DFT-assisted therapy processes are summarised in excellent reviews by Son et al.,[225] Feng et al.[224] and Yang et al. [226]

Among the three types of SCNs shown in Fig. 8c, small organic SCN molecules are traditionally used for sonotherapy. However, disadvantages, such as low stability, weak tumour enrichment abilities, inhomogeneous distribution, and low efficacies in generating ROS, hindering their wider application. In recent years, the self-assembly of organic SCNs with biocompatible components to form nanosystems emerged as a promising method to address the above problems, improving sonotherapy efficiency. Excellent candidates for SDT are hybrid organic/inorganic materials (MOFs, ZIFs and COFs), which are crystalline and porous materials with large surface area, high stability, and tunable electronic features. The morphology of these hybrid organic/inorganic SCNs is of particularly importance for sonotherapy applications since it affects the delivery of the SCN into the tumour cells and the generation of the ROS. Great efforts have been made in literature to control the synthesis of hybrid organic/inorganic SCNs to achieve a desired morphology. Liu et al. developed a facile two-step procedure to synthesise a library of hollow COFs with diverse nanostructural morphologies, including the bowl-like, yolk-shell, nanosphere, nanorods, capsule-like, and flower-like structures (Fig. 8d).[227] Each of these morphologies has its own targeted application corresponding to a particular sonodynamic cancer therapy.[228]

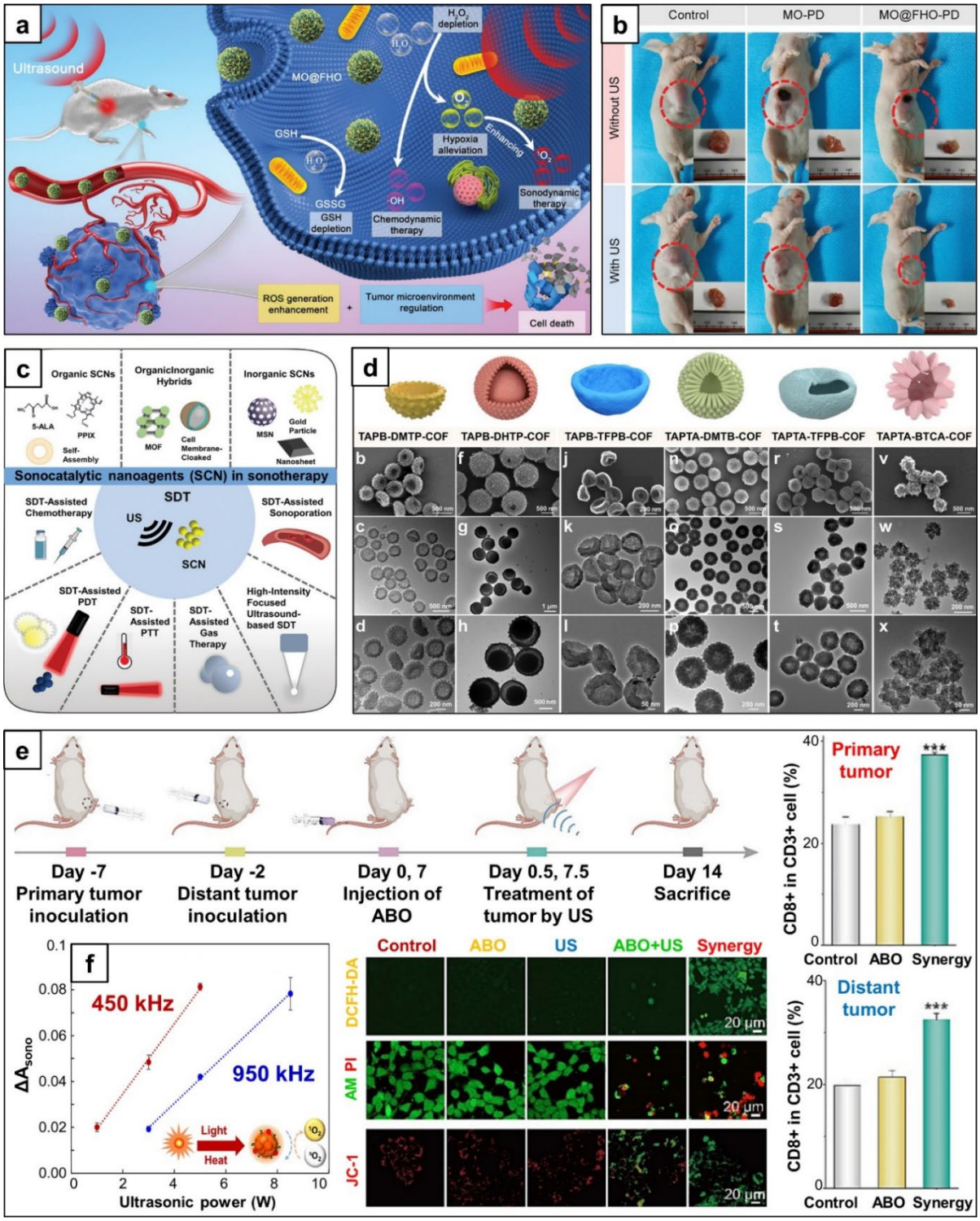

Figure 8. (a) Mechanism of cancer treatment and (b) images of the tumours present in mice during cancer treatment by sonotherapy using MnO_2@FeOOH nanospheres (called MO@FHO), reproduced from an open access publication.[223] (c) Sonocatalyst nanoagents (SCN) and their corresponding sonodynamic therapy (SDT) applications, reproduced with permission from Feng et al.[224] Copyright 2023, John Wiley and Sons. (d) SEM and TEM images of covalent organic frameworks (COF) synthesised with different functional morphologies for sonotherapy , reproduced with permission from Liu et al.[227] Copyright 2023, John Wiley and Sons. (e) In vivo treatment and results of 4T1 tumour-bearing mice on Au-Bi_2O_3 nanoheterojunction sonocatalysts (called ABO): images of DCFH-DA staining, Calcein-AM/PI staining, and JC-1 staining in 4T1 cells; cytometry patterns of maturation dendritic cells (DCs) in the primary and distal tumours, reproduced with permission from Chen et al.[229] Copyright 2024, Elsevier. (f) Sonotherapy efficiencies at different applied ultrasound frequencies and powers, reproduced with permission from Yagi et al.[230] Copyright 2022, American Chemical Society.

Inorganic materials compose one third of SCNs and are the most widely used material in SDT, owing to their versatile compositions, excellent stability, high activity, and selectivity. Usually, inorganic catalysts in SDT are heterostructures built from two solid phases. The activity and electronic properties of these materials can be fine-tuned via doping, alloying, functionalization or via metal/support interactions. This offers great flexibility for fabricating highly efficient catalysts for targeted applications in SDT. Chen et al. prepared nanoflowers of the Au-Bi_2O_3 nanoheterojunction (called ABO) for the therapy of 4T1 tumour cells.[229] The plasmonic resonance effect between metallic Au and semiconductor Bi_2O_3 phases induced the separation of electrons and holes of ABO under ultrasound, promoting ROS generation and enhancing photothermal effects of the Bi_2O_3 phase. Elevated ROS generation subsequently disrupted the redox balance of tumour cells by consuming their intratumoral overexpressed glutathione. Combined, these effects cooperatively induced immunogenic cell death, which was reflected in the in-vitro therapeutic test via a 2',7'-dichlorodihydrofluorescein diacetate (DCFH-DA) probe, calcein acetoxymethyl ester (Calcein-AM)/propidium iodide (PI) staining, and a JC-1 assay in 4T1 cells (Fig. 8e). In-vivo antitumour therapy was also conducted on mice and the combination of ABO + US was responsible for inhibiting the growth of both primary and distant tumours (Fig. 7e), emphasising the efficiency of this material in sonocatalytic therapy treatments.

Applied ultrasonic frequency and power are the most important parameters for sonocatalytic cancer treatment since they greatly influence the generation of ROS, Fig. 8f.[230] There is a need to optimise the ultrasonic frequency to find the conditions that maximise the ROS yield (often at moderate frequency around ~500 kHz) and also the penetration depth, which decreases as a function of increasing frequency.. The best practice is to choose the frequency that corresponds most strongly to the type of tumour cells under treatment. Despite its potential, sonocatalytic therapy is still in an early technological readiness level (TRL) or laboratory stage and has not been clinically tested or approved for cancer treatment. Extensive development in this field is still needed to connect experimental observations with clinical applications. More interdisciplinary studies will be required to fully understand the mechanism underlying sonocatalytic therapy processes. Ultimately, the goal

is to design novel sonodynamic nanoagents with better biocompatibility and higher catalytic efficiency, and to evaluate side effects and long-term toxicity before the scale-up.

3.4. Sonocatalysis in biomass conversion

According to the United Nations, the world population will grow to 9.8 billion by 2050.[231] This population growth will drastically increase the demand for energy, food, and chemicals. Sustainably meeting these demands while protecting our environment has become one of the highest priorities.[232] The progressive incorporation of renewable biomass resources, including carbohydrates, lignin, and polysaccharides, in the chemical industry is a revolutionary transition towards building a circular and sustainable chemical supply chain.[70, 71, 233] This contribution is driven by the fact that biomass is carbon-neutral and that it has a huge capacity to produce a wide range of fuels and chemicals that are essential for human life. However, controlling the selective conversion of the polyfunctional substrates comprising biomass is a grand challenge, and currently limits the potential of biomass transformation into high value-added specialty chemicals, such as bio-based products.

To address this selectivity challenge and facilitate biomass conversion, a new concept of assisted catalysis has emerged, wherein chemical reactions are driven at room temperature by external triggers like electrical potentials,[234] photons,[185, 235, 236] plasma,[234, 237] and ultrasound.[68, 69] Among these driving forces, ultrasound, in particular, is experiencing a renaissance. At high applied frequencies, ultrasound-generated radicals can participate in chemical reactions. Paquin et al. used ultrasound at a frequency of 170 kHz to significantly improve the cellulose oxidation to carboxylic acids.[238] Amaniampong et al. found that the carbohydrate concentration had a strong effect on the mechanism of the radical-driven conversion of biomass substrates (Fig. 9a).[239] The conversion of glucose under 550 kHz ultrasonic irradiation occurred via a pyrolysis-like mechanism at the liquid-bubble interface. Levoglucosan was generated in-situ as the key intermediate species and ultimately led to the formation of alkylpolyglycosides (APGs) as the main products, which have important applications in the food, cosmetics, detergent, and pharmaceutical industries.[74] The key advantage of ultrasound-assisted glucose conversion to APGs is its reaction at 40 °C without the use of

(bio)catalysts as in conventional methods, therefore preventing the degradation of carbohydrates. In contrast, at concentrations lower than 10 wt. %, glucose is oxidised by •OH radicals produced from water sonolysis, resulting in the formation of either gluconic or glucuronic acid under different gas atmospheres.[44] However, controlling the rate and optimising the selectivity of the reaction under high frequency ultrasonic irradiation remain significant technological challenges. Therefore, in the absence of catalysts, the homogeneously generated radicals of high frequency ultrasound (HFUS) are mainly used for the total oxidation of aqueous pollutants.

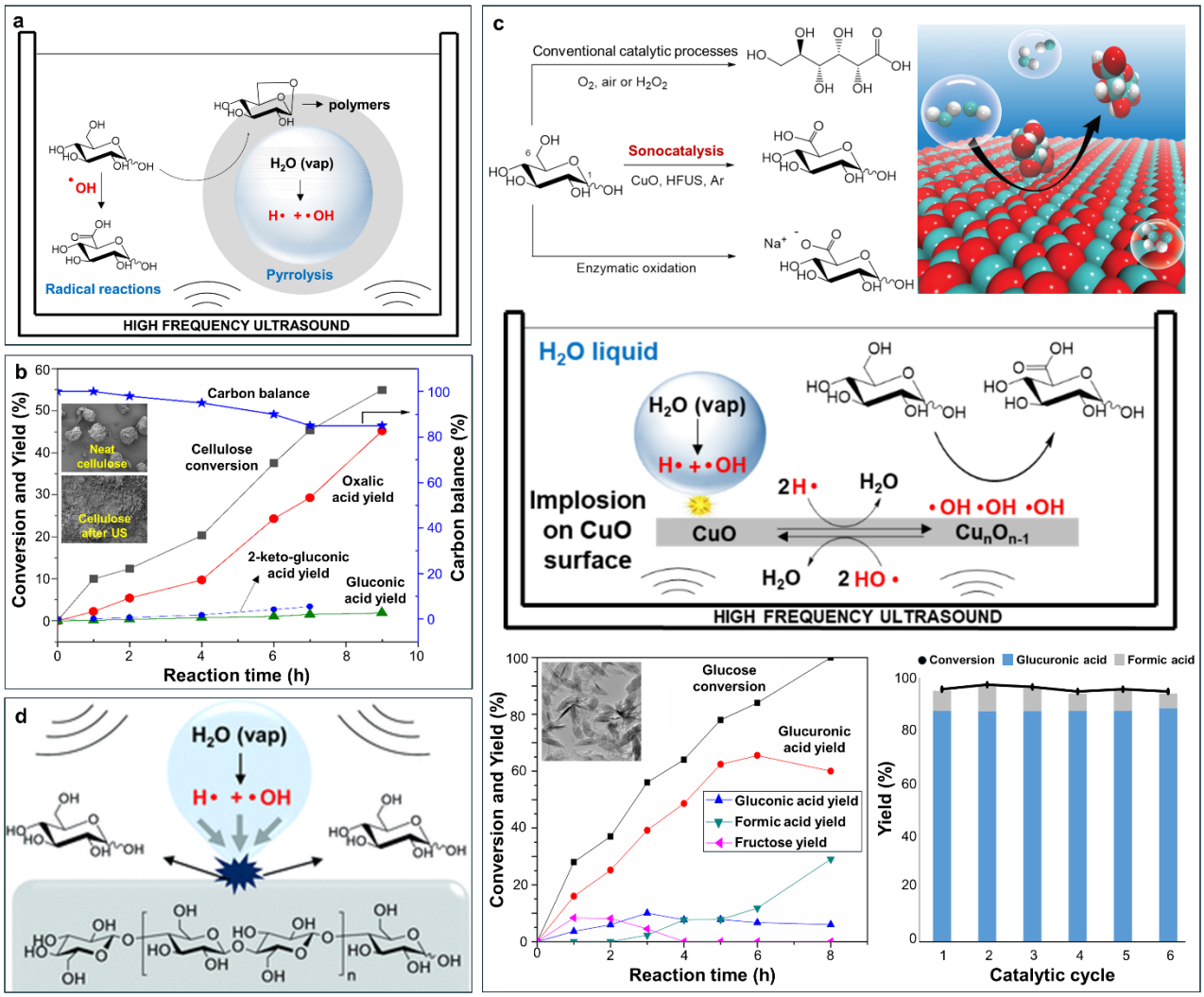

Figure 9. (a) Mechanisms and products of glucose conversion under ultrasonic irradiation depending on the reaction conditions, reproduced with permission from Amaniampong et al.[239] Copyright 2020, Elsevier. (b) Cellulose conversion over Au/Fe_2O_3 catalysts under ultrasonic irradiation, reproduced with permission from Amaniampong et al.[69] Copyright 2022, Royal Society of Chemistry. (c) Synergistic effect between CuO and HFUS in achieving selective glucose oxidation, reproduced with permission from Amaniampong et al.[68] Copyright 2019, American Chemical Society. (d) The complete depolymerization of cellulose to glucose under high frequency ultrasonic irradiation, reproduced from an open access publication.[73]

In the presence of nanoparticles, the formation of cavitation bubbles occurs preferentially on the nanoparticle surface via heterogeneous nucleation. In contrast to symmetrical cavitation bubble implosion in a homogeneous solution, the asymmetrical implosion of cavitation bubbles on a solid surface generates high-speed jets of liquid directed towards the surface. The enhanced mass transfer resulting from the high-speed jets is an effective means to concentrate radicals on the surface of catalysts, which allow them to participate in chemical reactions. So far, this strategy has mostly been applied in LFUS (<20 kHz) systems, where radical formation is negligible and the physical effects of cavitation (e.g., mixing, catalyst dispersion, and coke removal) are dominant for improving reaction rates.[240-243] For instance, Rinsant et al.[244] and Napoly et al.[245] used LFUS (20 kHz) to accelerate the iron-catalyzed oxidation of glucose by hydrogen peroxide. Sarwono et al.[246] and Marullo et al.[247] obtained a high conversion rate when using an ionic liquid with HY zeolite catalysts to convert a wide range of biomass substrates (glucose, fructose, sucrose, cellulose, and raw bamboo biomass) to a promising platform chemical, 5-hydroxymethylfurfural (HMF), under LFUS at 20 kHz. The transformation of biomass-derived platform chemicals (such as HMF, vanillyl alcohol, and glyoxal) to higher value-added chemicals by sonocatalysis was also reported.[242, 248]

Sonocatalysis is also effective for the conversion of lignin which constitutes 15-20% of lignocellulosic biomass.[249-251] Second generation lignocellulosic biomass, consisting of lignin, cellulose, and hemicellulose, is the largest renewable source of carbon.[252] The introduction of these feedstocks in the chemical industry promotes the production of environmentally friendly chemicals and a wide range of sustainable consumer products. Du et al. transformed lignin to bio-oil using a phosphotungstic acid (PTA) sonocatalyst under ultrasonic irradiation at 35 kHz.[253-255] In this study, 94.79% lignin depolymerization was achieved, with bio-oil composing 90.6% of the product yield and the remainder being a small quantity of phenolic monomers. Due to the low quantity of radical species produced in low frequency ultrasound, H_2O_2 typically needs to be added into the reactant mixture to provide a higher density of ROS,[244, 256, 257] which makes the process less “green”. However, if catalysts can be designed so that they generate higher amounts of ROS species, biomass conversion can be facilitated even at LFUS conditions. Recently, Amaniampong et al. carried out

the conversion of cellulose under LFUS on a catalyst composed of Au nanoparticles on a Fe_2O_3 support (Au/Fe_2O_3). They observed a 45% yield of oxalic acid, which is an industrial platform chemical with applications for polymers, leather manufacturing, celluloid production, and the synthesis of pharmaceutical intermediates (Fig. 9b).[69] The presence of ultrasonic energy was vital for fragmenting the cellulose particles (inserts in Fig. 9b), cleaving the β-1,4 glycosidic bonds and simultaneously generating H_2O_2 via cavitation events. The generated H_2O_2 was subsequently activated at interfacial sites of the Au/Fe_2O_3 catalyst to produce reactive surface atomic oxygen species (O*) that were responsible for cellulose oxidation. Most applications of LFUS in sonocatalysis primarily enhance the reaction rates, while controlling the reaction selectivity under LFUS is more challenging.

On the other hand, sonocatalysis using HFUS provides a better alternative for improving both the reaction rates and the reaction selectivity of biomass conversion. This is due to the high density of active radical species produced during rapid cavitation and simultaneously transferred to the catalyst surface. With an appropriate catalyst design, the affinity of the radicals to the catalyst surface can be increased. Tailoring these relative affinities can reduce parasitic reactions (e.g. unselective free radical annihilation) in the bulk solution, offering better control of the selectivity of the reaction towards the formation of a desired product. Recent progress has being made in the field of biomass conversion based on applying sonocatalysis under HFUS.[68, 258]

In 2019, guided by density functional theory (DFT) calculations, Amaniampong et al. reported that using a CuO nanoleaf catalyst under HFUS significantly increased the selectivity of glucose oxidation to glucuronic acid, which is an important pharmaceutical intermediate in the production of drugs for blood coagulation inhibitors, and antioxidants (Figure 9c).[68] Under optimised conditions, a total yield of 88% glucuronic acid was achieved. The catalyst remained highly stable even after 6 catalytic cycles (Fig.9c). This discovery represents a significant advancement since the conventional catalytic oxidation of glucose usually produces gluconic acid, a lower-value product used to make industrial cleaners, via oxidation of the anomeric position.[190, 259] Before this study, the heterogeneously catalyzed selective oxidation of glucose to glucuronic acid (oxidation via the C6

position) was not possible. This work also highlighted the importance of optimising the size of CuO nanoleaves for sonochemistry under HFUS. The efficient transfer of radicals from cavitation bubbles to the catalyst surface required nanostructured CuO with a specific size and morphology.[68] Recently, Bahry et al. reported the highly selective demethylenation of benzyl alcohol, a biomass-derived intermediate compound, on CuO catalysts at 578 kHz and an acoustic power of 0.11 W/mL.[258] The use of HFUS changed the selectivity of the products from benzaldehyde, typical for conventional thermal catalytic reactions, to phenol. Sonocatalysis using HFUS can even be applied for the conversion of raw cellulose, since it was reported that cellulose was selectively depolymerised to glucose by ultrasonic irradiation in water at high ultrasonic frequencies (Figure 9d).[70, 71, 73] These discoveries pave the way toward effectively fine-tuning reaction selectivity in the transformation of biomass-derive feedstocks to high value-added specialty chemicals, enabling access to chemicals that are generally not synthesizable by conventional routes.

3.5. Sonocatalysis in other sustainable chemistry applications.

With the increasing accumulation of CO_2 and greenhouse gas emissions in the atmosphere causing a severe impact on climate, significant efforts are being made in the field of CO_2 reduction, decarbonization, and the development of carbon-free, renewable energy sources to replace fossil fuels. This section introduces recent approaches using sonocatalysis for H_2 production, CO_2 activation, and N_2 fixation. These approaches are typical case studies of how sonocatalysis can contribute to addressing climate change. The activation of CO_2 is the first step for its utilization, which in turn contributes to the reduction of CO_2 levels in the atmosphere.[260, 261] H_2 is a high-density fuel source and its production is considered a promising energy alternative since its combustion only yields water. Therefore, producing H_2 from green methods will help to promote the development of a "hydrogen economy".[262-265] N_2 fixation is a chemical process that activates molecular N_2 and converts it to other useful nitrogenous compounds, like ammonia. Currently, N_2 fixation is a highly energy intensive process that produces a large amount of CO_2 emissions. Therefore, developing greener method of N_2 fixation via sonocatalysis can also help to address climate change.[266, 267]

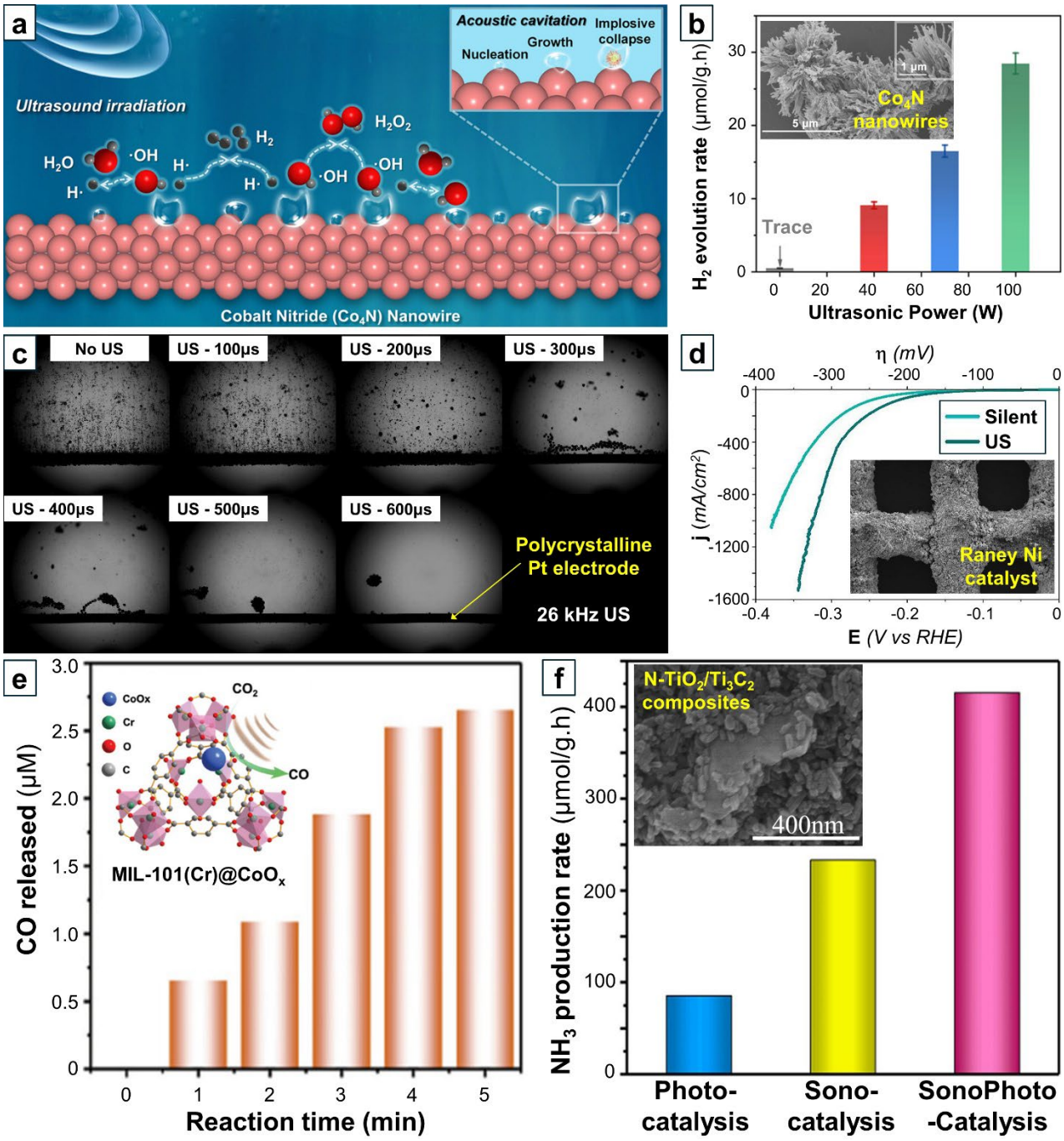

Figure 10. (a) Sonocatalytic mechanism of H_2 production and (b) influence of ultrasonic power on the H_2 production rate in the presence of catalytic Co_4N nanowires, reproduced with permission from Qi et al.[268] Copyright 2023, American Chemical Society. (c) Hydrogen evolution reaction (HER) on a Pt wire with and without ultrasound, reproduced with permission from Pollet et al.[269] Copyright 2020, Elsevier. (d) HER on a Raney-Ni catalyst under silent conditions (without ultrasound) and under ultrasonic irradiation at 408 kHz, reproduced from an open access publication.[270] (e) Amount of CO produced via CO_2 sono-reduction using MIL-101(Cr)@CoO_x catalysts, reproduced with permission from Zhang et al.[271] Copyright 2024, John Wiley and Sons. (f) NH_3 formation rate via sonocatalysis, photocatalysis, and sonophotocatalysis using composite N-TiO_2/Ti_3C_2 catalysts, reproduced with permission from Ding et al.[272] Copyright 2024, Elsevier.

Under the influence of ultrasound, cavitation events occur that result in the production of •H and •OH radicals via water sonolysis. These radicals diffuse into the bulk liquid and partially recombine

to form H_2 and H_2O_2, which can be measured experimentally. While the ROS generated from cavitation events are used as oxidising agents in sonocatalysis, the generation of gaseous hydrogen has received less attention from researchers. However, the production of H_2 during sonochemistry has received more attention since the perspective article by Rashwan et al. was published in 2019[273], coining the term "sono-hydro-gen". The same term was later used in the review article "The Sono-Hydro-Gen process (Ultrasound induced hydrogen production): Challenges and opportunities".[274] These papers highlighted the potential of H_2 production via sonochemical processes in thermochemical, electrochemical, photobiological, and photoelectrochemical technologies.[274, 275] The key reactions for H_2 production in sono-hydro-gen are:

$$H_2O \overset{)))}{\Leftrightarrow} \bullet H + \bullet OH \qquad (1)$$

$$\bullet H + \bullet H \overset{)))}{\Leftrightarrow} H_2 \qquad (2)$$

$$\bullet H + \bullet OH \overset{)))}{\Leftrightarrow} H_2 + \bullet O \qquad (3)$$

wherein reaction (1) is water sonolysis and reactions (2) and (3) are the two main reactions responsible for producing H_2. Merouani et al. measured the chemical kinetics of water sonolysis in combination with bubble dynamics in an acoustic field. They reported that reaction (3) contributed to 99.9% of hydrogen production,[276] while reaction (2) only had a minor contribution and occurred at the interface of the bubble.[277] With sono-hydro-gen, the average hydrogen production rate is only ~0.8 μM/min, which is much lower than the level applicable for commercialization, thus further improvements in performance and efficiency are necessary.[274, 278, 279]

Catalysts can be used to improve the H_2 production in a sono-hydro-gen process. In fact, utilising catalysts to enhance sonocatalysis-mediated hydrogen therapy has been reported recently.[280-282] Yuan et al. used Pt-Bi_2S_3 catalysts to facilitate the hydrogen evolution reaction under ultrasonic irradiation, which subsequently induced mitochondrial dysfunction and disrupted the tumour's antioxidation defence system, leading to cell death.[280] However, the use of sonocatalysis for direct H_2 production is still in its infancy, despites some promising recent studies. For example, Wang et

al. reported that Au/TiO_2 sonocatalysts were highly active for promoting water sonolysis and producing H_2 under untrasonic activation at 40 kHz.[283] Qi et al. carried out sonocatalytic H_2 production on flower-like Co_4N nanowires. The engineered nanostructures with rich nitrogen-vacancies led to stronger adsorption of the •H and •OH radicals generated by cavitation on the surface of the catalysts, facilitating H_2 production (Figure 10a).[268] Without ultrasound, only a trace amount of H_2 was detected. However, ultrasonic irradiation at 40 kHz and 100 W achieved a H_2 production rate of 28.5 μmol/g/h (Fig. 10b).[268] The hydrogen evolution reaction (HER), which produces hydrogen from water, was also enhanced on Pt polycrystalline catalysts. Pollet et al. recorded the HER on a Pt catalyst with a high-speed camera (Fig. 10c) and observed a hydrogen production efficiency increase of 250% under ultrasound at 26 kHz and 200 W.[269] Foroughi et al. also reported that the HER was facilitated on Raney-Ni catalysts under ultrasonic irradiation (at 408 kHz (Fig. 10d).[270] Zhang used $BaTiO_3$ nanofluid catalysts under ultrasound to achieve a high rate of 270 mmol/h/g for H_2 evolution.[284] These studies illustrate the promising role of sonocatalysis in H_2 production.

Activation of CO_2 is the first step in reutilising CO_2 to reduce its atmospheric concentration. The bond energy in CO_2 is extremely stable at ~800 kJ/mol,[285] therefore it only can be activated under high energy input or using extremely active catalysts. Recently, Islam et al. reported that the conversion of CO_2 to hydrocarbons (i.e., the Sabatier reaction) was feasible in the presence of ultrasonic irradiation and this discovery was subsequently named the "Islam-Pollet-Hihn process".[286] Using a sonoreactor coupled with a 488 kHz ultrasonic transducer, Islam et al. obtained the large amount of CO and a mixture of hydrocarbons, including CH_4, C_2H_4 and C_2H_6, as the main products. This study, reported in 2022, demonstrated that sonochemical activation could be used to convert CO_2, but the reaction efficiency was low and left a lot of room for improvement.[286] It is probable that the process could be made more efficient through the introduction of catalysts.

The concept of sonocatalysis in CO_2 activation has already been reported in ultrasound-assisted sonodynamic gas cancer therapy.[271, 287] Zhang et al. synthesised nanocatalysts by integrating CoO_x into metal-organic frameworks (called MIL-101(Cr)@CoO_x) and observed that these catalysts were

active in transforming endogenous CO_2 to CO under ultrasonic irradiation (Figure 10e).[271] The enhancement of CO supply inhibited cancer cell proliferation, resulting in a tumour regression rate of 86.4%,demonstrating the high efficiency of sonodynamic therapy. Despite this promising result, only few recent studies have utilised sonocatalysis to facilitate direct CO_2 activation. Islam et al. reported that Cu catalysts converted CO_2 to CO, CH_4, C_2H_4, HCOOH, and C_2H_5OH under ultrasonication at 24 kHz, whereas these products were absent under silent conditions.[288] Ma et al. investigated the sonocatalytic reduction of CO_2 using $H_2Ti_3O_7$ catalysts.[289] Applying ultrasound at 80 kHz resulted in the reduction of CO_2 to CO with 100% selectivity at a rate of 8.3 μmol/g/h using $H_2Ti_3O_7$ catalysts.[289] The high activity was caused by the synergy between the electronic properties of the catalyst and the sonoluminescence generated by the cavitation events. The $H_2Ti_3O_7$ catalysts also had good stability, with their activity remaining high after four consecutive cycles. The success of this approach is encouraging for future applications using sonocatalysis for CO_2 activation.

Finally, we introduce the perspective of using sonocatalysis in N_2 fixation. N_2 fixation (i.e., activation of the N_2 molecule) is a very important application due to its crucial role in agriculture. Similar to CO_2 activation, the $N \equiv N$ bond is extremely strong with a bond energy of 911 kJ/mol that often requires the activation of a catalyst. Due to the high energy input required, $N \equiv N$ bond activation occurs at elevated temperature (~500^{o}C) and pressure (~300 bar). These severe operating conditions make the process extremely energy intensive, thus contributing negatively to climate change. Several novel processes are being investigated to facilitate the activation of N_2 under ambient conditions, including electrocatalysis and plasma-catalysis. Sonocatalysis is also a promising approach to address this challenge. Recent works combining sonocatalysis and photocatalysis have demonstrated that this approach is feasible. Ding et al. synthesised N-TiO_2/Ti_3C_2 composite sonocatalysts and obtained good activity in converting N_2 to NH_3.[272] The efficiency of sonocatalysis was further synergised with photocatalysis, achieving a NH_3 production rate of 415.6 μmol/h/g under ultrasonic irradiation at 53 kHz (Fig. 10f). Maimaitizi et al. also reported the effectiveness of flower-like Pt/N-MoS_2 microspheres in the sonocatalytic conversion of N_2.[290] Ranjith et al. prepared the hybrid structure by intercalating WS_2 into MXene $Ti_3C_2T_x$

stacked with TiO_2 (called $Ti_3C_2T_x$ /TiO2-WS_2), which had an excellent charge transfer rate and high activity for sonophotocatalytic N_2 fixation.[291] The production rate of NH_3 from N_2 fixation on $Ti_3C_2T_x$/TiO_2-WS_2 reached 526 μmol/g/h at 40 kHz. These studies indicate that the development of sonocatalysts is a promising alternative for N_2 fixation.

4. Harnessing the power of microfluidics and materials nanostructuring in sonocatalysis.

4.1. Current technical hurdles in sonocatalysis: energy efficiency and reaction control.

Despite the promising synergy between heterogeneous catalysis and HFUS, the energy efficiency of current sonocatalytic processes is suboptimal. In sonochemical processes, the energy required to induce cavitation is supplied from electricity, which is converted by the piezoelectric transducer to generate ultrasound. Thus, electrical energy needs to be transformed to mechanical energy before producing the ultrasonic irradiation. Moholkar et al. described the chain of energy conversion from electrical energy to the cavitation energy.[292] This process includes the transformation of electrical energy into mechanical oscillations of the piezoelectric crystal in the transducer. The kinetic energy of the vibration subsequently converts to the acoustic energy of ultrasound waves before finally transforming into cavitation energy, inducing physical and chemical effects upon bubble collapse. Rashwan et al. estimated that approximately 80–90% of electric energy could be transferred to the liquid via acoustic waves,[274] but that the proportion of acoustic waves that release cavitation energy is much smaller. The energy efficiency, η, is expressed by the ratio of the ultrasonic energy, Q_{US}, to the total supplied electric energy, Q_e, in the equation: $\eta = \frac{Q_{US}}{Q_e}$. [293]

The term Q_{US} can be directly measured using calorimetry, and is determined from the rate of temperature increase during the ultrasonic irradiation using the equation: $Q_{US} = C_p M \frac{dT}{dt}$, where C_p, M, and dT/dt are the heat capacity of the solvent, the mass of solvent, and the rate of temperature rise, respectively.[293-295] This method is based on the assumption that mechanical energy in the transducer is fully converted to heat via cavitation and is solely responsible for the temperature change in the solution.[293] From the perspective of sonocatalysis, only the efficiency of the chemical effects resulting from cavitation events, e.g. the formation of ROS, is relevant. In some processes,

only a small amount of total supplied energy is transformed into cavitation activity (<20%) to produce the desired chemical effects.[296, 297] Therefore, other criteria, including sonochemical efficiency (SE),[298-300] cavitation yield[301, 302] and G-value,[303] are used for calibrating the efficiency of sonoreactors. The most popular criterion is the sonochemical efficiency, calculated as the number of •OH radicals produced per unit of supplied energy via the equation: $SE = \frac{n}{Q_e} = \frac{C \times V}{P \times t}$. In the previous equation, *n*, *C*, *V*, *P*, and *t* are the moles of •OH radicals produced, molar concentration of OH radicals, sonoreactor, supplied ultrasonic power, and irradiation time, respectively. The concentration of •OH radicals generated during ultrasonic irradiation can be detected using several methods, including potassium iodide (KI) dosimetry (Weissler method), ferrous sulphate dosimetry (Fricke dosimetry), terephthalic acid dosimetry, and TPPS dosimetry (monitoring the decomposition of porphyrin derivatives).[295, 304]

The sonochemical efficiency is influenced by many factors, including reactor design, applied ultrasonic frequency, power, temperature and choice of solvent.[298, 299, 302, 305-307] The three types of sonoreactors commonly reported in the literature are the emerged ultrasonic horn (Type-A), the bottom plate transducer/horn probe ultrasonic bath (Type-B) and the indirect ultrasonic bath (Type-C) (Figure 11a).[274] Existing sonochemical techniques rely on the inception of cavitation bubbles in the liquid phase under the influence of an acoustic field to induce sonochemical effects. Kim et al. investigated cavitation bubble collapse under ultrasonic radiation at 300 W and showed that the pressure and temperature profiles were not homogeneously distributed within the entire volume of the reactor.[308] Even though pressure oscillations radiate perpendicularly away from the probe tip to the bottom of the reactor, hot spot regions were concentrated around the ultrasound probe (Figure 11b).[274] Similarly, Niazi et al. simulated the ultrasonic activation of an aqueous solution saturated with oil at 25 °C in a glass cylindrical sonoreactor and obtained the formation of discrete active cavitation zones (Figure 11c).[309]

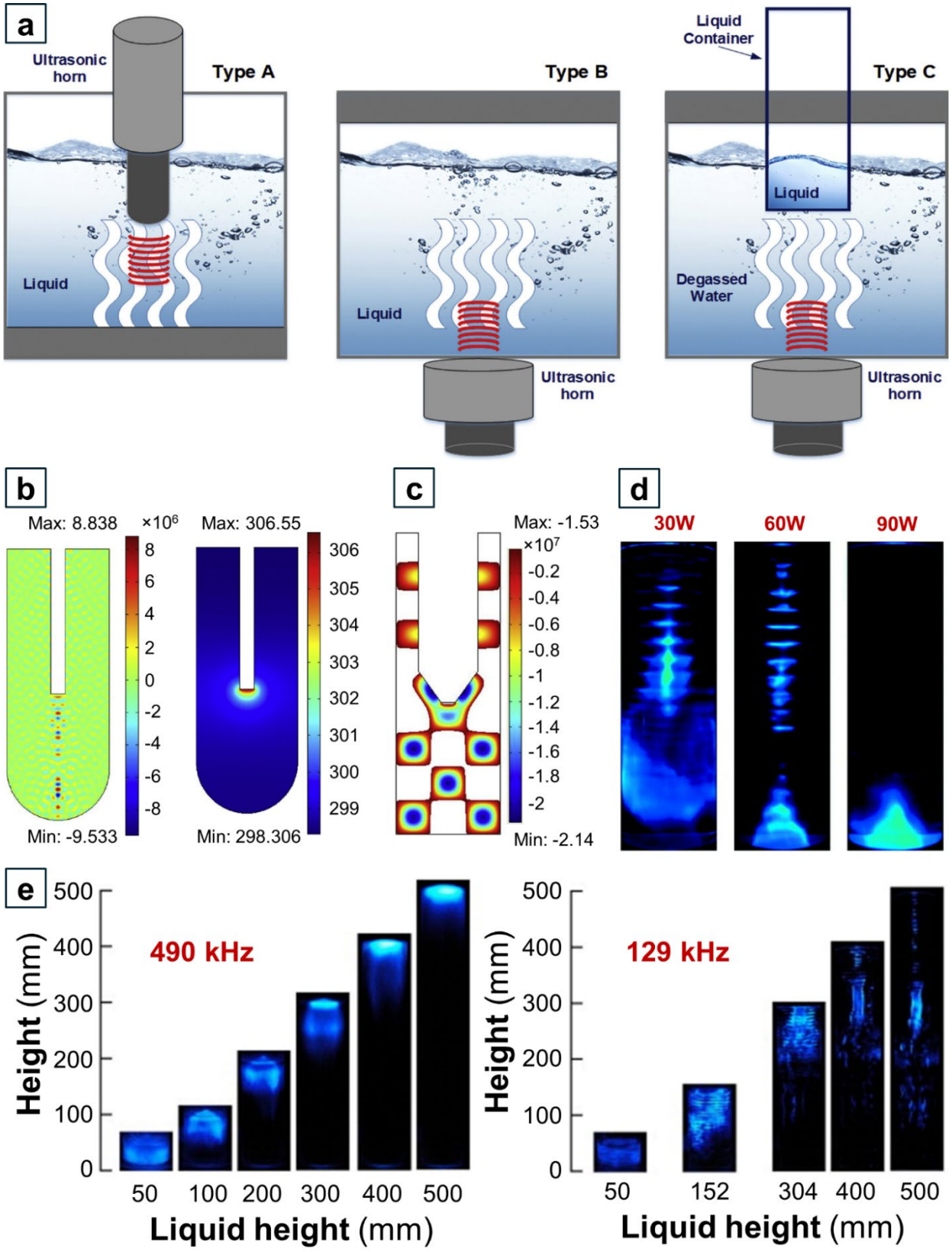

Figure 11. (a) Three typical configurations of a sonoreactor, reproduced with permission from Rashwan et al.[274] Copyright 2019, Elsevier. (b) Pressure profile (left) and temperature contour (right) from cavitation bubble collapse under ultrasonic irradiation at 300 W, reproduced with permission from Rashwan et al.[274] Copyright 2019, Elsevier. (c) Active cavitation zones in a sonoreactor with oil-water phases, reproduced with permission from Niazi et al.[309] Copyright 2014, Elsevier. (d) Sonochemical activity at different applied powers, expressed via chemiluminescence imaging, reproduced with permission from Son et al.[310] Copyright 2012, Elsevier. (e) Sonochemical luminescence at different ultrasonic frequencies and liquid heights of the cylindrical sonoreactor, reproduced with permission from Asakura et al.[311] Copyright 2008, Elsevier.

Due to the spatiotemporal unpredictability and stochastic nature of the bubble nucleation,[34] extremely high ultrasonic intensities and prolonged continuous ultrasonic irradiation are often required to generate a sufficiently high density of inertial cavitation events in the fluid. The resulting rapid bubble implosion is essential for generating radicals, such as •OH. However, these conditions lead to several undesirable side reactions and also induce unwanted secondary effects, such as high fluid shear stress and thermal effects.[43, 312] Furthermore, ultrasonic waves are quickly attenuated when propagating through the fluid at high ultrasonic intensities, resulting in the loss of acoustic energy to thermal energy as the liquid temperature increases during prolonged irradiation.[313] Son et al. examined the sonochemical activity in a reactor at different applied powers via chemiluminescence imaging with luminol.[310] The study found that the attenuation of ultrasound waves was stronger at higher applied ultrasound power. At a relatively high power (90 W), large cavitation bubbles were formed near the transducer.[314] The highly concentrated cloud of bubbles hindered the transmission of ultrasonic waves, leading to their attenuation (Figure 11d). The sonochemical efficiency also depends on the ultrasonic frequency. Asakura *et al.* visualised the sonochemical reaction field via chemiluminescence at different applied frequencies.[311] At higher ultrasonic frequencies, the intensity of sonochemical luminescence was stronger due to the production of more radicals. Sonochemical activity was even observed far away from the transducer (Figure 11e). However, the energy consumption, materials cost, and material stability are major concerns at high frequency operation.[315] At its current level, the sonochemical efficiency is still below its desired performance.[300, 316] Therefore, optimising the efficiency of sonocatalytic reactions by localising cavitation near the surface of the catalysts remains an important milestone in the field of sonocatalysis. The two most promising approaches for improving the energy efficiency of the sonochemical reactions are: (i) using nanostructured cavitation agents and (ii) optimising the design of sonoreactors. These two approaches are described in the subsequent sections.

Other challenges of sonocatalysis are the difficulty in exercising control over the reaction and in optimising the reactor performance. Due to the short lifespan of the active radicals generated from cavitation bubble collapse, very little mechanistic understanding has been gleaned for sonocatalytic

reactions. The exact mechanism by which reactive radicals interact with the active sites of a catalyst remains largely unknown. This lack of knowledge represents a significant challenge for the optimization of sonocatalytic reactions and the design of highly active catalysts. Furthermore, due to the discrete distribution of active cavitation zones in the sonoreactor, effective mass and heat transfer within the entire reactor volume is sometimes difficult to achieve. This is especially true in the sonochemical synthesis of high value-added specialty chemicals which require fine control over the reaction parameters. Optimisation of a sonoreactor is difficult since the overall sonochemical efficiency of a chemical process is influenced both by primary factors, such as frequency, intensity, and pressure, and secondary factors, like temperature and the choice of solvent. These complications lead to serious issues in the reproducibility of sonocatalytic research, hindering the development of its application. Finally, as most current sonoreactors are operated in batch-mode at laboratory-scale, scaling up the process poses an additional challenge. Significant time investments are necessary to perform the technical and economic evaluations of a sonocatalytic process, as well as the life cycle assessment of its sonoreactor.. It is also important to evaluate the stability and durability of sonocatalysts to ensure a consistent performance and longer lifespan. Future investigation will likely focus on integrating sonocatalysis with renewable energy resources to make the technology more sustainable and more suitable for industrial-scale trials.

4.2. Designing catalytic cavitation agent to improve the energy efficiency of sonocatalysis.

As described above, efficiently utilising ultrasonic energy for radical generation and chemical synthesis remains a key technical hurdle in the field of sonocatalysis. One method to overcome this problem is through the use of nanostructured cavitation agents that have engineered surface features to facilitate and localise cavitation. This method provides a convenient pathway to lower the acoustic energy consumption since the cavitation agent is able to compensate for the reduced energy input. In essence, cavitation events are confined near the active sites of these nanostructured materials, while no cavitation occurs in the bulk liquid. Indeed, spatial and temporal control of cavitation at specific ultrasonic frequencies and intensities is an issue that has already been addressed in biomedical acoustics, where HFUS cavitation is typically used for enhanced drug-delivery and

ultrasound contrast enhancement.[317-319] Importantly, the advances made in biomedical acoustics may have direct relevance in addressing the challenges in sonocatalysis using HFUS. Within the biomedical acoustics community, nanostructured cavitation agents are used to reduce the energy required for inertial cavitation by orders of magnitude.[34, 37, 318, 320, 321] Thus, in a well-defined acoustic field, one could control the acoustic energy at a suitable level so that cavitation only occurs at the sites predefined by the cavitation agents.

Kwan et al. succeeded in designing polymeric nanocups that trapped and nucleated inertial cavitation bubbles on their surfaces (Figure 12a).[322] High-speed imaging provided evidence that the implosion of the cavitation bubbles was occurring in close proximity of the cavitation agent, emphasising the effectiveness of this approach. Furthermore, the size of the nanocups could be easily tuned to make it suitable for various ultrasonic activation conditions. These nanocups improved the energy efficiency of sonochemical cavitation 30-fold. In other words, the inertial cavitation threshold is reduced from 30 MPa without the cavitation agents to only 1 MPa when the cavitation agents are included. Mannaris et al. prepared Au nanocones acting as cavitation agents and reported that their unique morphology was able to trap nanobubbles and facilitate inertial cavitation, greatly improving the sonochemical efficiency (Fig. 12b).[317] Mesoporous silica have also been used as cavitation agents to enhance sonochemical efficiency.[323, 324]

However, despite the increased research into solid cavitation agents in biomedical engineering, there have been very few reports using nanostructured cavitation agents to promote industrially relevant sonochemical reactions. Cavitation agents are usually engineered to have a large quantity of gas-stabilising sites, which are capable of nucleating, growing, and maintaining cavitation bubbles on their surface. However, in order to be used as a cavitation agent in sonocatalysis, the material also needs to be constructed from a catalytically active substance and/or possess a high density of active sites on its surface to facilitate chemical reactions. Therefore, to the nanoscale cavitation agents typically used in biomedical applications need to be redesigned to have dual functionality: as ultrasound-responsive cavitation agents and as heterogeneous catalysts.

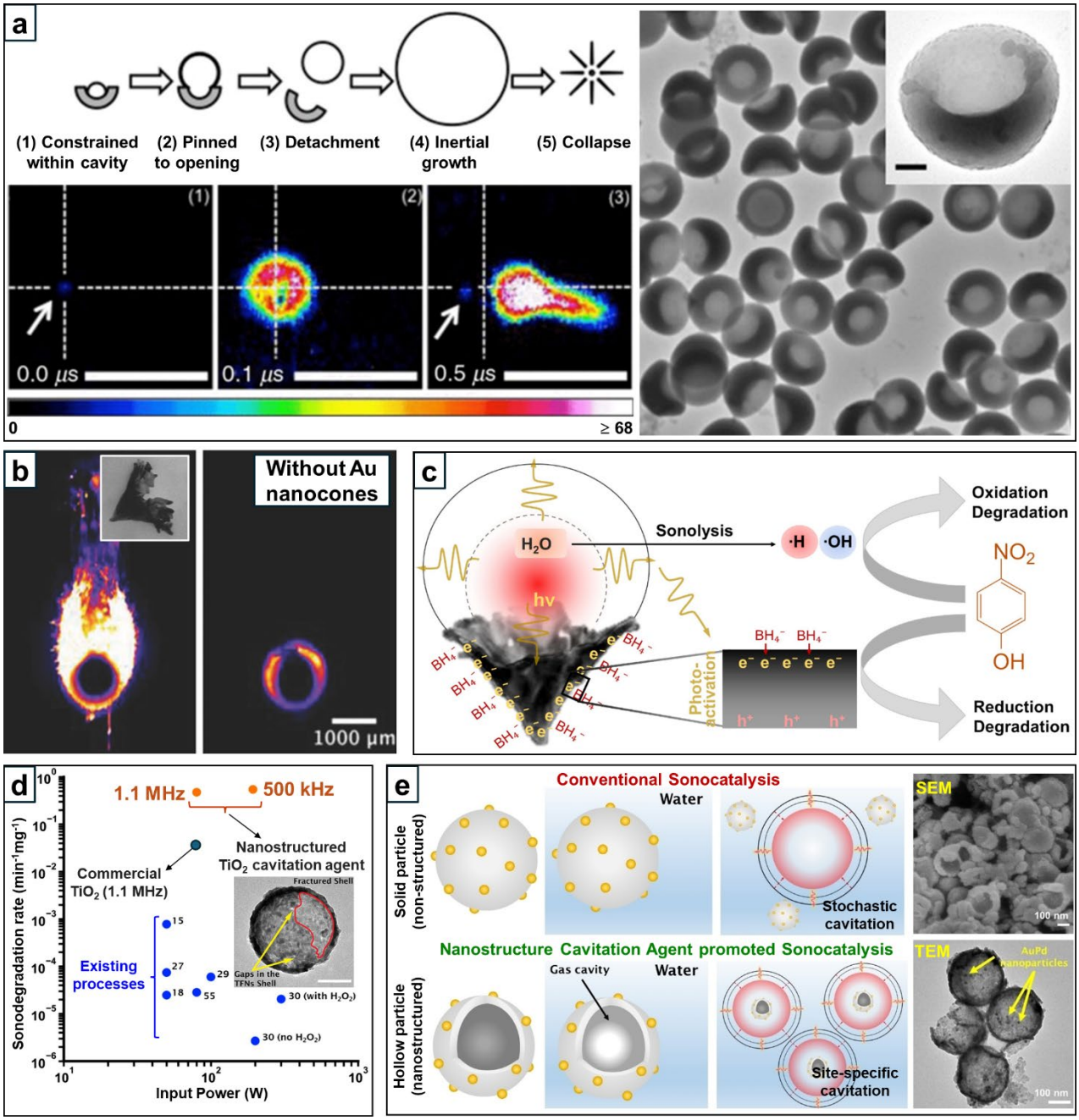

Figure 12. (a) The use of polymeric nanocups as effective cavitation agents. Experimental evidence showing stages (1), (2), and (3) of the cavitation nucleation mechanism, reproduced with permission from Kwan et al.[322] Copyright 2016, American Physical Society. (b) A cavitation event on a gold nanocone (left) and in the absence of a gold nanocone (right), reproduced with permission from Mannaris et al.[317] Copyright 2018, John Wiley and Sons. (c) Gas trapping and cavitation on a Au nanocone (Au NCs) resulting in the enhancement of its sonocatalytic activity, reproduced from an open access publication.[325] (d) Comparison of the sonochemical efficiency of nanostructured TiO_2 cavitation agents to other materials in the literature, reproduced from an open access publication.[326] (e) Enhanced energy efficiency and sonocatalytic activity of hollow AuPd/TiO_2 nanoshells (AuPd/TON), reproduced with permission from Jonnalagadda et al.[36] Copyright 2022, John Wiley and Sons.

Recently, progress has been made in this field with the introduction of the "catalytic cavitation agent".[36, 325-327] Su et al. employed Au nanocones, which were established as effective cavitation agents, to catalyse the sono-degradation of water pollutants using 4-nitrophenol and methylene blue

as model compounds (Fig. 12c).[325] The synergy between the ROS generated from cavitation events and the sonoluminescence-enhanced electron transfer resulting from the Au nanocones caused an 87-fold increase in the sonochemical degradation efficiency when compared to existing studies in literature. This demonstrates the vital role of localised cavitation events in sonocatalytic reactions. Jonnalagadda et al. synthesised TiO_2 fractured nanoshells that could serve as both effective cavitation nucleation agents and catalytically active sites.[326] The study showed that cavitation occurred locally on the TiO_2 fractured nanoshells, facilitating the in-situ generation of active radicals that consequently degraded the organic pollutants (methylene blue) in the aqueous fluid, resulting in an enhancement of three orders of magnitude as compared to conventional methods (Figure 12d). The sonocatalytic efficiency of TiO_2 fractured nanoshells was further improved after being decorated by AuPd nanoparticles that promoted both site-specific cavitation and high activity in the oxidation of benzyl alcohol to benzaldehyde (Figure 12e). Jonnalagadda et al. reported that AuPd nanoparticles supported on TiO_2 fractured nanoshells (called AuPd/TONs) significantly reduced the energy requirement whilst achieving the same or even faster reaction rates when compared to the current advanced methods.[36] These examples illustrate the great potential of synthesising cavitation agents using catalytically active materials to enable the direct utilization of radicals generated by cavitation for selective chemical reactions. The key point is that overall energy consumption of the process can be significantly reduced using these tailored nanostructured cavitation agents.

4.3. Harnessing the power of microfluidics in sonocatalysis.

Reengineering the reactor is another approach to improving the energy efficiency of sonocatalytic processes. Existing sonochemistry techniques induce sonochemical effects by relying on inception cavitation in the liquid phase in poorly defined acoustic fields. In conventional sonochemistry setups (consisting of an ultrasonic bath, probe sonicator, and plate sonicator reaction chambers), predicting and controlling the occurrence of cavitation events is difficult due to the complex acoustic fields that arise from overlapping acoustic interferences. An appropriate reactor design with well-defined acoustic fields could achieve a means to control the frequency and location of inertial cavitation, significantly improving the energy efficiency. Wong et al. built a sono-reactor (called SonoCYL)

with a cylindrically converging design that was capable of generating an intense and localised high acoustic pressure region (Figure 13a).[328] This innovative sonochemical reactor had a much higher •OH radical generation rate and energy efficiency than conventional reactors, demonstrating the crucial effect of reactor design son sonochemical activity.

Microfluidic reactors, also called microreactors are an important subset of sono-reactors. A microreactor is designed with channel sizes ranging from tens to hundreds of micrometers, allowing for fine control of chemical processes with a drastically reduced fluid volume. Whitesides has even stated that "microfluidics seems almost too good to be true: it offers so many advantages and so few disadvantages" in his Nature paper in 2006.[329] The core advantages of microfluidics can overcome most challenges of conventional sonocatalytic reactions, such as controlling heat transfer, optimising discrete active zones, and scaling up batch-mode operation. Another benefit of microfluidic reactors is that they can handle reactions involving unstable or hazardous reactants. Microreactors in chemical processes using heterogeneous catalysts have been widely reported in Yao et al.,[330] Suryawanshi et al.,[331] Tanimu et al.[332] and Feng et al.[333] The combination of microfluidics and sonochemistry started to receive attention during the 2000s and early 2010s.[334-340] Rivas et al. mentioned the term "micro-sono-reactor" as a green and efficient platform in his feature article in Chemical Communications in 2012[134], and later analysed the synergy of microfluidics and ultrasound as a process intensification concept in 2016.[135] One prominent advantage of microreactors for sonochemistry is their reproducibility, which is an issue that has often plagued conventional sonoreactors.

Recently, the combination of sonochemistry and ultrasound witnessed a surge of development thanks to the advances in acoustic engineering. With many new configurations possible for sono-micro-reactors, the energy efficiency has been significantly improved.[239, 341-344] The confined space within the microchannels allows for uniform distribution of active cavitation zones and generates well-defined acoustic fields and a means to control the frequency and location of inertial cavitation.[162, 345] Nieves et al. reported an enhancement of cavitation bubbles during the formation of mini-emulsions in microchannels, resulting in the reduction of droplet polydispersity by 24%.[346]

Liu et al. also obtained a significant increase in the mixing efficiency when using the ultrasonic cavitation in microchannels.[347] Zhao et al. monitored cancer cell spheroids in a vascularised microfluidic model and found that microbubbles generated under ultrasonic irradiation in microchannels greatly enhanced the efficiency of cancer therapy.[348] Liu et al. obtained higher cavitation activity and better quality organic nanoparticles in a microfluidic device under ultrasonic irradiation at 20 kHz than when the same synthesis was performed via conventional methods.[349] Zhao et al. observed an improved energy efficiency in the extraction of vanillin from water by an order of magnitude in a sono-micro-reactor.[350] Thanks to the development of the interdigital transducer (IDT), extremely high frequency ultrasound (from several to hundreds of MHz) can now be generated in microfluidic devices. This research field has come to be known as "acoustofluidics" and has been extensively used in nanomaterials synthesis, material processing, and biomedical applications.[351-356] However, the applications of acoustofluidics mainly relies on utilising the physical effects of sonochemistry, since the radical production at these extremely high ultrasonic frequencies is almost negligible (Fig. 6).

The combination of microfluidics and sonochemistry creates a platform that is highly effective and easily tuneable. Besides controlling the ultrasonic irradiation parameters (frequency and power), the flexibility of being able to use different transducer configurations and microchannel designs provide move degrees of freedom over which to optimise sonochemical reactions. The two main configurations of ultrasonic transducers inside a microreactor are Bulk Acoustic Wave (BAW) and Surface Acoustic Wave (SAW). In a BAW setup, the acoustic wave generated from the transducer is transferred to the bulk liquid and induces resonance modes in the microchannel (Figure 13b).[357] In a SAW setup, the acoustic waves generated from the transducer or interdigitated transducer (IDTs) propagate along the surface of the substrate and radiate into the liquid along its path (Figure 13c).[358] BAW microreactors are simpler, better characterised, and usually operate at a lower ultrasound frequency (tens kHz to 10 MHz) than SAW. SAW microreactors, on the other hand, require a more complicated fabrication process (patterning the transducer/IDT and bonding the microreactor on the substrate) but are often more precise, versatile, and flexible. More importantly,

SAW microreactors are more energy efficient than BAW microreactors since the acoustic energy generated in SAW microreactors is confined to the surface of a substrate, whereas the acoustic energy generated in BAW microreactor is distributed throughout the bulk of substrate.[359] Furthermore, the combination of multiple transducers/IDTs, even with different frequencies, can be used in SAW microreactors to generate different types of SAWs, such as the "travelling surface acoustic wave" (TSAW) and the "standing surface acoustic wave (SSAW)".[360] This capability allows for precise control of the generated acoustic wave, thus maximising the efficiency of manipulation processes, such as mixing, separation, concentration, sorting, trapping, and patterning.[361, 362] These unique features make SAW microreactors a promising platform for the continued development of sonocatalysis.

In addition to the flexibility in setting up the configuration of the transducers/IDTs, the microchannels for fluid flow inside microreactors are amenable to numerous designs.[360, 363] To enhance cavitation during sonochemical processes, a higher density of microbubbles must be generated. Novel setups in gas/liquid mixing and microreactor geometries have been developed using microfluidics, allowing for the production of microbubbles with uniform size (Figure 13d).[364] Changing the identity of the gas and tuning the gas and liquid flow rates allow for more precise control over the density and compositions of microbubbles.[365] Microchannels can also be designed inside special structures to enhance the cavitation efficiency, as is the case in sharp-edge acoustofluidics.[366] Rasouli et al. constructed sharp-edge structures along the length of a microfluidic device and achieved superior performance in the synthesis of polymeric nanoparticles and liposome in a low-power and highly controllable process.[367] Bachman et al. designed a SAW acoustofluidic device consisting of Tesla structures and periodic sharp-edge patterns, as depicted in Fig. 13c(i) and 13c(ii).[358] This device exhibited a much higher mixing efficiency than conventional passive hydrodynamic mixers and was able to operate at a wide range of operating conditions. The subfields "micro-elastofluidics" and "stretchable microfluidics" were recently developed in Nguyen's group at Griffith University. These microfluidics domains seek to manipulate the fluid-structure interactions of the sono-microreactor[368-371] to influence their sonochemical performance.

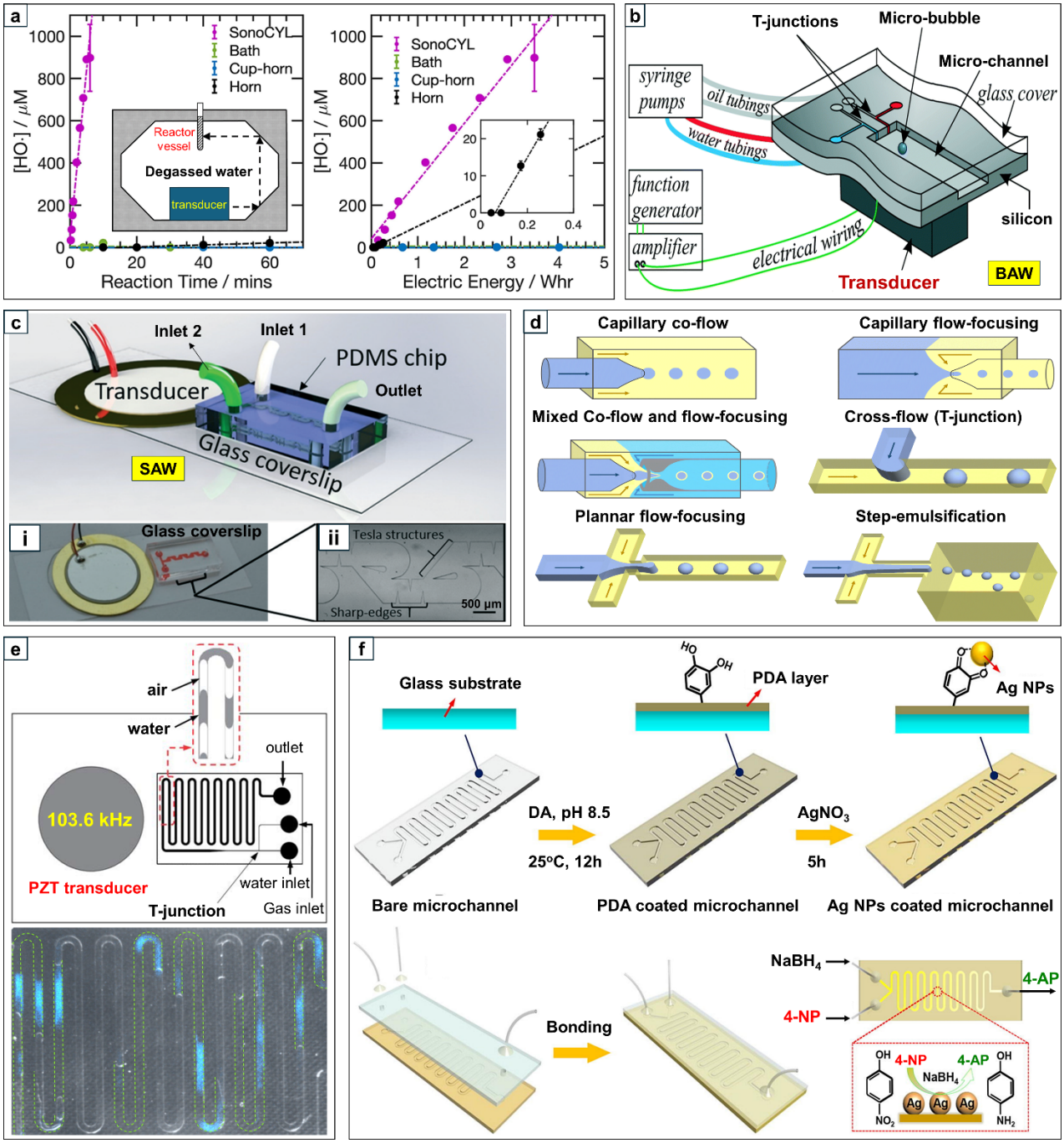

Figure 13. (a) Sonochemical efficiency of the novel sonoreactor SonoCYL, reproduced from an open access publication.[328] (b) Setup of the microfluidic device with Bulk Acoustic Wave (BAW), reproduced from an open access publication.[357] (c) Surface Acoustic Wave (SAW) setup: (i) Photo of the acoustofluidic device and (ii) a close-up of the microchannel design with sharp-edge structures and recirculation zones, reproduced with permission from Bachman et al.[358] Copyright 2020, Royal Society of Chemistry. (d) Different setups for generating droplets and microbubbles in a microreactor, reproduced with permission from Nan et al.[364] Copyright 2024, Royal Society of Chemistry. (e) Schematic of a microfluidic T-junction device driven by an attached transducer (top) and chemiluminescence image of cavitation bubbles in the microchannel (bottom), reproduced with permission from Tandiono et al.[372] Copyright 2010, Royal Society of Chemistry. (f) The process of immobilising Ag NPs on the wall of microchannels by polydopamine (PDA) coating and catalytic reduction of 4-NP to 4-AP in the microreactor, reproduced with permission from Zhang et al.[373] Copyright 2017, Elsevier.

Despite recent reports of the enhanced energy efficiency of sono-microreactors, studies of the improved sonochemical efficiency of microfluidic devices are not as prevalent, despite their direct effect on sonocatalytic performance. In 2004, Iida et al. pioneered the quantification of •OH radical formation inside microreactors under the influence of ultrasound using fluorometry and obtained the first confirmation of cavitation events at the microscale. Tandiono et al. investigated the cavitation activity driven by capillary SAW in a microfluidic device made from PDMS and glass.[372] The plate transducer was attached at a distance of 5 mm from the microreactor and produced ultrasonic waves at 103.6 kHz (Figure 13e). High-speed images showed that strong inertial cavitation occurred at 136 μs and that most of the cavitation bubbles collapsed at 752 μs. Chemiluminesence experiments using luminol were carried out using the same setup, confirming the intensive formation of •OH radicals at the confined gas–liquid interfaces (Figure 13e).[374] This study provided direct evidence that cavitation bubbles do not occur randomly in the bulk liquid (as in conventional sonoreactors) but only within a well-defined region in the microreactor, allowing for the spatial control of sonochemical reactions. Rivas et al. designed a BAW microreactor engineered with cylindrical pits acting as gas trapping sites to nucleate cavitation and computed the sonochemical efficiency for the formation of •OH radicals from water sonolysis occurring under different applied powers.[340, 375] They observed that the sonochemical efficiency was increased by an order of magnitude thanks to the presence of the designed pits, and that medium power delivered the highest performance in all cases. This study illustrates that the appropriate design of microchannel walls has the potential to intensify the formation of radical formations inside a sono-microreactor. Verhaagen et al. successfully scaled-up this pits-microreactor in 2016, increasing the sonochemical efficiency of the reactor by 45.1% and scaling up the capacity of the reactor by a factor of 25.[300] Thangavadivel et al. evaluated the sonochemical efficiency of the 4-channels microreactor via the degradation of methyl orange.[376] The formation of ROS from cavitation events was quantified by Fricke dosimetry and operational parameters including solution temperature, flow rate, and ultrasonic power were optimised to obtain the highest efficiency of the microreactor.

Heterogeneous catalysts need to be distributed homogeneously inside the microreactor in order to facilitate the reaction inside a microfluidic device as intended. Despite the challenge of mass transfer inside a narrow channel, several approaches have been developed to help accomplish this. The most popular approach is coating or immobilising solid catalysts on the wall of microchannels. Zhang et al. coated polydopamine (PDA) on the inside of a glass microchannel and used this PDA layer to anchor the Ag nanoparticles to the channel wall before bonding it with another glass cover to make the catalytic microreactor (Figure 13f).[373] Other approaches include loading the solid catalyst in a packed bed inside a microreactor or depositing catalysts via the functionalised monoliths in the microchannel.[332, 377] Recently, solid nanocatalysts were incorporated into the continuous phase of the microreactor, originally a mixture of liquid and gas, through the formation of Pickering emulsions, slurry Taylor segments, colloidal suspensions, and catalyst slurries. The homogeneous distribution of catalyst particles within the microfluidic channels helps to facilitate the reaction, enhancing the efficiency and overall conversion of microreactors.[378-380] This approach is highly successful in leveraging the dual functionality of catalytic cavitation agents inside microfluidic devices in order to achieve the best efficiency for sonocatalytic reactions.

4.4. Density functional theory (DFT) calculations to assist in studying the mechanism of sonocatalytic reactions and designing catalytic cavitation agents for sonocatalysis

One challenge in the development of sonocatalysis is the lack of insights into the reaction mechanism. Without this crucial information, designing sonoreactors and sonocatalysts that maximise the production of desired products is reduced toa “trial-and-error” approach, which is costly and ineffective. Mechanistic insight into sonocatalytic reaction mechanisms by experimentation is very challenging due to the short lifespan ROS and the large and inter-connected reaction network produced in ultrasonic irradiation. Computational studies via density functional theory (DFT) calculations provide a more tractable approach to gain a detailed understanding of sonochemical reactions at molecular level. Several DFT studies were reported recently that deliver novel insights into the reaction mechanism of the sonochemical transformation of biomass to high

value-added specialty chemicals, significantly advancing the knowledge in this field and leading to the development of more efficient catalytic processes.

Glucose oxidation using heterogeneous catalysts usually results in the formation of gluconic acid as the main product.[190] Gluconic acid is used to make consumer products like household cleaners, industrial cleaners, inks, paints, dyes, and metal finishing, and its market price is AU$92/kg. However, it is also possible to produce glucuronic acid, a much more valuable chemical building block, from glucose oxidation. In fact, the market price of glucuronic acid is AU$2.2M/kg because it is such a vital pharmaceutical intermediate in the production of drugs for blood coagulation inhibitors and antioxidants for immune system support. Glucuronic acid has been traditionally produced via enzymatic-catalysed routes and its production via heterogeneous catalysis was never effective enough to be commercially viable. However, in 2019, a successful strategy to produce glucuronic acid through the selective oxidation of glucose using a solid catalyst was proposed by Amaniampong et al.[68] Their work suggested that by using a CuO catalyst and tuning the reaction conditions, the glucose ring opening was inhibited and instead, selective oxidation at the C6 position was preferred, yielding glucuronic acid (Figure 14a(i)). DFT calculations showed that the ring opening of glucose was suppressed by the oxygen surface lattice of the CuO catalysts, which was able to trap the •H radicals produced by water sonolysis, as shown in Fig. 14a(ii).[68] DFT calculations predicted an activation barrier of 47 kJ/mol for glucose ring opening on a clean CuO(111) surface, but that the barrier increases to 121 kJ/mol under ultrasonic irradiation. Therefore, sonochemical conditions are a plausible alternative to controlling the opening of the glucose ring. Once glucose ring opening is suppressed, glucose in the closed-ring structure can be readily oxidised by •OH radicals, resulting in the highly selective production of glucuronic acid. The detailed reaction mechanism and computed activation barriers for all elementary steps are presented in Fig. 14a(iii). The presence of •OH radicals (from water sonolysis) on CuO(111) provides an alternative pathway with lower activation barriers (highlighted by blue arrows) for oxidising the glucose molecule. The mechanistic understanding reported herein is beneficial in thinking about how similar protocols can be implemented in modelling the conversion of other biomass resources via sonocatalysis.[258]

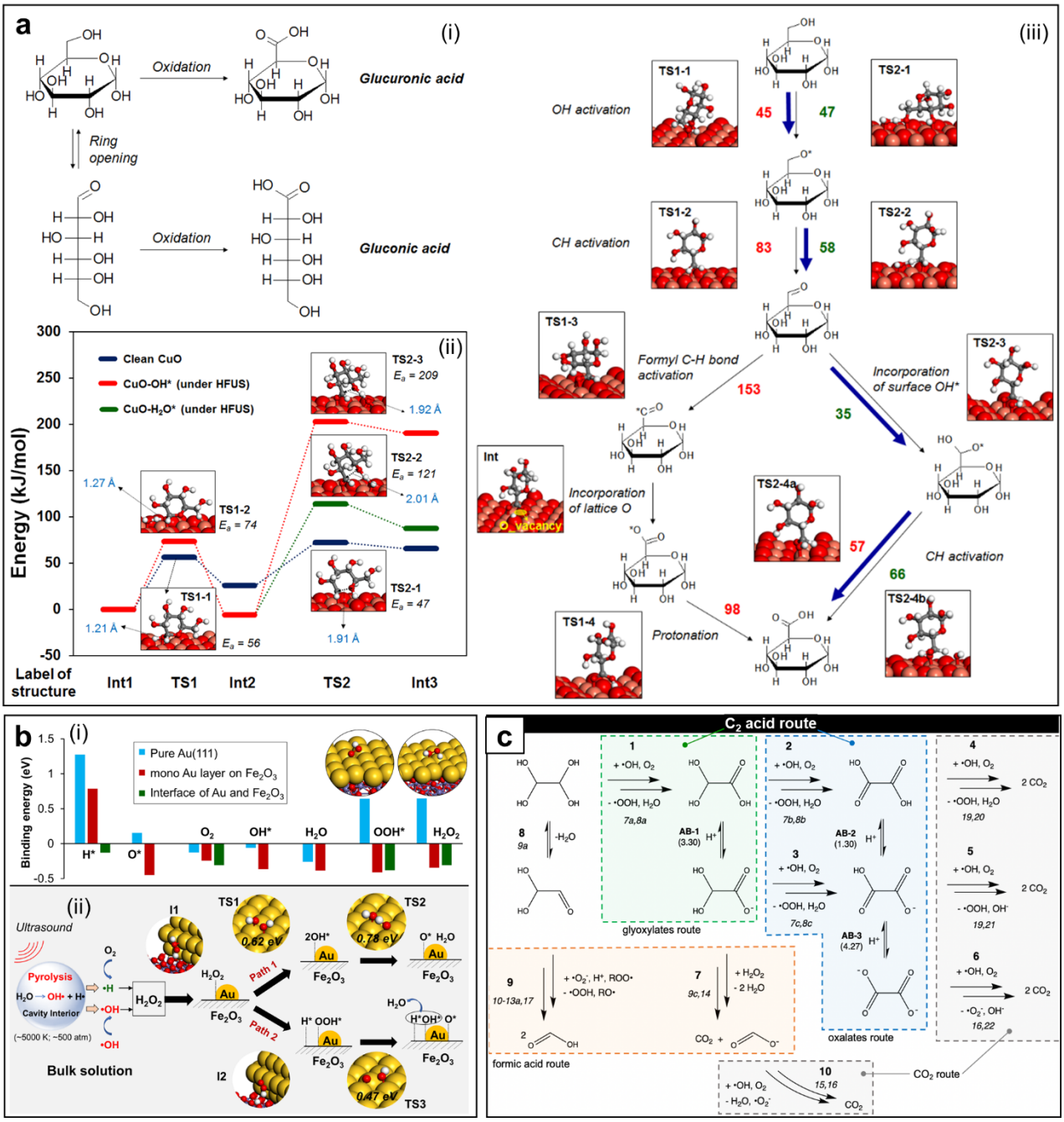

Figure 14. (a) Strategy for sonocatalytic conversion of glucose to glucuronic acid (i). The inhibition of glucose ring opening on CuO(111) surfaces under ultrasonic irradiation (ii). The detailed mechanism of glucose oxidation to glucuronic acid on CuO(111) surfaces under ultrasonic irradiation (iii), reproduced with permission from Amaniampong et al.[68] Copyright 2019, American Chemical Society. (b) Binding energies (i) and ROS formation mechanism using Au/Fe_2O_3 catalysts in the presence of ultrasonic irradiation (ii), reproduced with permission from Amaniampong et al.[69] Copyright 2022, Royal Society of Chemistry. (c) Reaction network that yields C_2 acids and CO_2 during sono-oxidation of glyoxal, reproduced from an open access publication.[381]

Another challenge for sonocatalysis is that the active sites of the catalyst are not always well-defined, hindering the improvement and development of novel catalytic materials. In 2022, DFT calculations were applied to study the sonochemical conversion of cellulose to oxalic acid using Au/Fe_2O_3 catalysts.[69] The predicted adsorption energies and electronic properties calculated for

different sites revealed that only the atoms located at narrow interfacial zones were active for cellulose oxidation (Fig. 14b(i)). DFT calculations showed that charge transfer between the Au nanoparticles and the Fe_2O_3 support induced a stronger stabilization of ROS at interfacial sites, facilitating the generation of oxidising agents (•OH, •OOH and •O) (Fig.14b(ii)). This investigation established methodology for the rational development of sonocatalysts. It particularly in the design of novel catalytic activation agents. This methodology was implemented in many studies using DFT calculations in order to design catalysts with higher activity and stability via doping and/or tuning the metal/support interactions.[382-390]

Finally, DFT calculations also provide useful predictions of sonocatalytic efficiency. All kinetic and thermodynamic parameters for each elementary step in a sonochemical reaction can be computed and used as input data for validating a microkinetic model. Consequently, this yield estimates of rate constants and rate efficiencies under different reaction conditions. Fischer et al. performed extensive DFT calculations for all elementary steps pertaining to the oxidation of glyoxal of hydroxyl radicals and constructed a detailed microkinetic model (Figure 14c).[381] This model was used to evaluate the sonochemical efficiency of the reaction and optimised operating conditions, such as pH and the ultrasonic frequency, in order to obtain the desired product composition. All of their theoretical predictions were consistent with experimental measurements. It is expected that DFT calculations will become a key tool in accelerating the development of sonocatalysis and sustainable chemistry.

5. Conclusions and perspectives.

This review provides a comprehensive picture of the past, current, and future perspectives of sonocatalysis, an important subsection of sonochemistry. Sonochemistry is now widely considered to be a vital green technology. Much progress has been made in tuning the selectivity of products, minimising the use of harmful chemicals or reagents, reducing waste, and shifting to renewable energy resources. Sonochemistry is highly effective in cleaning and extraction applications, environmental remediation, organic synthesis, biomedical treatment, and nanomaterial synthesis.

Sonocatalysis is based on the synergy between heterogeneous catalysis and ultrasound in order to facilitate chemical reactions. The core of this approach relies on generating highly reactive radicals via rapid cavitation under high frequency ultrasonic irradiation in the presence of a solid catalyst. Recent advances in wastewater treatment and sonotherapy via sonocatalysis were presented in this manuscript. In addition, the sonocatalytic mechanism was analysed, highlighting the synergy between solid catalysts and ultrasound, and giving insight into the design of more efficient sonochemical processes. This manuscript also focuses on the applications of sonocatalysis in biomass conversion, which is a promising approach for addressing climate change and promoting the development of a circular economy through sustainable chemistry. The introduction of renewable biomass resources in the chemical industry promotes the sustainable production of environmentally friendly chemicals and a wide range of products essential for human life (Figure 15). The application of sonocatalysis in biomass conversion allows for fine-tuning of the product distribution in order to transform biomass-derived feedstocks into high value-added specialty chemicals and access to chemicals that are generally impossible to produce by conventional routes. This research reviewed was compiled with the intention of analysing the current state of sonocatalysis, as well as highlighting the potential for further development in the future.

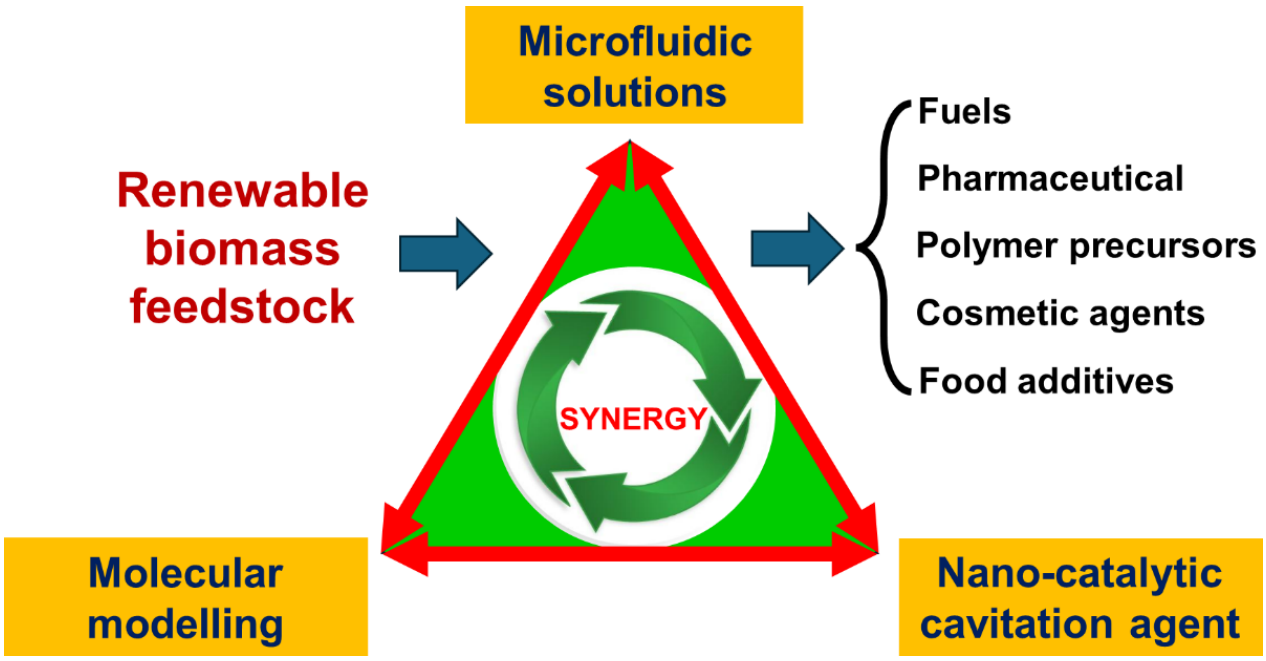

Figure 15. The synergy between microfluidics, catalytic cavitation agents, and molecular modelling in the sustainable transformation of renewable biomass to high value-added products.

The major technical hurdles of sonocatalysis in its current state are the low efficiency in utilising ultrasonic energy for radical generation, and the difficulties in reaction control. These challenges have been reviewed and analysed in detail. Several promising approaches to overcoming these problems have been identified, including the use of catalytic cavitation agents and the design of microfluidic sonoreactors. Using tailored nanostructured catalytic cavitation agents causes a significant reduction in the energy consumption of sonocatalytic processes. Implementing catalytic cavitation agents in a microfluidic sonoreactor with a well-defined acoustic field allows for fine control over the acoustic energy so that cavitation only occurs at the site of the nanostructured cavitation agents. In this way, the majority of radicals produced inside the cavitation bubble are transferred directly to a nano-engineered catalytic surface, enhancing the activity and selectivity of the reaction. The application of molecular modelling via density functional theory (DFT) calculations results in fundamental insight into the sonocatalytic reaction mechanism at the atomic scale. Microkinetic models supported by DFT calculations and validated by experimental measurements guide the design of novel bifunctional nanomaterials that serve as both effective cavitation agents and active catalysts. The integration of nanostructured catalytic cavitation agents, microfluidic solutions, and molecular modelling forms a trilateral methodology that allows researchers to unlock the full potential of sonocatalyis for sustainably chemistry.

Acknowledgement.

This work is financially supported by the Australian Research Council (FL230100023 and DE240100408). Y.C. acknowledges financial support from the Zhejiang University Luk's Scholarship for Graduates International Exchange for the cooperation research conducted at Griffith University. P.N.A. acknowledges the financial support from the European Research Council (ERC) funded/Co-funded by the European Union (ERC, ConCASM, project agreement number 101117070). Views and opinions expressed are however those of the author(s) only and do not necessarily reflect those of the European Union or the European Research Council. Neither the

European Union nor the granting authority can be held responsible for them. F.J. and P.N.A. also acknowledge financial support from the European Union (ERDF) and Région Nouvelle Aquitaine.

Conflict of Interest.

The authors declare no conflict of interest.

Keywords.

Sonocatalysis, sustainable chemistry, green chemistry, microfluidics, catalytic cavitation agent, density function theory (DFT) calculations, sonochemistry, biomass conversion, selective oxidation, environmental remediation, sonodynamic therapy.

References.

1. N. H. Ince, G. Tezcanli, R. K. Belen and İ. G. Apikyan, *Applied Catalysis B: Environmental*, 2001, **29**, 167-176.
2. S. K. Gujar, G. Divyapriya, P. R. Gogate and P. V. Nidheesh, *Critical Reviews in Environmental Science and Technology*, 2023, **53**, 780-802.
3. T. D. Pham, R. A. Shrestha, J. Virkutyte and M. Sillanpää, *Canadian Journal of Civil Engineering*, 2009, **36**, 1849-1858.
4. J. Li, Y. Ma, T. Zhang, K. K. Shung and B. Zhu, *BME Frontiers*, 2022, **2022**, 9764501.
5. H. Huang, Y. Zheng, M. Chang, J. Song, L. Xia, C. Wu, W. Jia, H. Ren, W. Feng and Y. Chen, *Chemical Reviews*, 2024, **124**, 8307-8472.
6. C. Xiouras, A. Fytopoulos, J. Jordens, A. G. Boudouvis, T. Van Gerven and G. D. Stefanidis, *Ultrasonics Sonochemistry*, 2018, **43**, 184-192.
7. P. W. Cains, P. D. Martin and C. J. Price, *Organic Process Research & Development*, 1998, **2**, 34-48.
8. H. Li, H. Li, Z. Guo and Y. Liu, *Ultrasonics Sonochemistry*, 2006, **13**, 359-363.
9. J. Ferreira, J. Opsteyn, F. Rocha, F. Castro and S. Kuhn, *Chemical Engineering Research and Design*, 2020, **162**, 249-257.
10. R. Crespo, P. M. Martins, L. Gales, F. Rocha and A. M. Damas, *Journal of Applied Crystallography*, 2010, **43**, 1419-1425.
11. Z. J. Dolatowski, J. Stadnik and D. Stasiak, *Acta Sci. Pol. Technol. Aliment*, 2007, **6**, 88-99.
12. T. S. Awad, H. A. Moharram, O. E. Shaltout, D. Asker and M. M. Youssef, *Food Research International*, 2012, **48**, 410-427.

13. M. Gallo, L. Ferrara and D. Naviglio, *Foods*, 2018, **7**, 164.
14. J. J. Hinman and K. S. Suslick, in *Sonochemistry: From Basic Principles to Innovative Applications*, eds. J. C. Colmenares and G. Chatel, Springer International Publishing, Cham, 2017, pp. 59-94.
15. J. H. Bang and K. S. Suslick, *Advanced Materials*, 2010, **22**, 1039-1059.
16. S. E. Skrabalak, *Physical Chemistry Chemical Physics*, 2009, **11**, 4930-4942.
17. M. Draye, G. Chatel and R. Duwald, *Pharmaceuticals*, 2020, **13**, 23.
18. M. A. Schiel, A. B. Chopa, G. F. Silbestri, M. B. Alvarez, A. G. Lista and C. E. Domini, in *Green Synthetic Approaches for Biologically Relevant Heterocycles*, ed. G. Brahmachari, Elsevier, Boston, 2015, pp. 571-601.
19. N. Pokhrel, P. K. Vabbina and N. Pala, *Ultrasonics Sonochemistry*, 2016, **29**, 104-128.
20. S. K. Bhangu and M. Ashokkumar, in *Sonochemistry: From Basic Principles to Innovative Applications*, eds. J. C. Colmenares and G. Chatel, Springer International Publishing, Cham, 2017, pp. 1-28.
21. L. H. Thompson and L. K. Doraiswamy, *Industrial & Engineering Chemistry Research*, 1999, **38**, 1215-1249.
22. T. J. Mason, *Practical Sonochemistry: User's Guide to Applications in Chemistry and Chemical Engineering*, E. Horwood, 1991.
23. E. A. Neppiras, *Physics Reports*, 1980, **61**, 159-251.
24. S. A. Elder, *The Journal of the Acoustical Society of America*, 1959, **31**, 54-64.
25. E. Webster, *Ultrasonics*, 1963, **1**, 39-48.
26. E. B. Flint and K. S. Suslick, *Science*, 1991, **253**, 1397-1399.
27. A. R. Rezk, H. Ahmed, S. Ramesan and L. Y. Yeo, *Advanced Science*, 2021, **8**, 2001983.
28. D. L. Miller, S. V. Pislaru and J. F. Greenleaf, *Somatic Cell and Molecular Genetics*, 2002, **27**, 115-134.
29. C.-Y. Lai, C.-H. Wu, C.-C. Chen and P.-C. Li, *Ultrasound in Medicine & Biology*, 2006, **32**, 1931-1941.
30. C.-D. Ohl, M. Arora, R. Ikink, N. de Jong, M. Versluis, M. Delius and D. Lohse, *Biophysical Journal*, 2006, **91**, 4285-4295.
31. W. Zhang, Y. Shi, S. Abd Shukor, A. Vijayakumaran, S. Vlatakis, M. Wright and M. Thanou, *Nanoscale*, 2022, **14**, 2943-2965.
32. A. L. Y. Kee and B. M. Teo, *Ultrasonics Sonochemistry*, 2019, **56**, 37-45.
33. B. Savun-Hekimoğlu, *Acoustics*, 2020, **2**, 766-775.
34. R. G. Thomas, U. S. Jonnalagadda and J. J. Kwan, *Langmuir*, 2019, **35**, 10106-10115.
35. Y. T. Shah, A. B. Pandit and V. S. Moholkar, in *Cavitation Reaction Engineering*, Springer US, Boston, MA, 1999, pp. 155-192.
36. U. S. Jonnalagadda, Q. Fan, X. Su, W. Liu and J. J. Kwan, *ChemCatChem*, 2022, **14**, e202200732.
37. J. J. Kwan, R. Myers, C. M. Coviello, S. M. Graham, A. R. Shah, E. Stride, R. C. Carlisle and C. C. Coussios, *Small*, 2015, **11**, 5305-5314.
38. M. Mrowetz, C. Pirola and E. Selli, *Ultrasonics Sonochemistry*, 2003, **10**, 247-254.
39. Z. Li, L. Li, S. Zhang, L. Zhang, Y. Cui and H. Shi, *Separation and Purification Technology*, 2024, **332**, 125799.

40. D. Meroni, M. Jiménez-Salcedo, E. Falletta, B. M. Bresolin, C. F. Kait, D. C. Boffito, C. L. Bianchi and C. Pirola, *Ultrasonics Sonochemistry*, 2020, **67**, 105123.

41. S. A. Asli and M. Taghizadeh, *ChemistrySelect*, 2020, **5**, 13720-13731.

42. D. Meroni, C. Gasparini, A. Di Michele, S. Ardizzone and C. L. Bianchi, *Ultrasonics Sonochemistry*, 2020, **66**, 105119.

43. T. G. McKenzie, F. Karimi, M. Ashokkumar and G. G. Qiao, *Chemistry – A European Journal*, 2019, **25**, 5372-5388.

44. P. N. Amaniampong, A. Karam, Q. T. Trinh, K. Xu, H. Hirao, F. Jérôme and G. Chatel, *Scientific Reports*, 2017, **7**, 40650.

45. K. S. Suslick, N. C. Eddingsaas, D. J. Flannigan, S. D. Hopkins and H. Xu, *Accounts of Chemical Research*, 2018, **51**, 2169-2178.

46. J. I. Thornycroft and S. W. Barnaby, *Journal of the American Society for Naval Engineers*, 1895, **7**, 711-736.

47. L. Rayleigh, *The London, Edinburgh, and Dublin Philosophical Magazine and Journal of Science*, 1917, **34**, 94-98.

48. R. W. Wood and A. L. Loomis, *The London, Edinburgh, and Dublin Philosophical Magazine and Journal of Science*, 1927, **4**, 417-436.

49. W. T. Richards and A. L. Loomis, *Journal of the American Chemical Society*, 1927, **49**, 3086-3100.

50. H. Frenzel and H. Schultes, *Zeitschrift für Physikalische Chemie*, 1934, **27B**, 421-424.

51. B. Von Claus, *Z. Tech. Phys.*, 1935, **16**, 80-82.

52. C. W. Porter and L. Young, *Journal of the American Chemical Society*, 1938, **60**, 1497-1500.

53. W. T. Richards, *Reviews of Modern Physics*, 1939, **11**, 36-64.

54. A. Weissler, H. W. Cooper and S. Snyder, *Journal of the American Chemical Society*, 1950, **72**, 1769-1775.

55. B. E. Noltingk and E. A. Neppiras, *Proceedings of the Physical Society. Section B*, 1950, **63**, 674.

56. A. Weissler, *The Journal of the Acoustical Society of America*, 1953, **25**, 651-657.

57. A. V. M. Parke and D. Taylor, *Journal of the Chemical Society (Resumed)*, 1956, 4442-4450.

58. C. F. Naude´ and A. T. Ellis, *Journal of Basic Engineering*, 1961, **83**, 648-656.

59. G. Chatel, *Sonochemistry*, WSPC (Europe), 2017.

60. J. L. Luche and J. C. Damiano, *Journal of the American Chemical Society*, 1980, **102**, 7926-7927.

61. K. S. Suslick, P. F. Schubert and J. W. Goodale, *Journal of the American Chemical Society*, 1981, **103**, 7342-7344.

62. T. Ando, S. Sumi, T. Kawate, J. Ichihara and T. Hanafusa, *Journal of the Chemical Society, Chemical Communications*, 1984, 439-440.

63. T. Mason, *Ultrasonics Sonochemistry*, 2015, **25**, 4-7.

64. T. Ando, T. J. Mason and K. S. Suslick, *Ultrasonics Sonochemistry*, 1994, **1**, S3.

65. D. F. Gaitan, L. A. Crum, C. C. Church and R. A. Roy, *The Journal of the Acoustical Society of America*, 1992, **91**, 3166-3183.

66. P. T. Anastas and J. C. Warner, *Green Chemistry: Theory and Practice*, Oxford University Press, Oxford, 1998.

67. P. N. Amaniampong, Q. T. Trinh, J. J. Varghese, R. Behling, S. Valange, S. H. Mushrif and F. Jérôme, *Green Chemistry*, 2018, **20**, 2730-2741.

68. P. N. Amaniampong, Q. T. Trinh, K. De Oliveira Vigier, D. Q. Dao, N. H. Tran, Y. Wang, M. P. Sherburne and F. Jérôme, *Journal of the American Chemical Society*, 2019, **141**, 14772-14779.

69. P. N. Amaniampong, Q. T. Trinh, T. Bahry, J. Zhang and F. Jérôme, *Green Chemistry*, 2022, **24**, 4800-4811.

70. P. N. Amaniampong, N. Y. Asiedu, E. Fletcher, D. Dodoo-Arhin, O. J. Olatunji and Q. T. Trinh, in *Valorization of Biomass to Value-Added Commodities: Current Trends, Challenges, and Future Prospects*, eds. M. O. Daramola and A. O. Ayeni, Springer International Publishing, Cham, 2020, pp. 193-220.

71. Q. T. Trinh, A. Banerjee, K. B. Ansari, D. Q. Dao, A. Drif, N. T. Binh, D. T. Tung, P. M. Q. Binh, P. N. Amaniampong, P. T. Huyen and M. T. Le, in *Biorefinery of Alternative Resources: Targeting Green Fuels and Platform Chemicals*, eds. S. Nanda, D.-V. N. Vo and P. K. Sarangi, Springer Singapore, Singapore, 2020, pp. 317-353.

72. T. T. Dang, T. L. A. Nguyen, K. B. Ansari, V. H. Nguyen, N. T. Binh, T. T. N. Phan, T. H. Pham, D. T. T. Hang, P. N. Amaniampong, E. Kwao-Boateng and Q. T. Trinh, in *Nanostructured Photocatalysts*, eds. V.-H. Nguyen, D.-V. N. Vo and S. Nanda, Elsevier, 2021, pp. 169-216.

73. S. Haouache, A. Karam, T. Chave, J. Clarhaut, P. N. Amaniampong, J. M. Garcia Fernandez, K. De Oliveira Vigier, I. Capron and F. Jérôme, *Chemical Science*, 2020, **11**, 2664-2669.

74. P. N. Amaniampong, J.-L. Clément, D. Gigmes, C. Ortiz Mellet, J. M. García Fernández, Y. Blériot, G. Chatel, K. De Oliveira Vigier and F. Jérôme, *ChemSusChem*, 2018, **11**, 2673-2676.

75. L. Ouyang, H. H. W. B. Hansen, H. Cha, X. Ji, J. Zhang, Q. Li, B. H. Tan, Q. T. Trinh, N.-T. Nguyen and H. An, *Colloids and Surfaces A: Physicochemical and Engineering Aspects*, 2024, **700**, 134773.

76. I. Tzanakis, G. S. B. Lebon, D. G. Eskin and K. A. Pericleous, *Ultrasonics Sonochemistry*, 2017, **34**, 651-662.

77. H. Xu, B. W. Zeiger and K. S. Suslick, *Chemical Society Reviews*, 2013, **42**, 2555-2567.

78. M. Ashokkumar, *ChemTexts*, 2018, **4**, 7.

79. S. Manickam, D. Camilla Boffito, E. M. M. Flores, J.-M. Leveque, R. Pflieger, B. G. Pollet and M. Ashokkumar, *Ultrasonics Sonochemistry*, 2023, **99**, 106540.

80. D. J. Flannigan and K. S. Suslick, *Nature*, 2005, **434**, 52-55.

81. M. M. Hasan and K. S. Iyengar, *Nature*, 1963, **199**, 995-996.

82. A. Brotchie, F. Grieser and M. Ashokkumar, *Physical Review Letters*, 2009, **102**, 084302.

83. K. S. Suslick, S. J. Doktycz and E. B. Flint, *Ultrasonics*, 1990, **28**, 280-290.

84. K. S. Suslick, *Science*, 1990, **247**, 1439-1445.

85. K. Feng, J. Eshraghi, P. P. Vlachos and H. Gomez, *Physics of Fluids*, 2024, **36**.

86. Y. Yang, M. Shan, Y. Zhang, H. Li, X. Kan and Q. Han, *Computers & Fluids*, 2024, **279**, 106325.

87. G. Chatel, L. Novikova and S. Petit, *Applied Clay Science*, 2016, **119**, 193-201.

88. R. F. Martínez, G. Cravotto and P. Cintas, *The Journal of Organic Chemistry*, 2021, **86**, 13833-13856.

89. G. Chatel, *Sonochemistry*.

90. P. T. Anastas and J. B. Zimmerman, *Environmental Science & Technology*, 2003, **37**, 94A-101A.

91. V. Sivakumar and P. G. Rao, *Transactions of the Indian National Academy of Engineering*, 2024, **9**, 1-24.

92. A. Taha, T. Hu, Z. Zhang, A. M. Bakry, I. Khalifa, S. Pan and H. Hu, *Ultrasonics Sonochemistry*, 2018, **49**, 283-293.

93. A. M. Andani, T. Tabatabaie, S. Farhadi and B. Ramavandi, *RSC Advances*, 2020, **10**, 32845-32855.

94. M. Vinatoru and T. J. Mason, *Molecules*, 2021, **26**, 755.

95. T. J. Mason, *Ultrasonics Sonochemistry*, 2003, **10**, 175-179.

96. M. L. Weththimuni and M. Licchelli, *Coatings*, 2023, **13**, 457.

97. E. Maisonhaute, C. Prado, P. C. White and R. G. Compton, *Ultrasonics Sonochemistry*, 2002, **9**, 297-303.

98. F. Reuter, S. Lauterborn, R. Mettin and W. Lauterborn, *Ultrasonics Sonochemistry*, 2017, **37**, 542-560.

99. G. Hu, Z. Wang and X. Wang, *Chemical Engineering Science*, 2023, **282**, 119267.

100. H. Luo and Z. Wang, *Journal of Environmental Chemical Engineering*, 2022, **10**, 107156.

101. X. Zhu, R. S. Das, M. L. Bhavya, M. Garcia-Vaquero and B. K. Tiwari, *Ultrasonics Sonochemistry*, 2024, **105**, 106850.

102. F. Chemat, H. Zill e and M. K. Khan, *Ultrasonics Sonochemistry*, 2011, **18**, 813-835.

103. M. Boukroufa, C. Boutekedjiret, L. Petigny, N. Rakotomanomana and F. Chemat, *Ultrasonics Sonochemistry*, 2015, **24**, 72-79.

104. I. D. Boateng, R. Kumar, C. R. Daubert, S. Flint-Garcia, A. Mustapha, L. Kuehnel, J. Agliata, Q. Li, C. Wan and P. Somavat, *Ultrasonics Sonochemistry*, 2023, **95**, 106418.

105. Y. Li, A. S. Fabiano-Tixier, V. Tomao, G. Cravotto and F. Chemat, *Ultrasonics Sonochemistry*, 2013, **20**, 12-18.

106. H. Bagherian, F. Zokaee Ashtiani, A. Fouladitajar and M. Mohtashamy, *Chemical Engineering and Processing: Process Intensification*, 2011, **50**, 1237-1243.

107. I. G. Moorthy, J. P. Maran, S. M. Surya, S. Naganyashree and C. S. Shivamathi, *International Journal of Biological Macromolecules*, 2015, **72**, 1323-1328.

108. S. R. Chia, K. W. Chew, H. Y. Leong, S. Manickam, P. L. Show and T. H. P. Nguyen, *Chemical Engineering Journal*, 2020, **398**, 125613.

109. J. Menzio, A. Binello, A. Barge and G. Cravotto, *Processes*, 2020, **8**, 1062.

110. J. L. Dias, S. Mazzutti, J. A. L. de Souza, S. R. S. Ferreira, L. A. L. Soares, L. Stragevitch and L. Danielski, *The Journal of Supercritical Fluids*, 2019, **145**, 10-18.

111. A. Görgüç, C. Bircan and F. M. Yılmaz, *Food Chemistry*, 2019, **283**, 637-645.

112. A. Mehmood, M. Ishaq, L. Zhao, S. Yaqoob, B. Safdar, M. Nadeem, M. Munir and C. Wang, *Ultrasonics Sonochemistry*, 2019, **51**, 12-19.

113. D. Wang, Y. Yuan, T. Xie, G. Tang, G. Song, L. Li, T. Yuan, F. Zheng and J. Gong, *Industrial Crops and Products*, 2023, **191**, 116021.

114. J. Xu, X. Zhu, J. Zhang, Z. Li, W. Kang, H. He, Z. Wu and Z. Dong, *Ultrasonics Sonochemistry*, 2023, **97**, 106451.

115. S. F. Sadeghian, M. Majdinasab, M. Nejadmansouri and S. M. H. Hosseini, *Ultrasonics Sonochemistry*, 2023, **92**, 106277.

116. S.-A. Hwangbo, S.-Y. Lee, B.-A. Kim and C.-K. Moon, *Nanomaterials*, 2022, **12**, 1547.

117. M. Liu, Y. Pan, M. Feng, W. Guo, X. Fan, L. Feng, J. Huang and Y. Cao, *Ultrasonics Sonochemistry*, 2022, **90**, 106201.

118. S. Potdar, U. Bagale, I. Potoroko, V. S. Hakke, Y. Maralla, M. Sivakumar and S. Sonawane, *Materials Today: Proceedings*, 2022, **57**, 1619-1625.

119. S. Mohamadi Saani, J. Abdolalizadeh and S. Zeinali Heris, *Ultrasonics Sonochemistry*, 2019, **55**, 86-95.

120. C. Guzmán, M. A. Rojas and M. Aragón, *Cosmetics*, 2021, **8**, 1.

121. M. Draye, J. Estager and N. Kardos, in *Activation Methods*, 2019, pp. 1-93.

122. M. Draye and N. Kardos, *Topics in Current Chemistry*, 2016, **374**, 74.

123. T. J. Mason, *Chemical Society Reviews*, 1997, **26**, 443-451.

124. R. Jayarajan, H. B. Chandrashekar, A. K. Dalvi and D. Maiti, *Chemistry – A European Journal*, 2020, **26**, 11426-11430.

125. J. L. Luche, C. Einhorn, J. Einhorn and J. V. Sinisterra-Gago, *Tetrahedron Letters*, 1990, **31**, 4125-4128.

126. R. E. Apfel, in *Methods in Experimental Physics*, ed. P. D. Edmonds, Academic Press, 1981, vol. 19, pp. 355-411.

127. H. Mohapatra, M. Kleiman and A. P. Esser-Kahn, *Nature Chemistry*, 2017, **9**, 135-139.

128. K. Kubota, Y. Pang, A. Miura and H. Ito, *Science*, 2019, **366**, 1500-1504.

129. Y. Pang, J. W. Lee, K. Kubota and H. Ito, *Angewandte Chemie International Edition*, 2020, **59**, 22570-22576.

130. J. Yoon, J. Kim, F. Tieves, W. Zhang, M. Alcalde, F. Hollmann and C. B. Park, *ACS Catalysis*, 2020, **10**, 5236-5242.

131. J. Ling, K. Wang, Z. Wang, H. Huang and G. Zhang, *Ultrasonics Sonochemistry*, 2020, **61**, 104819.

132. K. R. Campos, P. J. Coleman, J. C. Alvarez, S. D. Dreher, R. M. Garbaccio, N. K. Terrett, R. D. Tillyer, M. D. Truppo and E. R. Parmee, *Science*, 2019, **363**, 244.

133. B. von Boehn, M. Foerster, M. von Boehn, J. Prat, F. Macià, B. Casals, M. W. Khaliq, A. Hernández-Mínguez, L. Aballe and R. Imbihl, *Angewandte Chemie International Edition*, 2020, **59**, 20224-20229.

134. D. Fernandez Rivas, P. Cintas and H. J. G. E. Gardeniers, *Chemical Communications*, 2012, **48**, 10935-10947.

135. D. Fernandez Rivas and S. Kuhn, *Topics in Current Chemistry*, 2016, **374**, 70.

136. K. F. Jensen, B. J. Reizman and S. G. Newman, *Lab on a Chip*, 2014, **14**, 3206-3212.

137. B. Gutmann, D. Cantillo and C. O. Kappe, *Angewandte Chemie International Edition*, 2015, **54**, 6688-6728.

138. T. S. Tran, S. J. Park, S. S. Yoo, T.-R. Lee and T. Kim, *RSC Advances*, 2016, **6**, 12003-12008.

139. N.-K. Nguyen, M.-T. Ha, H. Y. Bui, Q. T. Trinh, B. N. Tran, V. T. Nguyen, T. Q. Hung, T. T. Dang and X. H. Vu, *Catalysis Communications*, 2021, **149**, 106240.

140. J. Li, S. G. Ballmer, E. P. Gillis, S. Fujii, M. J. Schmidt, A. M. E. Palazzolo, J. W. Lehmann, G. F. Morehouse and M. D. Burke, *Science*, 2015, **347**, 1221-1226.

141. M. Trobe and M. D. Burke, *Angewandte Chemie International Edition*, 2018, **57**, 4192-4214.

142. A.-C. Bédard, A. Adamo, K. C. Aroh, M. G. Russell, A. A. Bedermann, J. Torosian, B. Yue, K. F. Jensen and T. F. Jamison, *Science*, 2018, **361**, 1220-1225.

143. D. Angelone, A. J. S. Hammer, S. Rohrbach, S. Krambeck, J. M. Granda, J. Wolf, S. Zalesskiy, G. Chisholm and L. Cronin, *Nature Chemistry*, 2021, **13**, 63-69.

144. B. J. Shields, J. Stevens, J. Li, M. Parasram, F. Damani, J. I. M. Alvarado, J. M. Janey, R. P. Adams and A. G. Doyle, *Nature*, 2021, **590**, 89-96.

145. Y. Shi, P. L. Prieto, T. Zepel, S. Grunert and J. E. Hein, *Accounts of Chemical Research*, 2021, **54**, 546-555.

146. D. Schieppati, F. Galli, M. L. Peyot, V. Yargeau, C. L. Bianchi and D. C. Boffito, *Ultrasonics Sonochemistry*, 2019, **54**, 302-310.

147. E. A. Serna-Galvis, J. Lee, F. Hernández, A. M. Botero-Coy and R. A. Torres-Palma, in *Removal and Degradation of Pharmaceutically Active Compounds in Wastewater Treatment*, eds. S. Rodriguez-Mozaz, P. Blánquez Cano and M. Sarrà Adroguer, Springer International Publishing, Cham, 2021, pp. 349-381.

148. İ. Deveci and B. Mercimek, *Ultrasonics Sonochemistry*, 2019, **51**, 197-205.

149. D. Meroni, C. L. Bianchi, D. C. Boffito, G. Cerrato, A. Bruni, M. Sartirana and E. Falletta, *Ultrasonics Sonochemistry*, 2021, **75**, 105615.

150. S. Aluthgun Hewage, J. H. Batagoda and J. N. Meegoda, *Environmental Pollution*, 2021, **274**, 116538.

151. A. Agarwal, Y. Zhou and Y. Liu, *Environmental Science and Pollution Research*, 2016, **23**, 23876-23883.

152. F. Zhao, Q. Yan and D. Cheng, *Ultrasonics Sonochemistry*, 2021, **78**, 105745.

153. S. He, X. Tan, X. Hu and Y. Gao, *Environmental Technology*, 2019, **40**, 1401-1407.

154. J.-Y. Oh, S.-D. Choi, H.-O. Kwon and S.-E. Lee, *Ultrasonics Sonochemistry*, 2016, **33**, 61-66.

155. J. Bandelin, T. Lippert, J. E. Drewes and K. Koch, *Ultrasonics Sonochemistry*, 2018, **42**, 672-678.

156. S. Anandan, V. Kumar Ponnusamy and M. Ashokkumar, *Ultrasonics Sonochemistry*, 2020, **67**, 105130.

157. Q. Xu, H. Zhang, H. Leng, H. You, Y. Jia and S. Wang, *Ultrasonics Sonochemistry*, 2021, **78**, 105750.

158. K. M. Tripathi, T. S. Tran, Y. J. Kim and T. Kim, *ACS Sustainable Chemistry & Engineering*, 2017, **5**, 3982-3992.

159. D. Xia, J. Wu and K. Su, *Journal of Environmental Chemical Engineering*, 2022, **10**, 108685.

160. E. A. Serna-Galvis, J. Silva-Agredo, J. Lee, A. Echavarría-Isaza and R. A. Torres-Palma, *Molecules*, 2023, **28**, 1113.

161. L. Stępniak and E. Stańczyk-Mazanek, *Energies*, 2022, **15**, 5186.

162. A. Rosales Pérez and K. Esquivel Escalante, *ChemPlusChem*, 2024, **89**, e202300660.

163. D. Meroni, R. Djellabi, M. Ashokkumar, C. L. Bianchi and D. C. Boffito, *Chemical Reviews*, 2022, **122**, 3219-3258.

164. S. Sengupta and V. K. Balla, *Journal of Advanced Research*, 2018, **14**, 97-111.

165. Z. Izadifar, P. Babyn and D. Chapman, *Journal of Medical and Biological Engineering*, 2019, **39**, 259-276.

166. C. C. Church and E. L. Carstensen, *Ultrasound in Medicine & Biology*, 2001, **27**, 1435-1437.

167. P. Ma, X. Lai, Z. Luo, Y. Chen, X. J. Loh, E. Ye, Z. Li, C. Wu and Y.-L. Wu, *Nanoscale Advances*, 2022, **4**, 3462-3478.

168. M. Grundy, L. Bau, C. Hill, C. Paverd, C. Mannaris, J. Kwan, C. Crake, C. Coviello, C. Coussios and R. Carlisle, *Nanomedicine*, 2021, **16**, 37-50.

169. M. T. Reza, N. N. I. Moubarak, M. R. Islam, M. R. H. Khan and M. M. Nishat, *Sensing and Bio-Sensing Research*, 2023, **39**, 100553.

170. A. Shanei, H. Akbari-Zadeh, N. Attaran, M. R. Salamat and M. Baradaran-Ghahfarokhi, *Ultrasonics*, 2020, **102**, 106061.

171. Q. Lacerda, H. Falatah, J.-B. Liu, C. E. Wessner, B. Oeffinger, A. Rochani, D. B. Leeper, F. Forsberg, J. M. Curry, G. Kaushal, S. W. Keith, P. O'Kane, M. A. Wheatley and J. R. Eisenbrey, *Pharmaceutics*, 2023, **15**, 1302.

172. X. Su, M. Rakshit, P. Das, I. Gupta, D. Das, M. Pramanik, K. W. Ng and J. Kwan, *ACS Applied Materials & Interfaces*, 2021, **13**, 24422-24430.

173. B. Lyons, J. Hettinga, J. Balkaran, A. Collins, M. Maardalen, P. Katti, C. Mannaris, L. Bau, C. Smith, M. Gray, J. Kwan, R. Carlisle and C. Coussios, *The Journal of the Acoustical Society of America*, 2021, **150**, A54-A54.

174. G. Kim, J. Won, C.-W. Kim, J.-R. Park and D. Park, *Langmuir*, 2024, **40**, 91-99.

175. Y. Shen, J. Ou, X. Chen, X. Zeng, L. Huang, Z. Pi, Y. Hu, S. Chen and T. Chen, *BioMedical Engineering OnLine*, 2020, **19**, 52.

176. P. Shrimal, G. Jadeja and S. Patel, *International Journal of Pharmaceutics*, 2022, **620**, 121754.

177. H. Horsley, J. Owen, R. Browning, D. Carugo, J. Malone-Lee, E. Stride and J. L. Rohn, *Journal of Controlled Release*, 2019, **301**, 166-175.

178. G. Wang, W. Wu, J.-J. Zhu and D. Peng, *Ultrasonics Sonochemistry*, 2021, **79**, 105781.

179. R. V. Kumar, Y. Diamant and A. Gedanken, *Chemistry of Materials*, 2000, **12**, 2301-2305.

180. J. A. Fuentes-García, J. Santoyo-Salzar, E. Rangel-Cortes, G. F. Goya, V. Cardozo-Mata and J. A. Pescador-Rojas, *Ultrasonics Sonochemistry*, 2021, **70**, 105274.

181. A.-L. Morel, S. I. Nikitenko, K. Gionnet, A. Wattiaux, J. Lai-Kee-Him, C. Labrugere, B. Chevalier, G. Deleris, C. Petibois, A. Brisson and M. Simonoff, *ACS Nano*, 2008, **2**, 847-856.

182. S. Anandan, F. Grieser and M. Ashokkumar, *The Journal of Physical Chemistry C*, 2008, **112**, 15102-15105.

183. T. S. Tran, N. K. Dutta and N. R. Choudhury, *Advances in Colloid and Interface Science*, 2018, **261**, 41-61.

184. T. S. Tran, N. K. Dutta and N. R. Choudhury, *ACS Applied Nano Materials*, 2020, **3**, 11608-11619.

185. Q. T. Trinh, T. Le Van, T. T. N. Phan, K. P. Ong, H. Kosslick, P. N. Amaniampong, M. B. Sullivan, H.-S. Chu, H. An, T.-K. Nguyen, J. Zhang, J. Zhang, P. T. Huyen and N.-T. Nguyen, *Journal of Alloys and Compounds*, 2024, **1002**, 175322.

186. T. S. Tran, R. Balu, C. K. Nguyen, J. Mata, V. K. Truong, N. K. Dutta and N. R. Choudhury, *ACS Applied Nano Materials*, 2023, **6**, 908-917.

187. T. S. Tran, R. Balu, L. de Campo, N. K. Dutta and N. R. Choudhury, *Energy Advances*, 2023, **2**, 365-374.

188. P. Myagmarsereejid, S. Suragtkhuu, Q. T. Trinh, T. Gould, N. T. Nguyen, M. Bat-Erdene, E. Campbell, M. T. Hoang, W.-H. Chiu, Q. Li, H. Wang, Y. L. Zhong and M. Batmunkh, *npj 2D Materials and Applications*, 2024, **8**, 38.

189. T. S. Tran, R. Balu, J. Mata, N. K. Dutta and N. R. Choudhury, *Nano Trends*, 2023, **2**, 100011.

190. P. N. Amaniampong, Q. T. Trinh, B. Wang, A. Borgna, Y. Yang and S. H. Mushrif, *Angewandte Chemie International Edition*, 2015, **54**, 8928-8933.

191. J. J. Varghese, Q. T. Trinh and S. H. Mushrif, *Catalysis Science & Technology*, 2016, **6**, 3984-3996.

192. J. Mondal, Q. T. Trinh, A. Jana, W. K. H. Ng, P. Borah, H. Hirao and Y. Zhao, *ACS Applied Materials & Interfaces*, 2016, **8**, 15307-15319.

193. C. Sarkar, S. C. Shit, D. Q. Dao, J. Lee, N. H. Tran, R. Singuru, K. An, D. N. Nguyen, Q. V. Le, P. N. Amaniampong, A. Drif, F. Jerome, P. T. Huyen, T. T. N. Phan, D.-V. N. Vo, N. Thanh Binh, Q. T. Trinh, M. P. Sherburne and J. Mondal, *Green Chemistry*, 2020, **22**, 2049-2068.

194. R. Singuru, Q. T. Trinh, B. Banerjee, B. Govinda Rao, L. Bai, A. Bhaumik, B. M. Reddy, H. Hirao and J. Mondal, *ACS Omega*, 2016, **1**, 1121-1138.

195. N. H. Tran, L. Hoang, L. D. Nghiem, N. M. H. Nguyen, H. H. Ngo, W. Guo, Q. T. Trinh, N. H. Mai, H. Chen, D. D. Nguyen, T. T. Ta and K. Y.-H. Gin, *Science of The Total Environment*, 2019, **692**, 157-174.

196. Y. Zhao, D. Liu, W. Huang, Y. Yang, M. Ji, L. D. Nghiem, Q. T. Trinh and N. H. Tran, *Bioresource Technology*, 2019, **288**, 121619.

197. N. H. Tran, Q. T. Trinh and Q. B. Nguyen, *Science of The Total Environment*, 2019, **685**, 1308-1309.

198. P. Qiu, B. Park, J. Choi, B. Thokchom, A. B. Pandit and J. Khim, *Ultrasonics Sonochemistry*, 2018, **45**, 29-49.

199. G. Wang and H. Cheng, *Molecules*, 2023, **28**, 3706.

200. S. Soni, A. Kumari, S. Sharma, A. Sharma, V. Sheel, R. Thakur, S. K. Bhatia and A. K. Sharma, *Journal of the Taiwan Institute of Chemical Engineers*, 2024, 105565.

201. P. Liu, Z. Wu, A. V. Abramova and G. Cravotto, *Ultrasonics Sonochemistry*, 2021, **74**, 105566.

202. J. Abdi, A. J. Sisi, M. Hadipoor and A. Khataee, *Journal of Hazardous Materials*, 2022, **424**, 127558.

203. P. Dhull, A. Sudhaik, P. Raizada, S. Thakur, V.-H. Nguyen, Q. Van Le, N. Kumar, A. A. Parwaz Khan, H. M. Marwani, R. Selvasembian and P. Singh, *Chemosphere*, 2023, **333**, 138873.

204. B.-M. Jun, J. Han, C. M. Park and Y. Yoon, *Ultrasonics Sonochemistry*, 2020, **64**, 104993.

205. A. Ucar, *Russian Journal of Applied Chemistry*, 2022, **95**, 1364-1372.

206. M. Dastborhan, A. Khataee, S. Arefi-Oskoui and Y. Yoon, *Ultrasonics Sonochemistry*, 2022, **87**, 106058.

207. K. Saravanakumar, A. Fayyaz, S. Park, Y. Yoon, Y. M. Kim and C. M. Park, *Journal of Molecular Liquids*, 2021, **344**, 117740.

208. S. S. Magdum, M. Bhosale, G. Palanisamy, K. Selvakumar, S. Thangarasu and T. H. Oh, *Journal of Water Process Engineering*, 2024, **59**, 104997.

209. M. Sadeghi, S. Farhadi and A. Zabardasti, *New Journal of Chemistry*, 2020, **44**, 20878-20894.

210. A. Jamal Sisi, A. Khataee, M. Fathinia, B. Vahid and Y. Orooji, *Journal of Molecular Liquids*, 2020, **316**, 113801.

211. Y. Vasseghian, E.-N. Dragoi, F. Almomani and V. T. Le, *Chemosphere*, 2022, **287**, 132387.

212. G. Li, Y. Cao, L. Yi, J. Wang and Y. Song, *Journal of Chemical Technology & Biotechnology*, 2020, **95**, 1756-1772.

213. G. Wang and H. Cheng, *Science of The Total Environment*, 2023, **901**, 165833.

214. J. Qiao, H. Zhang, G. Li, S. Li, Z. Qu, M. Zhang, J. Wang and Y. Song, *Separation and Purification Technology*, 2019, **211**, 843-856.

215. G. Wang, S. Li, X. Ma, J. Qiao, G. Li, H. Zhang, J. Wang and Y. Song, *Ultrasonics Sonochemistry*, 2018, **45**, 150-166.

216. J. Qiao, M. Lv, Z. Qu, M. Zhang, X. Cui, D. Wang, C. Piao, Z. Liu, J. Wang and Y. Song, *Science of The Total Environment*, 2019, **689**, 178-192.

217. M. F. Dadjour, C. Ogino, S. Matsumura and N. Shimizu, *Biochemical Engineering Journal*, 2005, **25**, 243-248.

218. M. Farshbaf Dadjour, C. Ogino, S. Matsumura, S. Nakamura and N. Shimizu, *Water Research*, 2006, **40**, 1137-1142.

219. C. Ogino, M. Farshbaf Dadjour, K. Takaki and N. Shimizu, *Biochemical Engineering Journal*, 2006, **32**, 100-105.

220. K. Shanmugam Ranjith, S. Majid Ghoreishian, S. Han, N. R. Chodankar, G. Seeta Rama Raju, S. J. Marje, Y. S. Huh and Y.-K. Han, *Ultrasonics Sonochemistry*, 2023, **99**, 106570.

221. S. Haddadi, A. Khataee, S. Arefi-Oskoui, B. Vahid, Y. Orooji and Y. Yoon, *Ultrasonics Sonochemistry*, 2023, **92**, 106255.

222. Á. d. J. Ruíz-Baltazar, *Ultrasonics Sonochemistry*, 2021, **73**, 105521.

223. Q. Liu, L. Shi, Y. Liao, X. Cao, X. Liu, Y. Yu, Z. Wang, X. Lu and J. Wang, *Advanced Science*, 2022, **9**, 2200005.

224. Z. Feng, X. Xiang, J. Huang, L. Wang, B. Zhu, H. Zhou, H. Pang, C. Cheng, L. Ma and L. Qiu, *Advanced Functional Materials*, 2023, **33**, 2302579.

225. S. Son, J. H. Kim, X. Wang, C. Zhang, S. A. Yoon, J. Shin, A. Sharma, M. H. Lee, L. Cheng, J. Wu and J. S. Kim, *Chemical Society Reviews*, 2020, **49**, 3244-3261.

226. F. Yang, J. Lv, W. Ma, Y. Yang, X. Hu and Z. Yang, *Small*, 2024, **n/a**, 2402669.

227. S. Liu, K. Dou, B. Liu, M. Pang, P. a. Ma and J. Lin, *Angewandte Chemie International Edition*, 2023, **62**, e202301831.

228. M. Chang, L. Zhang, Z. Wang, L. Chen, Y. Dong, J. Yang and Y. Chen, *Advanced Drug Delivery Reviews*, 2024, **205**, 115160.

229. G. Chen, J. Du, L. Gu, Q. Wang, Q. Qi, X. Li, R. Zhang, H. Yang, Y. Miao and Y. Li, *Chemical Engineering Journal*, 2024, **482**, 148953.

230. J. Yagi, A. Ikeda, L.-C. Wang, C.-S. Yeh and H. Kawasaki, *The Journal of Physical Chemistry C*, 2022, **126**, 19693-19704.

231. J. Fouladi, A. AlNouss and T. Al-Ansari, *Journal of Cleaner Production*, 2023, **418**, 138071.

232. J. G. Segovia-Hernández, G. Contreras-Zarazúa and C. Ramírez-Márquez, *RSC Sustainability*, 2023, **1**, 1332-1353.

233. K. B. Ansari, S. Z. Hassan, S. A. Farooqui, R. Hasib, P. Khan, A. R. S. Rahman, M. S. Khan and Q. T. Trinh, in *Green Diesel: An Alternative to Biodiesel and Petrodiesel*, eds. M. Aslam, S. Shivaji Maktedar and A. K. Sarma, Springer Nature Singapore, Singapore, 2022, pp. 351-375.

234. D. B. Nguyen, S. Saud, Q. T. Trinh, H. An, N.-T. Nguyen, Q. H. Trinh, H. T. Do, Y. S. Mok and W. G. Lee, *Plasma Chemistry and Plasma Processing*, 2023, **43**, 1475-1488.

235. R. Paul, R. Das, N. Das, S. Chakraborty, C.-W. Pao, Q. Thang Trinh, G. T. K. Kalhara Gunasooriya, J. Mondal and S. C. Peter, *Angewandte Chemie International Edition*, 2023, **62**, e202311304.

236. G. Liu, P. R. Narangari, Q. T. Trinh, W. Tu, M. Kraft, H. H. Tan, C. Jagadish, T. S. Choksi, J. W. Ager, S. Karuturi and R. Xu, *ACS Catalysis*, 2021, **11**, 11416-11428.

237. A. Denra, S. Saud, D. B. Nguyen, Q. T. Trinh, T.-K. Nguyen, H. An, N.-T. Nguyen, S. Teke and Y. S. Mok, *Journal of Cleaner Production*, 2024, **436**, 140618.

238. M. Paquin, É. Loranger, V. Hannaux, B. Chabot and C. Daneault, *Ultrasonics Sonochemistry*, 2013, **20**, 103-108.

239. P. N. Amaniampong and F. Jérôme, *Current Opinion in Green and Sustainable Chemistry*, 2020, **22**, 7-12.

240. A. Hernoux-Villière, U. Lassi and J.-M. Lévêque, *Ultrasonics Sonochemistry*, 2013, **20**, 1341-1344.

241. M. Kunaver, E. Jasiukaitytė and N. Čuk, *Bioresource Technology*, 2012, **103**, 360-366.

242. M. Montalbo-Lomboy, L. Johnson, S. K. Khanal, J. van Leeuwen and D. Grewell, *Bioresource Technology*, 2010, **101**, 351-358.

243. S. Tallarico, P. Costanzo, S. Bonacci, A. Macario, M. L. Di Gioia, M. Nardi, A. Procopio and M. Oliverio, *Scientific Reports*, 2019, **9**, 18858.

244. D. Rinsant, G. Chatel and F. Jérôme, *ChemCatChem*, 2014, **6**, 3355-3359.

245. F. Napoly, N. Kardos, L. Jean-Gérard, C. Goux-Henry, B. Andrioletti and M. Draye, *Industrial & Engineering Chemistry Research*, 2015, **54**, 6046-6051.

246. A. Sarwono, Z. Man, N. Muhammad, A. S. Khan, W. S. W. Hamzah, A. H. A. Rahim, Z. Ullah and C. D. Wilfred, *Ultrasonics Sonochemistry*, 2017, **37**, 310-319.

247. S. Marullo, C. Rizzo, A. Meli and F. D'Anna, *ACS Sustainable Chemistry & Engineering*, 2019, **7**, 5818-5826.

248. R. Behling, G. Chatel and S. Valange, *Ultrasonics Sonochemistry*, 2017, **36**, 27-35.

249. B. Liu, B. Du, Y. Sun, M. Zhu, Y. Yang, X. Wang and J. Zhou, *Fuel Processing Technology*, 2020, **203**, 106387.

250. Z. M. A. Bundhoo and R. Mohee, *Ultrasonics Sonochemistry*, 2018, **40**, 298-313.

251. M. J. Bussemaker, F. Xu and D. Zhang, *Bioresource Technology*, 2013, **148**, 15-23.

252. Q. T. Trinh, B. K. Chethana and S. H. Mushrif, *The Journal of Physical Chemistry C*, 2015, **119**, 17137-17145.

253. B. Du, C. Chen, Y. Sun, M. Yu, M. Yang, X. Wang and J. Zhou, *Fuel Processing Technology*, 2020, **206**, 106479.

254. B. Du, B. Liu, X. Wang and J. Zhou, *ChemistryOpen*, 2019, **8**, 643-649.

255. B. Du, B. Liu, Y. Yang, X. Wang and J. Zhou, *Catalysts*, 2019, **9**, 399.

256. P. Bujak, P. Bartczak and J. Polanski, *Journal of Catalysis*, 2012, **295**, 15-21.

257. B. Toukoniitty, J. Kuusisto, J.-P. Mikkola, T. Salmi and D. Y. Murzin, *Industrial & Engineering Chemistry Research*, 2005, **44**, 9370-9375.

258. T. Bahry, S. Jiang, U. Jonnalagadda, W. Liu, B. Teychene, F. Jerome, S. H. Mushrif and P. N. Amaniampong, *Catalysis Science & Technology*, 2023, **13**, 2982-2993.

259. P. N. Amaniampong, Q. T. Trinh, K. Li, S. H. Mushrif, Y. Hao and Y. Yang, *Catalysis Today*, 2018, **306**, 172-182.

260. K. B. Ansari, A. Banerjee, S. Z. Hassan, M. Danish, I. Arman, P. Khan, A. R. Shakeelur Rahman, Q. N. Ahmad and Q. T. Trinh, in *2D Nanomaterials for CO2 Conversion into Chemicals and Fuels*, eds. K. K. Sadasivuni, K. Kannan, A. M. Abdullah and B. Kumar, The Royal Society of Chemistry, 2022, p. 0.

261. O. Mohan, Q. T. Trinh, A. Banerjee and S. H. Mushrif, *Molecular Simulation*, 2019, **45**, 1163-1172.

262. Q. Hassan, S. Algburi, A. Z. Sameen, M. Jaszczur and H. M. Salman, *Environment Systems and Decisions*, 2024, **44**, 327-350.

263. Q. T. Trinh, J. Yang, J. Y. Lee and M. Saeys, *Journal of Catalysis*, 2012, **291**, 26-35.

264. R. Li, Z. Liu, Q. T. Trinh, Z. Miao, S. Chen, K. Qian, R. J. Wong, S. Xi, Y. Yan, A. Borgna, S. Liang, T. Wei, Y. Dai, P. Wang, Y. Tang, X. Yan, T. S. Choksi and W. Liu, *Advanced Materials*, 2021, **33**, 2101536.

265. M. A. Tekalgne, K. V. Nguyen, D. L. T. Nguyen, V.-H. Nguyen, T. P. Nguyen, D.-V. N. Vo, Q. T. Trinh, A. Hasani, H. H. Do, T. H. Lee, H. W. Jang, H. S. Le, Q. V. Le and S. Y. Kim, *Journal of Alloys and Compounds*, 2020, **823**, 153897.

266. P. J. Buchanan, Z. Chase, R. J. Matear, S. J. Phipps and N. L. Bindoff, *Nature Communications*, 2019, **10**, 4611.

267. N. Ojha, K. K. Pant and E. Coy, *Industrial & Engineering Chemistry Research*, 2023, **62**, 21885-21908.

268. W. Qi, J. Liu, X. Guo, H. Guo, T. Thomas, Y. Zhu, S. Liu and M. Yang, *ACS Applied Nano Materials*, 2023, **6**, 2636-2645.

269. B. G. Pollet, F. Foroughi, A. Y. Faid, D. R. Emberson and M. H. Islam, *Ultrasonics Sonochemistry*, 2020, **69**, 105238.

270. F. Foroughi, C. Immanuel Bernäcker, L. Röntzsch and B. G. Pollet, *Ultrasonics Sonochemistry*, 2022, **84**, 105979.

271. T. Zhang, Q. Zheng, J. Huang and X. Li, *Advanced Functional Materials*, 2024, **34**, 2311029.

272. Z. Ding, M. Sun, W. Liu, W. Sun, X. Meng and Y. Zheng, *Separation and Purification Technology*, 2021, **276**, 119287.

273. S. S. Rashwan, I. Dincer and A. Mohany, *International Journal of Energy Research*, 2019, **43**, 1045-1048.

274. S. S. Rashwan, I. Dincer, A. Mohany and B. G. Pollet, *International Journal of Hydrogen Energy*, 2019, **44**, 14500-14526.

275. M. H. Islam, O. S. Burheim and B. G. Pollet, *Ultrasonics Sonochemistry*, 2019, **51**, 533-555.

276. S. Merouani, O. Hamdaoui, Y. Rezgui and M. Guemini, *International Journal of Hydrogen Energy*, 2016, **41**, 832-844.

277. S. Merouani, O. Hamdaoui, Y. Rezgui and M. Guemini, *Ultrasonics Sonochemistry*, 2015, **22**, 41-50.

278. S. S. Rashwan, I. Dincer and A. Mohany, *International Journal of Hydrogen Energy*, 2020, **45**, 20808-20819.

279. L. Venault, R. Guillaumont and P. Université de, 1997.

280. M. Yuan, S. Liang, L. Yang, F. Li, B. Liu, C. Yang, Z. Yang, Y. Bian, P. a. Ma, Z. Cheng and J. Lin, *Advanced Materials*, 2023, **35**, 2209589.

281. J. Shi, *National Science Review*, 2023, **10**.

282. C. Xia, A. Wu, Z. Jin, L. Zeng, L. Jiang, Q. Xu, M. Fan and Q. He, *Biomaterials*, 2023, **296**, 122090.

283. Y. Wang, D. Zhao, H. Ji, G. Liu, C. Chen, W. Ma, H. Zhu and J. Zhao, *The Journal of Physical Chemistry C*, 2010, **114**, 17728-17733.

284. Y. Zhang, H. Khanbareh, S. Dunn, C. R. Bowen, H. Gong, N. P. H. Duy and P. T. T. Phuong, *Advanced Science*, 2022, **9**, 2105248.

285. G. Glockler, *The Journal of Physical Chemistry*, 1958, **62**, 1049-1054.

286. M. H. Islam, O. S. Burheim, J.-Y. Hihn and B. G. Pollet, *Ultrasonics Sonochemistry*, 2021, **73**, 105474.

287. M. Yuan, L. Yang, Z. Yang, Z. Ma, J. Ma, Z. Liu, P. a. Ma, Z. Cheng, A. Maleki and J. Lin, *Advanced Science*, 2024, **11**, 2308546.

288. M. H. Islam, H. Mehrabi, R. H. Coridan, O. S. Burheim, J.-Y. Hihn and B. G. Pollet, *Ultrasonics Sonochemistry*, 2021, **72**, 105401.

289. J. Ma, X. Xiong, C. Ban, K. Wang, J.-Y. Dai and X. Zhou, *Applied Physics Letters*, 2022, **121**.

290. H. Maimaitizi, A. Abulizi, T. Zhang, K. Okitsu and J.-j. Zhu, *Ultrasonics Sonochemistry*, 2020, **63**, 104956.

291. K. S. Ranjith, S. M. Ghoreishian, R. Umapathi, G. S. R. Raju, H. U. Lee, Y. S. Huh and Y.-K. Han, *Ultrasonics Sonochemistry*, 2023, **100**, 106623.

292. V. S. Moholkar and M. M. C. G. Warmoeskerken, *AIChE Journal*, 2003, **49**, 2918-2932.

293. M. Toma, S. Fukutomi, Y. Asakura and S. Koda, *Ultrasonics Sonochemistry*, 2011, **18**, 197-208.

294. J. j. Zhou, H. m. Peng and J. h. Hu, 2011.

295. S. Koda, T. Kimura, T. Kondo and H. Mitome, *Ultrasonics Sonochemistry*, 2003, **10**, 149-156.

296. N. P. Vichare, P. Senthilkumar, V. S. Moholkar, P. R. Gogate and A. B. Pandit, *Industrial & Engineering Chemistry Research*, 2000, **39**, 1480-1486.

297. J.-M. Löning, C. Horst and U. Hoffmann, *Ultrasonics Sonochemistry*, 2002, **9**, 169-179.

298. J. A. Kewalramani, B. Bezerra de Souza, R. W. Marsh and J. N. Meegoda, *Ultrasonics Sonochemistry*, 2023, **98**, 106529.

299. Y. Asakura and K. Yasuda, *Ultrasonics Sonochemistry*, 2021, **81**, 105858.

300. B. Verhaagen, Y. Liu, A. G. Pérez, E. Castro-Hernandez and D. Fernandez Rivas, *ChemistrySelect*, 2016, **1**, 136-139.

301. R. Feng, Y. Zhao, C. Zhu and T. J. Mason, *Ultrasonics Sonochemistry*, 2002, **9**, 231-236.

302. S. Asgharzadehahmadi, A. A. Abdul Raman, R. Parthasarathy and B. Sajjadi, *Renewable and Sustainable Energy Reviews*, 2016, **63**, 302-314.

303. Y. T. Didenko and K. S. Suslick, *Nature*, 2002, **418**, 394-397.

304. D. B. Rajamma, S. Anandan, N. S. M. Yusof, B. G. Pollet and M. Ashokkumar, *Ultrasonics Sonochemistry*, 2021, **72**, 105413.

305. M. W. A. Kuijpers, M. F. Kemmere and J. T. F. Keurentjes, *Ultrasonics*, 2002, **40**, 675-678.

306. I. Garcia-Vargas, O. Louisnard and L. Barthe, *Ultrasonics Sonochemistry*, 2023, **99**, 106542.

307. K. Yasuda, T. T. Nguyen and Y. Asakura, *Ultrasonics Sonochemistry*, 2018, **43**, 23-28.

308. K. Y. Kim, K.-T. Byun and H.-Y. Kwak, *Chemical Engineering Journal*, 2007, **132**, 125-135.

309. S. Niazi, S. H. Hashemabadi and M. M. Razi, *Chemical Engineering Research and Design*, 2014, **92**, 166-173.

310. Y. Son, M. Lim, J. Khim and M. Ashokkumar, *Ultrasonics Sonochemistry*, 2012, **19**, 16-21.

311. Y. Asakura, T. Nishida, T. Matsuoka and S. Koda, *Ultrasonics Sonochemistry*, 2008, **15**, 244-250.

312. J. Collins, T. G. McKenzie, M. D. Nothling, M. Ashokkumar and G. G. Qiao, *Polymer Chemistry*, 2018, **9**, 2562-2568.

313. M. A. Beckett and I. Hua, *The Journal of Physical Chemistry A*, 2001, **105**, 3796-3802.

314. S. Merouani and O. Hamdaoui, *Ultrasonics Sonochemistry*, 2016, **32**, 320-327.

315. J. Chen, C. Fei, D. Lin, P. Gao, J. Zhang, Y. Quan, D. Chen, D. Li and Y. Yang, *Frontiers in Materials*, 2022, **8**.

316. M. Singla and N. Sit, in *Energy Aspects of Acoustic Cavitation and Sonochemistry*, eds. O. Hamdaoui and K. Kerboua, Elsevier, 2022, pp. 349-373.

317. C. Mannaris, B. M. Teo, A. Seth, L. Bau, C. Coussios and E. Stride, *Advanced Healthcare Materials*, 2018, **7**, 1800184.

318. Z. Gao, W. Wu and B. Wang, *Journal of Fluid Mechanics*, 2021, **911**, A20.

319. R. Myers, C. Coviello, P. Erbs, J. Foloppe, C. Rowe, J. Kwan, C. Crake, S. Finn, E. Jackson, J.-M. Balloul, C. Story, C. Coussios and R. Carlisle, *Molecular Therapy*, 2016, **24**, 1627-1633.

320. A. Sazgarnia, A. Shanei, A. R. Taheri, N. T. Meibodi, H. Eshghi, N. Attaran and M. M. Shanei, *Journal of Ultrasound in Medicine*, 2013, **32**, 475-483.

321. A. Yildirim, R. Chattaraj, N. T. Blum and A. P. Goodwin, *Chemistry of Materials*, 2016, **28**, 5962-5972.

322. J. J. Kwan, G. Lajoinie, N. de Jong, E. Stride, M. Versluis and C. C. Coussios, *Physical Review Applied*, 2016, **6**, 044004.

323. Y. Zhao, Y. Zhu, J. Fu and L. Wang, *Chemistry – An Asian Journal*, 2014, **9**, 790-796.

324. Q. Feng, W. Zhang, X. Yang, Y. Li, Y. Hao, H. Zhang, L. Hou and Z. Zhang, *Advanced Healthcare Materials*, 2018, **7**, 1700957.

325. X. Su, U. S. Jonnalagadda, L. D. Bharatula and J. J. Kwan, *Ultrasonics Sonochemistry*, 2021, **79**, 105753.

326. U. S. Jonnalagadda, X. Su and J. J. Kwan, *Ultrasonics Sonochemistry*, 2021, **73**, 105530.

327. Z. Zong, E. Gilbert, C. C. Y. Wong, L. Usadi, Y. Qin, Y. Huang, J. Raymond, N. Hankins and J. Kwan, *Ultrasonics Sonochemistry*, 2023, **101**, 106669.

328. C. C. Y. Wong, J. L. Raymond, L. N. Usadi, Z. Zong, S. C. Walton, A. C. Sedgwick and J. Kwan, *Ultrasonics Sonochemistry*, 2023, **99**, 106559.

329. G. M. Whitesides, *Nature*, 2006, **442**, 368-373.

330. X. Yao, Y. Zhang, L. Du, J. Liu and J. Yao, *Renewable and Sustainable Energy Reviews*, 2015, **47**, 519-539.

331. P. L. Suryawanshi, S. P. Gumfekar, B. A. Bhanvase, S. H. Sonawane and M. S. Pimplapure, *Chemical Engineering Science*, 2018, **189**, 431-448.

332. A. Tanimu, S. Jaenicke and K. Alhooshani, *Chemical Engineering Journal*, 2017, **327**, 792-821.

333. H. Feng, Y. Zhang, J. Liu and D. Liu, *Molecules*, 2022, **27**, 8052.

334. J. Jordens, A. Honings, J. Degrève, L. Braeken and T. V. Gerven, *Ultrasonics Sonochemistry*, 2013, **20**, 1345-1352.

335. L. Johansson, J. Enlund, S. Johansson, I. Katardjiev and V. Yantchev, *Biomedical Microdevices*, 2012, **14**, 279-289.

336. J. Friend and L. Y. Yeo, *Reviews of Modern Physics*, 2011, **83**, 647-704.

337. Y. Iida, K. Yasui, T. Tuziuti, M. Sivakumar and Y. Endo, *Chemical Communications*, 2004, DOI: 10.1039/B410015H, 2280-2281.

338. Y. Iida, T. Tuziuti, K. Yasui, A. Towata and T. Kozuka, *Ultrasonics Sonochemistry*, 2007, **14**, 621-626.

339. S. Hübner, S. Kressirer, D. Kralisch, C. Bludszuweit-Philipp, K. Lukow, I. Jänich, A. Schilling, H. Hieronymus, C. Liebner and K. Jähnisch, *ChemSusChem*, 2012, **5**, 279-288.

340. D. Fernandez Rivas, A. Prosperetti, A. G. Zijlstra, D. Lohse and H. J. G. E. Gardeniers, *Angewandte Chemie International Edition*, 2010, **49**, 9699-9701.

341. P. Mohanty, R. Mahapatra, P. Padhi, C. V. V. Ramana and D. K. Mishra, *Nano-Structures & Nano-Objects*, 2020, **23**, 100475.

342. B. Richard, C. Shahana, R. Vivek, A. R. M and P. A. Rasheed, *Nanoscale*, 2023, **15**, 18156-18172.

343. K. Yiannacou and V. Sariola, *Langmuir*, 2021, **37**, 4192-4199.

344. W. Kim, B. Cha, J. S. Jeon and J. Park, *Sensors and Actuators B: Chemical*, 2023, **393**, 134132.

345. Y. Bian, F. Guo, S. Yang, Z. Mao, H. Bachman, S.-Y. Tang, L. Ren, B. Zhang, J. Gong, X. Guo and T. J. Huang, *Microfluidics and Nanofluidics*, 2017, **21**, 132.

346. E. Nieves, G. Vite, A. Kozina and L. F. Olguin, *Ultrasonics Sonochemistry*, 2021, **74**, 105556.

347. Y. Liu, J. Ran, S. Yin, S. Li, W. Huang and L. Zhang, *Chemical Engineering and Processing - Process Intensification*, 2023, **194**, 109573.

348. P. Zhao, Y. Peng, Y. Wang, Y. Hu, J. Qin, D. Li, K. Yan and Z. Fan, *Ultrasonics Sonochemistry*, 2023, **101**, 106709.

349. Z. Liu, M. Yang, W. Yao, T. Wang and G. Chen, *Chemical Engineering Science*, 2023, **280**, 119052.

350. S. Zhao, C. Yao, L. Liu and G. Chen, *Chemical Engineering Journal*, 2022, **450**, 138185.

351. H. Wang, F. Yuan, Z. Xie, C. Sun, F. Wu, R. Mikhaylov, M. Shen, J. Yang, Y. Zhou, D. Liang, X. Sun, Z. Wu, Z. Yang and X. Yang, *Applied Acoustics*, 2023, **205**, 109258.

352. D. Huang, J. Wang, J. Che, B. Wen and W. Kong, *Biomedical Technology*, 2023, **1**, 1-9.

353. Y. Fan, X. Wang, J. Ren, F. Lin and J. Wu, *Microsystems & Nanoengineering*, 2022, **8**, 94.

354. J. M. Rothberg, T. S. Ralston, A. G. Rothberg, J. Martin, J. S. Zahorian, S. A. Alie, N. J. Sanchez, K. Chen, C. Chen, K. Thiele, D. Grosjean, J. Yang, L. Bao, R. Schneider, S. Schaetz, C. Meyer, A. Neben, B. Ryan, J. R. Petrus, J. Lutsky, D. McMahill, G. Corteville, M. R. Hageman, L. Miller and K. G. Fife, *Proceedings of the National Academy of Sciences*, 2021, **118**, e2019339118.

355. N. Ota, Y. Yalikun, T. Suzuki, S. W. Lee, Y. Hosokawa, K. Goda and Y. Tanaka, *Royal Society Open Science*, 2019, **6**, 181776.

356. Y. Li, S. Cai, H. Shen, Y. Chen, Z. Ge and W. Yang, *Biomicrofluidics*, 2022, **16**.

357. I. Leibacher, P. Reichert and J. Dual, *Lab on a Chip*, 2015, **15**, 2896-2905.

358. H. Bachman, C. Chen, J. Rufo, S. Zhao, S. Yang, Z. Tian, N. Nama, P.-H. Huang and T. J. Huang, *Lab on a Chip*, 2020, **20**, 1238-1248.

359. X. Ding, P. Li, S.-C. S. Lin, Z. S. Stratton, N. Nama, F. Guo, D. Slotcavage, X. Mao, J. Shi, F. Costanzo and T. J. Huang, *Lab on a Chip*, 2013, **13**, 3626-3649.

360. Z. Chen, Z. Pei, X. Zhao, J. Zhang, J. Wei and N. Hao, *Chemical Engineering Journal*, 2022, **433**, 133258.

361. X. Zhao, Z. Chen, Y. Qiu and N. Hao, *Materials Advances*, 2023, **4**, 988-994.

362. P. Zhang, H. Bachman, A. Ozcelik and T. J. Huang, *Annual Review of Analytical Chemistry*, 2020, **13**, 17-43.

363. A. Mudugamuwa, U. Roshan, S. Hettiarachchi, H. Cha, H. Musharaf, X. Kang, Q. T. Trinh, H. M. Xia, N.-T. Nguyen and J. Zhang, *Small*, **2024**, 2404685.

364. L. Nan, H. Zhang, D. A. Weitz and H. C. Shum, *Lab on a Chip*, 2024, **24**, 1135-1153.

365. H. Lin, J. Chen and C. Chen, *Medical & Biological Engineering & Computing*, 2016, **54**, 1317-1330.

366. Z. Chen, P. Liu, X. Zhao, L. Huang, Y. Xiao, Y. Zhang, J. Zhang and N. Hao, *Applied Materials Today*, 2021, **25**, 101239.

367. M. R. Rasouli and M. Tabrizian, *Lab on a Chip*, 2019, **19**, 3316-3325.

368. H. Fallahi, H. Cha, H. Adelnia, Y. Dai, H. T. Ta, S. Yadav, J. Zhang and N.-T. Nguyen, *Nanoscale Horizons*, 2022, **7**, 414-424.

369. H. M. Musharaf, U. Roshan, A. Mudugamuwa, Q. T. Trinh, J. Zhang and N.-T. Nguyen, *Micromachines*, 2024, **15**, 897.

370. D. T. Tran, A. S. Yadav, N.-K. Nguyen, P. Singha, C. H. Ooi and N.-T. Nguyen, *Small*, **n/a**, 2303435.

371. H. H. Vu, N.-T. Nguyen, N.-K. Nguyen, C. H. Luu, S. Hettiarachchi and N. Kashaninejad, *Advanced Engineering Materials*, 2023, **25**, 2300821.

372. Tandiono, S.-W. Ohl, D. S.-W. Ow, E. Klaseboer, V. V. T. Wong, A. Camattari and C.-D. Ohl, *Lab on a Chip*, 2010, **10**, 1848-1855.

373. L. Zhang, Z. Liu, Y. Wang, R. Xie, X.-J. Ju, W. Wang, L.-G. Lin and L.-Y. Chu, *Chemical Engineering Journal*, 2017, **309**, 691-699.

374. S.-W. Ohl, D. S. W. Ow, E. Klaseboer, V. V. Wong, R. Dumke and C.-D. Ohl, *Proceedings of the National Academy of Sciences*, 2011, **108**, 5996-5998.

375. D. Fernandez Rivas, M. Ashokkumar, T. Leong, K. Yasui, T. Tuziuti, S. Kentish, D. Lohse and H. J. G. E. Gardeniers, *Ultrasonics Sonochemistry*, 2012, **19**, 1252-1259.

376. K. Thangavadivel, M. Konagaya, K. Okitsu and M. Ashokkumar, *Journal of Environmental Chemical Engineering*, 2014, **2**, 1841-1845.

377. A. Hommes, A. J. ter Horst, M. Koeslag, H. J. Heeres and J. Yue, *Chemical Engineering Journal*, 2020, **399**, 125750.

378. Z. Peng, G. Wang, B. Moghtaderi and E. Doroodchi, *Chemical Engineering Science*, 2022, **247**, 117040.

379. J. Zong and J. Yue, *Frontiers in Chemical Engineering*, 2022, **3**.

380. J. Zong and J. Yue, *Industrial & Engineering Chemistry Research*, 2022, **61**, 6269-6291.

381. F. Fischer, T. Bahry, Z. Xie, K. Qian, R. Li, J. Kwan, F. Jérôme, S. Valange, W. Liu, P. N. Amaniampong and T. S. Choksi, *ChemRxiv*, 2024. DOI: 10.26434/chemrxiv-2024-01sv9.

382. L. Rekhi, Q. T. Trinh, A. M. Prabhu and T. S. Choksi, *ACS Catalysis*, 2024, **14**, 13839-13859.

383. Q. T. Trinh, K. Bhola, P. N. Amaniampong, F. Jérôme and S. H. Mushrif, *The Journal of Physical Chemistry C*, 2018, **122**, 22397-22406.

384. Q. T. Trinh, A. Banerjee, Y. Yang and S. H. Mushrif, *The Journal of Physical Chemistry C*, 2017, **121**, 1099-1112.

385. Q. T. Trinh, A. V. Nguyen, D. C. Huynh, T. H. Pham and S. H. Mushrif, *Catalysis Science & Technology*, 2016, **6**, 5871-5883.

386. Q. T. Trinh, K. F. Tan, A. Borgna and M. Saeys, *The Journal of Physical Chemistry C*, 2013, **117**, 1684-1691.

387. K. Bhola, Q. T. Trinh, D. Liu, Y. Liu and S. H. Mushrif, *Catalysis Science & Technology*, 2023, **13**, 6764-6779.

388. G. Liu, Q. T. Trinh, H. Wang, S. Wu, J. M. Arce-Ramos, M. B. Sullivan, M. Kraft, J. W. Ager, J. Zhang and R. Xu, *Small*, 2023, **19**, 2301379.

389. R. Paul, S. C. Shit, T. Fovanna, D. Ferri, B. Srinivasa Rao, G. T. K. K. Gunasooriya, D. Q. Dao, Q. V. Le, I. Shown, M. P. Sherburne, Q. T. Trinh and J. Mondal, *ACS Applied Materials & Interfaces*, 2020, **12**, 50550-50565.

390. C. Sarkar, S. Pendem, A. Shrotri, D. Q. Dao, P. Pham Thi Mai, T. Nguyen Ngoc, D. R. Chandaka, T. V. Rao, Q. T. Trinh, M. P. Sherburne and J. Mondal, *ACS Applied Materials & Interfaces*, 2019, **11**, 11722-11735.